National Library of Canada
Canadian Theses Service
Ottawa, Canada
K1A 0N4

Bibliothèque nationale du Canada
Services des thèses canadiennes

CANADIAN THESES

THÈSES CANADIENNES

NOTICE

The quality of this microfiche is heavily dependent upon the quality of the original thesis submitted for microfilming. Every effort has been made to ensure the highest quality of reproduction possible.

If pages are missing, contact the university which granted the degree.

Some pages may have indistinct print especially if the original pages were typed with a poor typewriter ribbon or if the university sent us an inferior photocopy.

Previously copyrighted materials (journal articles, published tests, etc.) are not filmed.

Reproduction in full or in part of this film is governed by the Canadian Copyright Act, R.S.C. 1970, c. C-30.

AVIS

La qualité de cette microfiche dépend grandement de la qualité de la thèse soumise au microfilmage. Nous avons tout fait pour assurer une qualité supérieure de reproduction.

S'il manque des pages, veuillez communiquer avec l'université qui a conféré le grade.

La qualité d'impression de certaines pages peut laisser à désirer, surtout si les pages originales ont été dactylographiées à l'aide d'un ruban usé ou si l'université nous a fait parvenir une photocopie de qualité inférieure.

Les documents qui font déjà l'objet d'un droit d'auteur (articles de revue, examens publiés, etc.) ne sont pas microfilmés.

La reproduction, même partielle, de ce microfilm est soumise à la Loi canadienne sur le droit d'auteur, SRC 1970, c. C-30.

THIS DISSERTATION
HAS BEEN MICROFILMED
EXACTLY AS RECEIVED

LA THÈSE A ÉTÉ
MICROFILMÉE TELLE QUE
NOUS L'AVONS REÇUE

Canada

NL-339 (r. 86/06)

THE UNIVERSITY OF ALBERTA

# GENESIS OF THE DEER TRAIL Zn-Pb-Ag VEIN DEPOSIT, WASHINGTON, U.S.A.

by

DARRELL WAYNE FLUET

A THESIS

SUBMITTED TO THE FACULTY OF GRADUATE STUDIES AND RESEARCH

IN PARTIAL FULFILMENT OF THE REQUIREMENTS FOR THE DEGREE

OF MASTER OF SCIENCE

DEPARTMENT OF GEOLOGY

EDMONTON, ALBERTA

Spring, 1986

Permission has been granted to the National Library of Canada to microfilm this thesis and to lend or sell copies of the film.

The author (copyright owner) has reserved other publication rights, and neither the thesis nor extensive extracts from it may be printed or otherwise reproduced without his/her written permission.

L'autorisation a été accordée à la Bibliothèque nationale du Canada de microfilmer cette thèse et de prêter ou de vendre des exemplaires du film.

L'auteur (titulaire du droit d'auteur) se réserve les autres droits de publication; ni la thèse ni de longs extraits de celle-ci ne doivent être imprimés ou autrement reproduits sans son autorisation écrite.

ISBN 0-315-30212-7

THE UNIVERSITY OF ALBERTA

**RELEASE FORM**

NAME OF AUTHOR DARRELL WAYNE FLUET

TITLE OF THESIS GENESIS OF THE DEER TRAIL Zn-Pb-Ag VEIN DEPOSIT, WASHINGTON, U.S.A.

DEGREE FOR WHICH THESIS WAS PRESENTED MASTER OF SCIENCE

YEAR THIS DEGREE GRANTED Spring, 1986

Permission is hereby granted to THE UNIVERSITY OF ALBERTA LIBRARY to reproduce single copies of this thesis and to lend or sell such copies for private, scholarly or scientific research purposes only.

The author reserves other publication rights, and neither the thesis nor extensive extracts from it may be printed or otherwise reproduced without the author's written permission.

(SIGNED) Darrell Fluet

PERMANENT ADDRESS:

10 Westbrook Dr.
Edmonton, Alberta, CDN.
T6J 2C9

DATED April 7 1986

THE UNIVERSITY OF ALBERTA

FACULTY OF GRADUATE STUDIES AND RESEARCH

The undersigned certify that they have read, and recommend to the Faculty of Graduate Studies and Research, for acceptance, a thesis entitled GENESIS OF THE DEER TRAIL Zn-Pb-Ag VEIN DEPOSIT, WASHINGTON, U.S.A. submitted by DARRELL WAYNE FLUET in partial fulfilment of the requirements for the degree of MASTER OF SCIENCE.

.....

Supervisor

.....

.....

.....

Date April 7, 1986

## DEDICATION

To Karin

For making it possible for me to do this study,

For helping me over the rough spots,

and

For putting up with me while I worked on it.

## ABSTRACT

The Deer Trail Pb-Zn-Ag veins of northeastern Washington, U.S.A., are hosted in dilatent fractures within metasediments of the Deer Trail series. This series is a member of the Missoula Group of sediments, which make up the upper portion of the Belt Supergroup.

Vein fill took place in three stages; the pre-ore, ore and post-ore stages and the temperature, salinity and $CO_2$ content of the hydrothermal fluid fell with time. The maximum temperature was approximately 300°C during the pre-ore stage, ranged between 250°C and 150°C during the ore stage and fell below 150°C in the post-ore stage. Salinity had a maximum value of about 8 wt.% in the pre-ore stage and fell to less than 3 wt.% during the post-ore stage. The $CO_2$ content of the fluid was also highest during the pre-ore stage and had fallen to nill by the post-ore stage. Pressure during vein formation had an absolute minimum value of approximately 80 bars, actual pressures were probably between 500 and 1000 bars.

The pre-ore stage fluid had a maximum calculated $\delta^{18}O$ value of nearly 10‰. Ore stage fluids had a mean $\delta^{18}O$ value of approximately of approximately 5‰, and fluids had a maximum $\delta^{18}O$ value of -5‰ during the post-ore stage. Very late calcite, formed after faulting of the vein, reflects a parent fluid $\delta^{18}O$ value of approximately -11‰. Wall rocks adjacent to the vein are depleted in $^{18}O$.

All hydrothermal fluids had $\delta D$ values between -125‰ and -140‰, except for early ore stage fluids which had $\delta D$ values between -89‰ and -111‰. These values are significantly higher than those of the pre-ore and post-ore stage fluids, which were dominanted by meteoric water, and may indicate the presence of magmatic or metamorphic water during that period. Alternatively, these high D values may have been the result of re-equilibration of meteoric water with the Loon Lake batholith at low water/rock ratios. All fluids underwent O exchange with the high-$^{18}O$ host rocks which resulted in a wide range of $\delta^{18}O$ fluid values throughout the system's history.

Sphalerite and galena from the mine have a narrow range of $\delta^{34}S$ values between 4.5‰ and 11.9‰. Geothermometry based on coeval sphalerite/galena pairs supports the ore stage temperature range determined from fluid inclusions. Sulfur isotopes also indicate a sedimentary sulfur source, probably the host Deer Trail series metasediments, and an $H_2S$ dominated system.

Oxygen and hydrogen isotope results are very similar to those found for the Coeur d'Alene deposits of Idaho. Sulfur isotopes are also similar, though somewhat lower in the case of Coeur d'Alene. The Idaho deposits are in the same host rocks, are associated with an intrusion of similar age and type, and have a mineralogy similar to that of the Deer Trail veins. Such similarities indicate that the Deer Trail and Coeur d'Alene deposits, and possible other similar deposits in southern British Columbia and northern Washington, were formed and controlled by the same geological events and processes.

## ACKNOWLEDGMENTS

The author wishes to thank Dr. R. D. Morton for his advice and supervision, and for teaching me to work and think independently.

Thanks also to ;

Dr. John Gray, for the use of his lab and mass spectrometer during the hydrogen isotope work.

Dr. Bruce Nesbitt, for his suggestions and instruction.

Dr. H. Krouse, for performing the sulfur isotope analyses and for helpful suggestions.

and

Dr. K. Meuhlenbachs, for the use of his lab during the oxygen isotope analyses.

Dr. H. A. K. Charlesworths' instruction, and the use of his TRIPOD program, are also gratefully acknowledged.

The author particularly appreciated the continuous help and suggestions of Dr. A. Changkakoti and all the members of the third floor 'Economic Geology Research Unit'.

Finally, thanks to Madre Mining Ltd. for their assistance in completing this study.

## Table of Contents


Chapter — Page

I. INTRODUCTION ..... 1

A. PURPOSE OF STUDY ..... 1

B. LOCATION AND CLIMATE ..... 3

C. PREVIOUS WORK ..... 6

D. HISTORY OF MINE DEVELOPMENT ..... 7

II. REGIONAL SETTING AND GEOLOGY ..... 8

A. INTRODUCTION ..... 8

B. BELTIAN METASEDIMENTS ..... 11

The Togo Formation ..... 14

The Edna Dolomite ..... 14

The McHale Slate ..... 15

The Stensgar Dolomite ..... 15

The Buffalo Hump Formation ..... 16

C. HUCKLEBERRY FORMATION AND LATER INTRUSIVES ..... 17

The Huckleberry Formation ..... 17

Intrusives ..... 18

D. STRUCTURAL GEOLOGY ..... 19

Folding ..... 19

Faulting ..... 20

III. LOCAL GEOLOGY AND DEPOSIT DESCRIPTION ..... 21

A. HOST ROCKS OF THE DEPOSIT ..... 21

B. INTRUSIONS ..... 22

C. FAULTS ..... 23

Parallel Faults ..... 23

Cut-Off Faults ..... 23

D. DEPOSIT DESCRIPTION ..... 28

Madre Vein ..... 28
The Elephant Vein ..... 28
Sister Vein ..... 30
Replacement bodies ..... 30
IV. VEIN PETROGENESIS, MINERALOGY AND PARAGENESIS ..... 31
A. BACKGROUND AND METHODS ..... 31
B. VEIN PETROGENESIS AND MINERALOGY ..... 32
Gangue Minerals ..... 32
Opaque Minerals : Non Silver-Bearing ..... 33
Opaque Minerals : Silver-Bearing ..... 35
Native Elements ..... 38
C. PARAGENETIC SEQUENCE AND DISCUSSION ..... 39
V. FLUID INCLUSION STUDIES ..... 42
A. INTRODUCTION ..... 42
Inclusion types and their recognition ..... 43
Information available from fluid inclusion studies ..... 44
B. FLUID INCLUSIONS IN THE DEER TRAIL VEINS ..... 45
C. TESTING METHODS AND RESULTS ..... 47
Freezing Tests ..... 47
Heating Tests - homogenization ..... 55
Crushing Stage ..... 58
D. INTERPRETATION AND DATA CORRECTIONS ..... 59
E. CONCLUSIONS ..... 64
VI. OXYGEN AND HYDROGEN ISOTOPE STUDIES ..... 65
A. INTRODUCTION TO OXYGEN AND HYDROGEN ISOTOPES ..... 65
B. OXYGEN ISOTOPE STUDY ..... 70
Method ..... 70

Analytical Results ..... 70
C. HYDROGEN ISOTOPE STUDY ..... 76
Method ..... 76
Analytical Results ..... 77
Discussion ..... 80
VII. SULFUR ISOTOPES ..... 82
A. INTRODUCTION TO SULFUR ISOTOPES ..... 82
B. SULFUR ISOTOPE STUDY ..... 85
Method ..... 85
Analytical Results ..... 85
Sulfur Isotope Geothermometry ..... 87
VIII. FLUID CHEMISTRY ..... 89
A. METHOD ..... 89
B. INTERPRETATION ..... 100
IX. SUMMARY AND CONCLUSIONS ..... 104
X. REFERENCES CITED ..... 108
XI. APPENDIX - TEST, CALCULATION AND CALIBRATION METHODS ..... 117
A. ELECTRON MICROPROBE ..... 117
B. STAGE CALIBRATION ..... 118
C. SULFUR ISOTOPES ..... 123
D. OXYGEN AND HYDROGEN ISOTOPES ..... 128

## List of Tables

Table 3-1: Sequence of major events in the development of the Deer Trail district. .....27

Table 4-1: Freibergite analyses - electron microprobe .....36

Table 5-1: Fluid inclusion heating and freezing results .....48

Table 6-1: Quartz O isotope analysis results.....71

Table 6-2: Calcite and dolomite O isotope analysis results .....72

Table 6-3: Results of H/D isotope analysis of fluid inclusion waters .....78

Table 7-1: Sulfide S isotope analysis results and geothermometry .....86

Table 8-1: Calculated parent fluid $\delta^{34}S$ values.....97

Table A-1: Stage calibration standards..... 120

Table A-2: Equilibrium coefficients for calculations and diagrams used in this study..... 124

## List of Figures

Figure 1-1: General location map ..... 4

Figure 1-2: General geology of Stevens county with relevent mines ..... 5

Figure 2-1: General geology of mine area ..... 9

Figure 2-2: Cross-section of mine area ..... 10

Figure 2-3: Correlation of Belt and Purcell Supergroups ..... 12

Figure 2-4: Column of formations, Deer Trail series ..... 13

Figure 3-1: Plan view of mines on the Deer Trail veins ..... 24

Figure 3-2: Three dimensional view of Hoodoo Madre vein fault blocks ..... 25

Figure 3-3: TRIPOD projection of Deer Trail veins ..... 29

Figure 4-1: Paragenetic sequence of the Deer Trail veins ..... 40

Figure 5-1: Types of fluid inclusions from Deer Trail vein material ..... 46

Figure 5-2: Liquid/gas curves for the NaCl $H_2O$ - $CO_2$ system ..... 53

Figure 5-3: Freezing point depression of the $CO_2$ clathrate in NaCl solutions ..... 54

Figure 5-4a: Inclusion homogenization temperatures of upper vein inclusion set ..... 56

Figure 5-4b: Inclusion homogenization temperatures of lower vein inclusion set ..... 57

Figure 5-5: Combined pressure vs. temperature water and carbon dioxide isochor plot ..... 60

Figure 5-6a: Combined homogenization data of upper and lower inclusion sets ..... 63

Figure 5-6b: Approximate temperature ranges of stages of vein formation ..... 63

Figure 6-1: Oxygen and deuterium analysis results ..... 74

Figure 8-1: Temperature vs. pH at given $CO_2$ fugacities, ionic strength = 1 molar ..... 92

Figure 8-2: $fO_2$ vs. $fS_2$ diagram, Fe-O-S system at 250°C ..... 93

Figure 8-3: pH vs. $fO_2$ diagram of sulfur species at 250°C ..... 95

Figure 8-4a: $\Delta\delta^{34}S$(sphalerite-galena) vs. $\delta^{34}S$(sphalerite, galena) diagram, fluid $\delta^{34}S$ value = 10‰ ..... 99

Figure 8-4b: $\Delta\delta^{34}S$(sphalerite-galeba) vs. $\delta^{34}S$(sphalerite, galena) diagram, $\delta^{34}S$ values from this study ..... 99

Figure 8-5: $\delta^{34}S$ ranges of Deer Trail vein sulfides and possible S sources ..... 101

Figure A-1: Indicated stage temperature vs. actual stage temperature ..... 121

Figure A-2: Indicated stage temperature vs. necessary temperature correction ..... 122

# I. INTRODUCTION

## A. PURPOSE OF STUDY

Numerous studies dealing with low to moderate temperature, epithermal, gold-dominated quartz veins in rhyolitic to dacitic volcanics have been published. A study of the isotopes and fluid inclusions of the veins of western Nevada are a good example (Vikre 1985). A second group of papers have dealt with moderate to high temperature base-metal dominated vein deposits, such as Butte, Montana (Sheppard and Taylor 1974). These deposits are associated with granitic intrusions and porphyries and are hosted either within the intrusions or the surrounding sediments.

It has been found that the hydrothermal system which formed both types of deposit were driven by either a cooling pluton or volcanic plug and were dominated by meteoric water, which had undergone varying degrees of oxygen exchange with the wall rocks and intrusions. Magmatic water may also have been involved in some of the base metal vein deposits. Between these two well studied classes of deposits lies a third class, of which the Deer Trail deposit is a member, that has been much less thoroughly studied.

The Deer Trail deposit is made up of a set of Zn-Pb-Ag bearing quartz veins which are hosted in Precambrian Belt metasediments, including argillite, slate, dolostone and limestone, and are associated with a large granitic to quartz monzonitic intrusion. This study was undertaken to determine the nature and genesis of these veins, and to try to discern the relationship between this deposit and other similar deposits such as Coeur d'Alene, Idaho.

To achieve this, four aspects of the deposit were studied;

1. Relative ages of veins, faults and intrusions.
2. Vein controls, petrogenesis and mineralogy.
3. Ore fluid characteristics.
4. Source of sulfur and constituent ore/gangue metals.

New information relating to these aspects may help in the mining and processing of ore from this deposit, and from other deposits of the same type. A better understanding of the mode of formation and controls on this deposit will also be helpful during exploration for analagous new deposits in the area, or in similar geological settings.

## B. LOCATION AND CLIMATE

The Deer Trail mine is located approximately 70 km northwest of Spokane, within the Hunters Quadrangle of Stevens County, Washington, U.S.A. (Fig. 1-1). It is situated at the southern end of a long array of similar deposits which stretch over 50 km to the northeast. All of these deposits are hosted by limestone or dolostone units within the Belt Supergroup and are associated with fractures or faults (Fig. 1-2).

The Deer Trail mine is situated near the midline of the Huckleberry Mountains, just below the head of Cedar Canyon; latitude 48° 02' N, longitude 118° 06' W. The minesite may be reached by traveling west from Spokane to Davenport, then north to Fruitland. An oiled road heading east from Fruitland leads to the foot of the Huckleberry Mountains, where a gravel 'Bureau of Land Management' road continues to the minesite.

The mountains around the mine are rugged and have a maximum elevation of approximately 1500 meters. The immediate Deer Trail mine area is dominated by a series of parallel ridges and valleys which trend 10° to 15° E of N, subparallel to the strike of bedding and structures in the area. The valley in which the Deer Trail mine is located seems to have been only slightly affected by glacial action which may explain the presence of preserved supergene-enriched deposits in the upper portions of the veins which were discovered in the late 1800's and mined soon after.

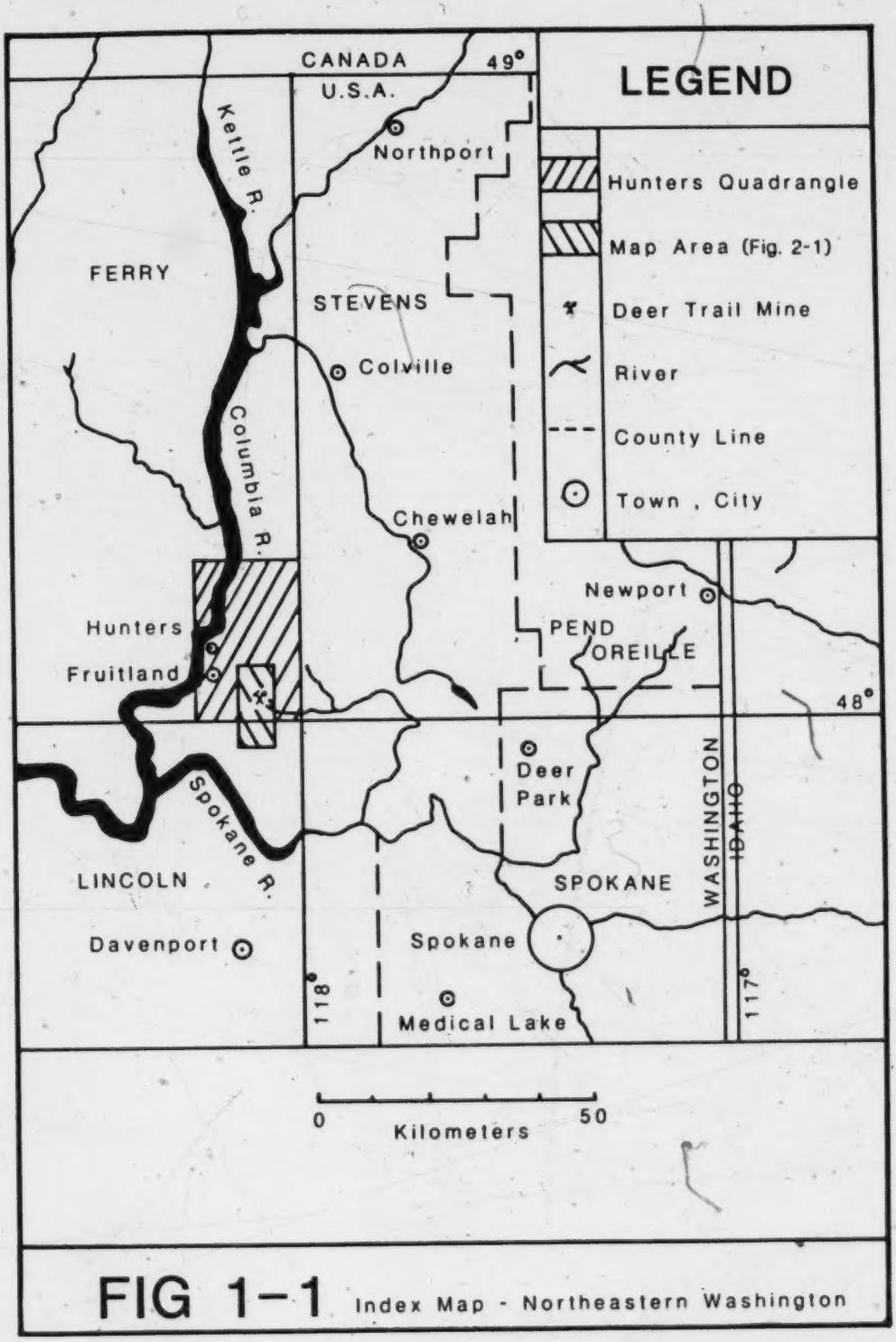


FIG 1-1 Index Map - Northeastern Washington

**FIG. 1–2** Highly Generalized Geology of Stevens County. modified from Mills , 1977.

## C. PREVIOUS WORK

Most of the studies of the Zn-Pb-Ag vein deposits of northeastern Washington were overviews of mining in the area, essentially just compilations of mine data.

The first compilation was written by Bancroft, in 1914. This report listed several important mining properties, outlined their general geology, and listed the ore minerals found in each mine. This paper was soon followed by two more from the Washington Geological Survey. Weavers' paper (1920) was essentially a summary of the Bancroft paper, with some additional information. Whitwell and Patty (1921), however, covered many mines not referred to by Bancroft or Weaver. Finally the Washington Division of Geology published a paper by Jenkens (1924) which covered essentially all of the then important mines in northeastern Washington.

The Campbell and Loofbourow report (1962), entitled 'Geology of the Magnesite Belt of Stevens County, Washington', included a description and map of the host rocks of the magnesite deposits and the major Zn-Pb-Ag veins of the area. Regional mapping was extended by the 'Preliminary Geology Map of Hunters Quadrangle' (Campbell and Raup 1964). This map showed that the Precambrian rocks of Hunters Quadrangle lie in a western extension of the Precambrian Belt basin of Idaho. A paper dealing with the tectonics of northeastern Washington (Yates *et al.* 1966) indicated that the entire Deer Trail district was located in the overturned west limb of a major NE-SW trending anticline.

Small (1973) studied the Pb isotopes of galena from many ore deposits in northeastern Washington, including the Deer Trail mine Togo, Aichanbee, and Queen & Seal mines. His results indicated that the Pb in these deposits was anomalous (radiogenic) and was probably the product of a multistage evolution, and that the formation of these deposits may have been related to the emplacement of the Loon Lake batholith.

## D. HISTORY OF MINE DEVELOPMENT

The original discovery in the Deer Trail district was made in 1894. Two hunters stumbled across a heavily weathered supergene-enriched vein in a deer trail - thus the origin of the name. Panning of material from the vein revealed the presence of abundant native silver. The hunters immediately staked the area and numerous additional claims were soon staked around the discovery outcrop. Many one-man or family-run mines, as well as larger developments, were operated in the area until about 1910, when the rich and easily accessible supergene-enriched deposits were exhausted. The Zn, Pb, Ag and Au(minor) produced during this short boom period was worth almost $3 million U.S. dollars at turn of the century metal prices (Thurmond 1928).

In the 1920's and early 1930's many of the claims in the district were acquired by the Venus Silver Mining Company. Development and mining was done on the Hoodoo level, but when the vein was lost, and the remaining ore apparently exhausted, the mine was again closed.

Very little further work was done on the property until 1980 when it was purchased by Madre Mining Limited. Extensive development work was done on several levels of the mine. A new haulage way, called the Madre tunnel, was driven to intersect the vein below the Hoodoo level. The Madre, Hoodoo and Midway levels were joined by raises and exploration and development work was done on all three levels. A new 150 ton per day floatation mill was installed, the concentrates from which were shipped to the Cominco plant at Trail, B.C., for processing. Almost $2 million worth of Zn, Pb and Ag concentrate was produced from the startup date to May, 1984. The mine is now closed due to low silver prices, though sulfide rich quartz veins still remain in open stopes and in undeveloped portions of the vein system.

## II. REGIONAL SETTING AND GEOLOGY

### A. INTRODUCTION

The Deer Trail veins are hosted by a suite of Belt Supergroup metasediments termed the Deer Trail series. This suite lies to the east of the southern tip of the Kootenay arc and is a western extension of the main body of Beltian sediments of Idaho and Montana (Campbell and Raup 1964). The Deer Trail series forms a lobe which is bounded on three sides by the Jurassic-Cretaceous Loon Lake batholith. The metasediments have been folded on both local and regional scales, but have a consistent strike of 30° to 40° E of N. All beds in the map area dip at between 51° northwestward and 60° southeastward, the southeast dipping beds being overturned (Fig. 2-1).

Two major sets of faults cut the Deer Trail series. The first strikes between 25° and 35° E of N, slightly less than that of the metasediments, and dips almost vertically. The maximum dip slip of these faults is approximately 1000 meters, east side down (Fig. 2-2), the amount of strike slip is unknown but right lateral in nature. A second set of faults cut diagonally across the Deer Trail series and strike at 90° to 110° E of N. Their strike slip may be up to 500 meters right lateral, while their dip slip is unknown (Campbell and Loofbourow 1962).

The Deer Trail series has been intruded by plugs, dykes and sills of quartz monzonitic to granitic composition. These are presumably coeval and consanguineous with the Loon Lake batholith. These plugs are very common and only the larger ones are shown in Figure 2-1. Older greenstone and diabase dykes are also present within the metasediments.

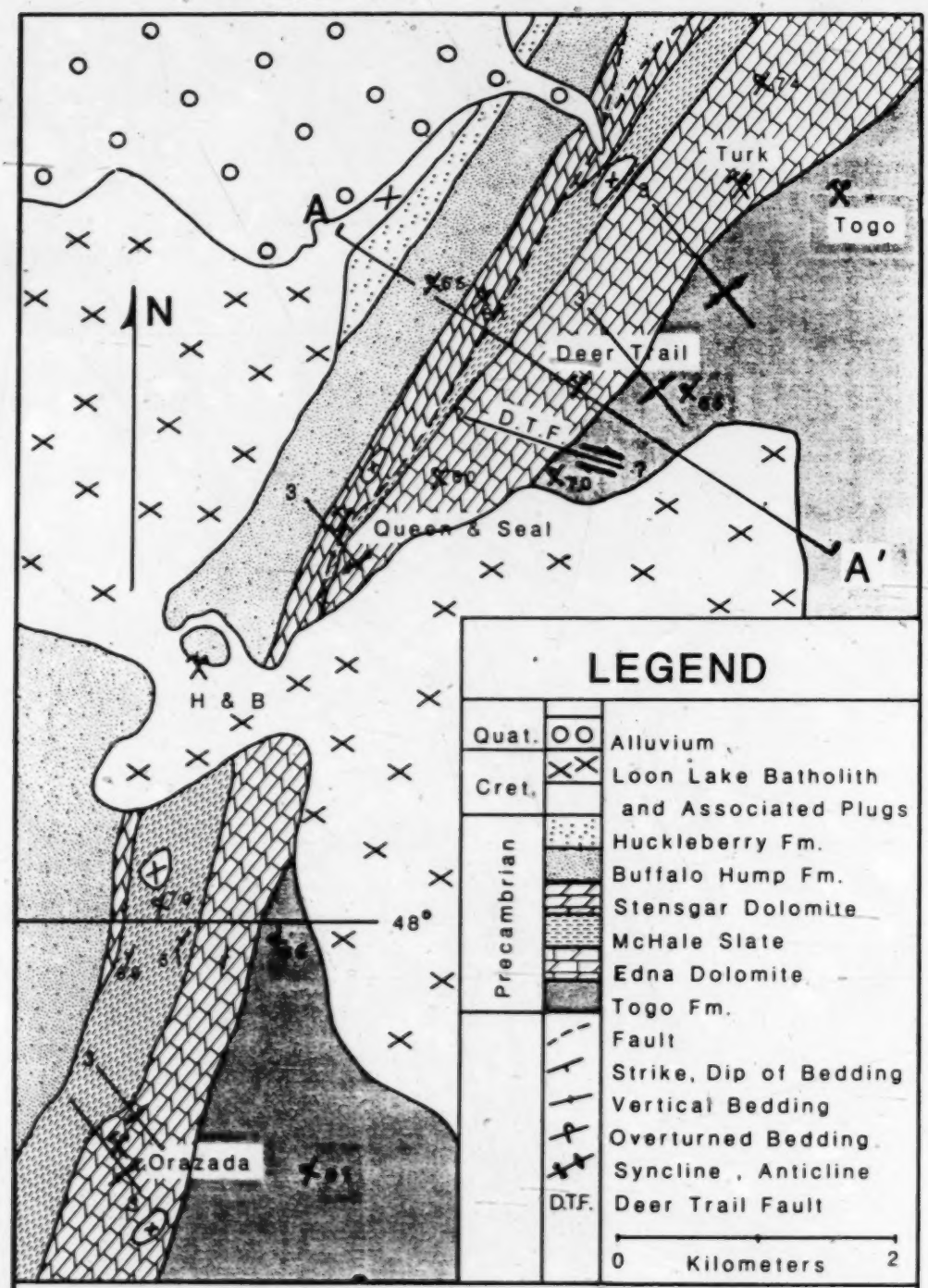


**FIG. 2-1** General Geology of Map Area
After Cambell and Raup, 1964

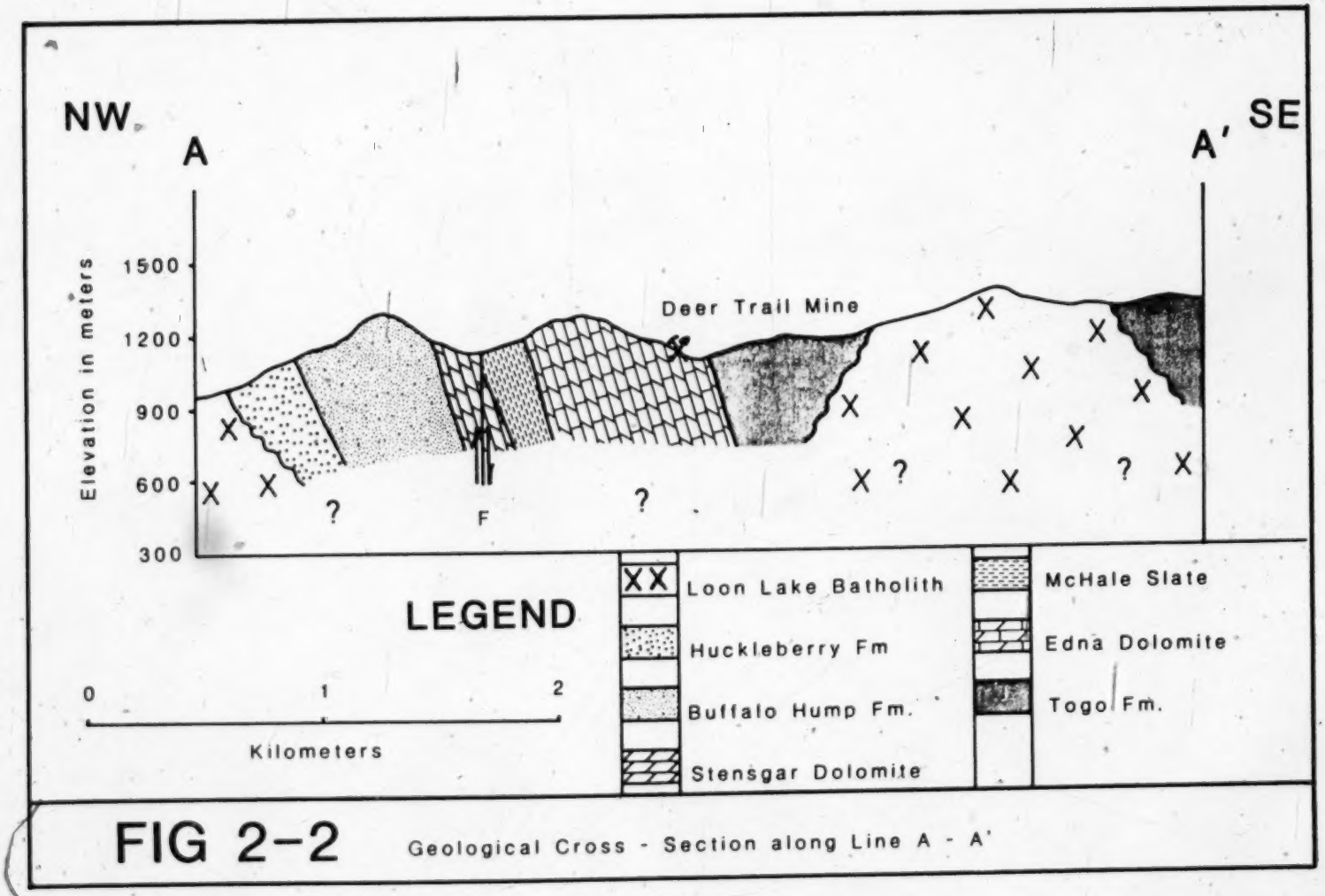


FIG 2-2 Geological Cross - Section along Line A - A'

## B. BELTIAN METASEDIMENTS

The Belt Supergroup is composed of a sequence of Precambrian metasediments which may reach 20,000 meters in thickness (Harrison and Grimes 1970). The sediments were probably originally deposited in a shallow epicratonic reentrant of the sea as rock types include slate, argillite, quartzite and carbonate. The maximum age of the Belt Supergroup is about 1700 Ma and deposition had probably ended by 1400 Ma ago (Small 1973; Harrison 1972). Horizontal and vertical facies changes within the metasediments are generally gradational and the rocks may best be described as monotonous. The maximum grain size over wide areas is medium grained sand or less, while color may range from grey to grey-green to brown. This makes correlation of specific units and formations difficult on anything but a local scale.

The rocks of the Deer Trail series are part of the upper Missoula Group, located at the top of the Belt Supergroup, and have been regionally metamorphosed to the greenschist facies. The metamorphism may have preceeded folding or the two events may have been contemporaneous. Intrusive plugs and the Loon Lake batholith have conspicuous metamorphic aureoles and are definitely post metamorphic (Campbell and Loofbourow 1962).

The Deer Trail series is made up of the following formations:

The Buffalo Hump Formation.

The Stensgar Dolomite - host of the Queen & Seal veins.

The McHale Slate.

The Edna Dolomite - host of the Deer Trail veins.

The Togo Formation - the base of which is unexposed.

The Deer Trail series correlates with the Dutch Creek/Mt. Nelson Formations of western Canada (Fig. 2-3), and has a minimum thickness of 3400 meters. It is overlain unconformably by the Huckleberry Formation (Campbell and Loofborow 1962) (Fig. 2-4).

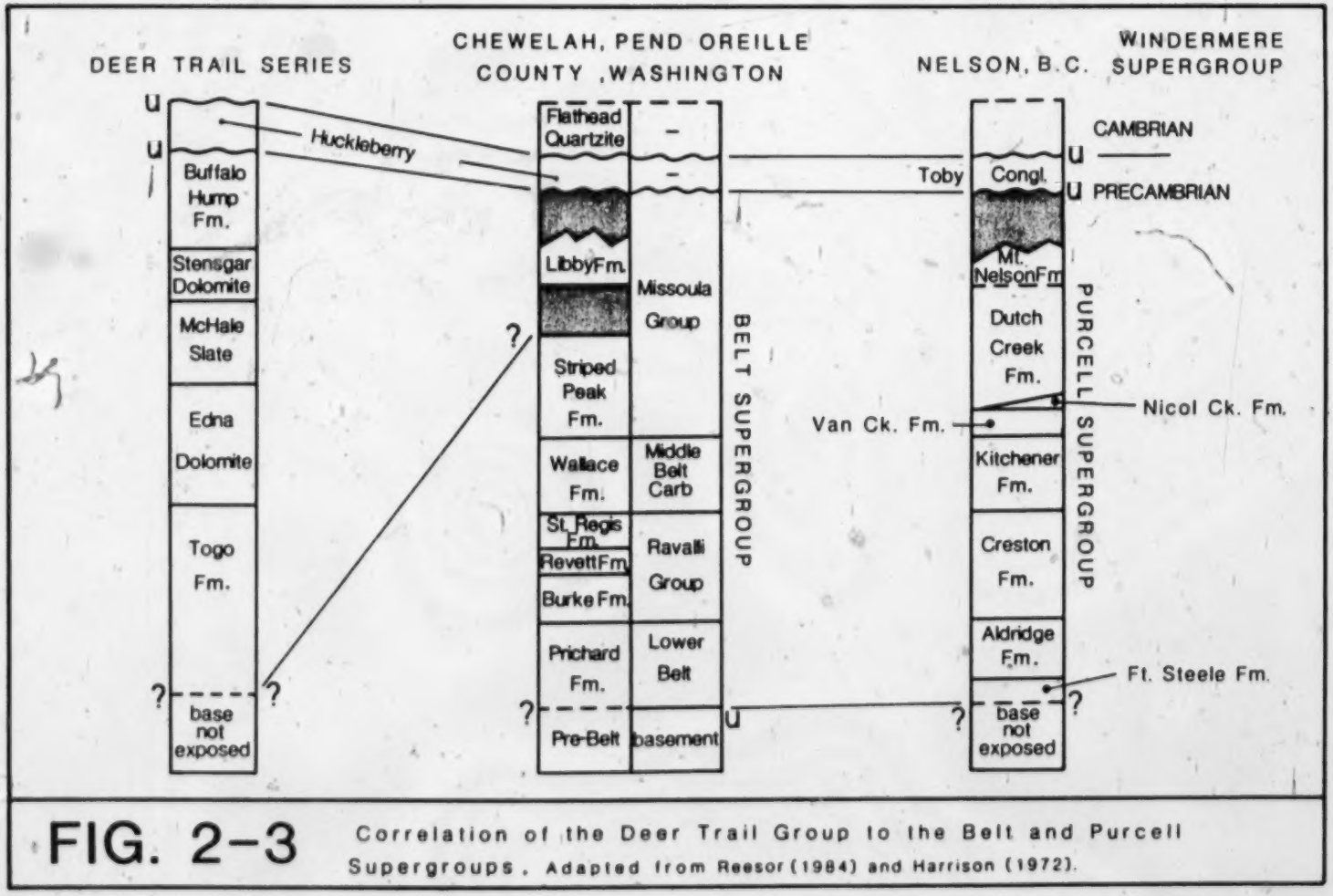


**FIG. 2-3** Correlation of the Deer Trail Group to the Belt and Purcell Supergroups. Adapted from Reesor (1984) and Harrison (1972).

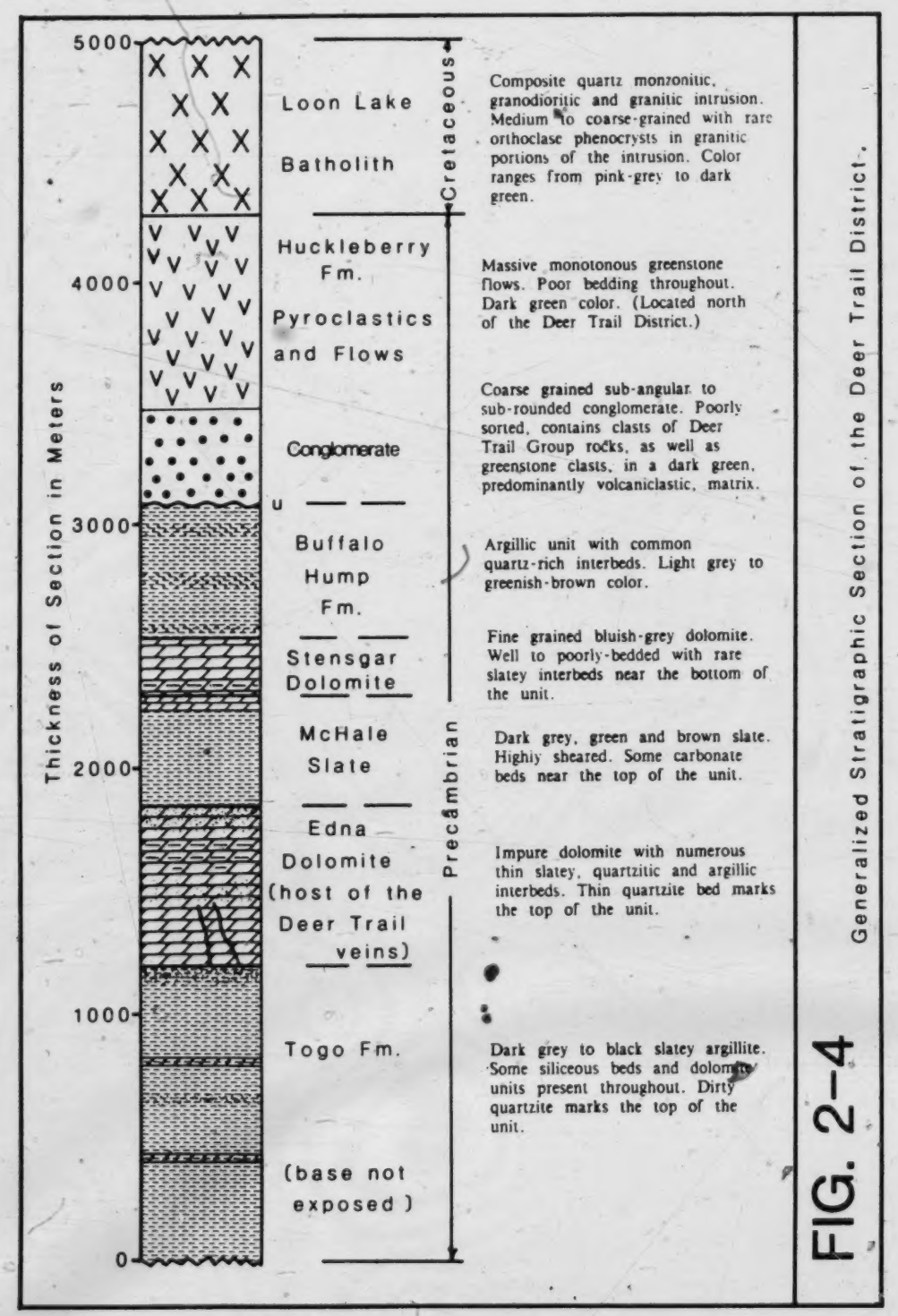
5000
4000
3000
2000
1000
0
Thickness of Section in Meters
Loon Lake Batholith
Cretaceous
Composite quartz monzonitic, granodioritic and granitic intrusion. Medium to coarse-grained with rare orthoclase phenocrysts in granitic portions of the intrusion. Color ranges from pink-grey to dark green.
Huckleberry Fm. Pyroclastics and Flows
Massive monotonous greenstone flows. Poor bedding throughout. Dark green color. (Located north of the Deer Trail District.)
Conglomerate
Coarse grained sub-angular to sub-rounded conglomerate. Poorly sorted, contains clasts of Deer Trail Group rocks, as well as greenstone clasts, in a dark green, predominantly volcaniclastic, matrix.
u
Buffalo Hump Fm.
Argillic unit with common quartz-rich interbeds. Light grey to greenish-brown color.
Stensgar Dolomite
Fine grained bluish-grey dolomite. Well to poorly-bedded with rare slatey interbeds near the bottom of the unit.
McHale Slate
Dark grey, green and brown slate. Highly sheared. Some carbonate beds near the top of the unit.
Edna Dolomite (host of the Deer Trail veins)
Impure dolomite with numerous thin slatey, quartzitic and argillic interbeds. Thin quartzite bed marks the top of the unit.
Precambrian
Togo Fm.
Dark grey to black slatey argillite. Some siliceous beds and dolomite units present throughout. Dirty quartzite marks the top of the unit.
(base not exposed)
Generalized Stratigraphic Section of the Deer Trail District.
FIG. 2-4

**The Togo Formation**

The Togo Formation is the oldest member of the Deer Trail series. It has an exposed thickness of over 1200 meters but, as it is cut to the east by the Loon Lake batholith, its true thickness is impossible to determine. The formation consists of monotonous, recessive, dark grey to black, slatey argillite. Thin beds of dark green-, black- and grey-striped silicic slate are common and produce limited resistant outcrops. Thin discontinuous beds of limestone and dolostone are present in the upper half of the formation. The top of the Togo Formation is marked by a distinct and continuous quartz-stringer rich facies whose thickness, and whose quartz content, rises markedly to the south. This facies acts as an excellent marker horizon within the Deer Trail series.

Though the contact is not well exposed, there appears to be an abrupt change in the character of the rocks at the Togo Formation/Edna dolomite interface. Adjacent outcrops show very different lithologies, indicating a non-gradational change from the quartzitic argillites of the Togo Formation to the dolomites and limestones of the Edna Dolomite.

**The Edna Dolomite**

The Edna Dolomite consists of impure dolostone with interbedded limestone, argillite, calcareous slate, phyllite, talcose slate and quartzite. It has a thickness of approximately 650 meters and is usually recessive. The main dolostone may range from very light grey to green, brown and black in color. Some beds are highly siliceous to cherty, while others are chalky. The chalky beds are not mentioned in the literature, but have been observed in drill core from the Deer Trail mine. Bedding is on the scale of millimeters to meters and may be highly contorted.

The base of this formation is a relatively clean dolomite. Most of the argillite and slate occur in the upper half of the formation, while quartzite beds are generally confined to the upper quarter of the formation.

**The McHale Slate**

The McHale Slate conformably overlies the Edna Dolomite throughout the entire map area. It is a slaty unit with interbeds of argillite and phyllite which exhibit little or no slaty cleavage. Several beds exhibit alternate bands of grey to brown color on a scale of millimeters to centimeters which may represent original bedding. The slate is generally dark grey, brown or green in color but changes to a light grey or buff near the top of the formation.

The McHale Slate has been intensely deformed so its actual thickness is difficult to determine. It may have acted as an incompetent bed between two competent units, the Stensgar and Edna Dolomites, and been more intensely folded and sheared than the rest of the Deer Trail series metasediments. On average it appears to be approximately 450 meters thick (Campbell and Loofbourow 1962). Interbeds of dolomite are present near the top of the formation, indicating a gradational change to the overlying Stensgar Dolomite.

**The Stensgar Dolomite**

The Stensgar Dolomite is an important marker horizon in the map area because of its continuity and its distinctive lithology. It consists of dense, well bedded, fine grained, pinkish- to bluish-grey dolostone. Argillitic and slaty beds are found near the base of the formation, but these gradually disappear upwards. The dolomite is resistive and forms numerous outcrops, though the complete section is never exposed.

In the north end of the map area the Stensgar Dolomite has a maximum thickness of 240 meters. It thins to the south and eventually pinches out completely at about latitude 48° north. This pinchout may represent an erosional unconformity or, more likely, is the result of offset along an unmapped extension of the Queen & Seal fault. The southern end of the formation has been extensively recrystallized and, occassionally, completely altered to a dolomitic marble. The Stensgar Dolomite hosts many large magnesite deposits and quartz veins, such as the Queen & Seal, which are very similar to the Deer Trail veins.

**The Buffalo Hump Formation**

This formation embraces all units above the Stensgar Dolomite and below the Huckleberry Formation. It is made up of interbedded slates, argillites and quartzites and its average thickness is approximately 550 meters. The top and bottom of the formation are slate- and argillite-rich, while the middle is dominantly quartzite and quartzitic slate. The color of the slates ranges from tan to dark-grey to green and brown. Their color and textures make these slates virtually indistinguishable from slates in other formations within the Deer Trail series.

The middle quartz-rich unit thins and thickens rapidly, though its thickness generally increases to the south. Its color ranges from light grey to yellow-brown, though in some areas it may have a bluish tint. Grain size generally varies from fine to coarse sand, but thin discontinuous beds of quartzitic slate are common. Rare quartz pebble conglomerate stringers are also present. As mentioned above, this unit generally overlies the Stensgar Dolomite. As a result of the Stensgar Dolomite pinchout, however, the Buffalo Hump Formation in the south of the map area lies directly upon the McHale Slate.

## C. HUCKLEBERRY FORMATION AND LATER INTRUSIVES

### The Huckleberry Formation

Only one non-Beltian sedimentary unit is present in the map area, namely the conglomerate member of the Huckleberry Formation. This 400 meter thick formation unconformably overlies the Buffalo Hump Formation and is neither part of the Deer Trail series nor a member of the Belt Supergroup, though it is also Precambrian in age. It is easily recognizable, unlike the sometimes indistinguishable units and formations of the Belt Supergroup.

The conglomerate unit is coarse grained and poorly sorted. Clasts range in size from less than 1 mm to over 10 cm in diameter, though the majority are less than 1 cm. Most clasts are composed of slate and phyllite, though rare limestone, dolomite and quartz pebbles are present. The high percentage of slate and phyllite clasts has produced a conglomerate with an apparent schistosity resulting from imbricate clast alignment. The matrix is dark to medium green, fine grained, and composed partly of eroded Belt sediments and partly of pyroclastic tuff material (Campbell and Loofbourow 1962). The monotonous green color and the lack of a fining-upwards sequence makes correlation within the unit virtually impossible.

The conglomerate is conformably overlain by the Huckleberry lavas, which are generally basaltic in composition. This unit is composed of massive flows with a few interbedded glassy and tuffaceous lenses, and has a maximum thickness of approximately 800 meters. These flows are only present to the north of the map area.

**Intrusives**

The Deer Trail series has been intruded by a Mesozoic quartz monzonitic to granodioritic batholith termed the Loon Lake batholith (Fig. 2-1). The batholith was emplaced in late Jurassic or early Cretaceous times and had been unroofed by the Tertiary (Waters and Krauskopf 1941). While the main body of the batholith is composed of quartz monzonite and granodiorite, some small granitic bodies and high-level rhyolitic intrusions, presumably apophyses of the main body, are present within the surrounding metasediments.

Within the map area the intrusion is generally light grey to pink in color and contains black biotite flakes up to 5 mm in diameter. It is usually medium grained but may range in texture from rhyolitic to porphyritic, sometimes with orthoclase phenocrysts up to 5 cm in length. The batholith, often less resistant to weathering than the surrounding metasediments, forms low-lying flat areas and is well exposed only along streams and rivers (Campbell and Loofbourow 1962).

Diabase dykes and sills are scattered throughout the Deer Trail series, though all are too small to show on the map. These dykes are not known to cross-cut any rocks younger than the Huckleberry conglomerate, and are thus presumed to be of Precambrian age. Campbell and Loofbourow (1962) feel that they may have acted as feeders and outlets for the basaltic flows which overlie the Huckleberry conglomerate.

## D. STRUCTURAL GEOLOGY

### Folding

The Deer Trail series has undergone one major and possibly two minor periods of folding. The axial traces of the major, and oldest, set of folds, $F_1$, are north plunging and trend approximately 20° to 40° E of N, coincident with the general strike of bedding in the area. These folds are large-scale, tight anticlines and synclines. The west limbs of the anticlines and east limbs of the synclines are locally overturned (Yates *et al.* 1966). The map area is completely within an overturned panel.

The axial traces of the second set of folds, $F_2$, parallel those of the first phase and may merely be minor parasitic folds associated with $F_1$. These folds have folded the limbs of the $F_1$ folds and produced highly variable dips within and between the formations of the Deer Trail series (Fyles and Hewlet 1959). The third set of folds, $F_3$, trend approximately 100° to 130° E of N, almost perpendicular to the axes of the $F_1$ and $F_2$ folds, and have kinked the limbs of the earlier folds (Fig. 2-1).

The $F_1$ and $F_2$ folds developed approximately 200 Ma ago. The $F_3$ folds are younger than $F_1$, $F_2$, but older than 100 Ma (Mills and Nordstrom 1973).

**Faulting**

Two major sets of faults are present in the region.

The first, the longitudinal set, is composed of high-angle faults which strike approximately 25° to 35° E of N, nearly parallel to the strike of bedding and the axes of the $F_1$ and $F_2$ folds. The longitudinal faults developed before the $F_3$ folds as the Queen & Seal fault, which passes southeast of the Queen & Seal mine, has been folded (Fig. 2-1). Another of these folded faults is located north of the map area.

The Queen & Seal fault, with a dip slip of nearly 500 meters, splits into two splays in the northern section of the map area. Both splays displace their eastern blocks upwards. The Queen & Seal fault is truncated by the Loon Lake batholith and is not recognized south of the intrusion (Campbell and Loofbourow 1962). This may be the result of poor mapping, the fault may actually continue and separate the McHale Slate from the Stensgar Dolomite and the Buffalo Hump Formation, explaining the peculiar pinch out of the Stensgar Dolomite in that area.

A second set of faults, the transverse, cut diagonally across the trend of the Deer Trail series and exhibit near vertical dips and strikes of between 110° and 120° E of N, nearly parallel to the axes of the $F_3$ folds. Their strike slip sense of motion is right lateral, with a maximum displacement of 4000 meters (Mills 1977).

A point of interest is the fact that these faults have nearly identical orientations, and identical senses of motion, as those of the Osborn and Placer Creek faults of Idaho, which are two major lineaments of northern Idaho,which affect the Coeur d'Alene district.

## III. LOCAL GEOLOGY AND DEPOSIT DESCRIPTION

### A. HOST ROCKS OF THE DEPOSIT

The host rock of the Deer Trail veins is the Edna Dolomite. Within the mine, this unit is generally a dark grey to black silty dolostone, often containing stringers of silty or sandy material, as well as fine grained green-brown banded quartzite beds up to 4 meters thick. Several highly siliceous to cherty beds of light brown to grey colored dolomite are also present. Massive dark grey to black limestone units are common, and rare buff colored chalky units are also found. These chalky units seem to have formed when limey sections of Edna dolomite were altered by nearby intrusive bodies.

Within one to three meters of the veins the dolomite has been hydrothermally altered to a calc-silicate rich material. It is often dedolomitized and contains epidote, clinozoisite, zoisite, green biotite, quartz, calcite, and rare hematite and chlorite. The rock is generally a dark green color and is often highly sheared. This lithology is mistakenly listed as the 'argillite' host rock of the veins in several publications, including Moen (1976) and Mills (1977). Bedding in the mine strikes between 30° and 50° E of N, and dips range from 80° northwest to 70° southeast. All east dipping beds are overturned.

Within one to ten centimeters of the of the veins the dolomite has been highly altered to a light grey rock. This material is rich in quartz and calcite and contains minor kaolinite, muscovite, hematite and pyrite. All green biotite has been destroyed, possibly indicating that Mg was removed by the hydrothermal fluids.

The Edna Dolomite has also been locally metamorphosed by intruding plugs, dykes and sills. Intrusions are often surrounded by an aureole of hornfels or marble, depending upon the original rock type. These hornfels-marble aureoles contain calcite, epidote, amphibole, biotite, chlorite and, rarely, tourmaline. Small localized skarns contain calcite, garnet, pyrite, epidote and minor tourmaline.

## B. INTRUSIONS

Intrusions encountered in the mine range from granodioritic to granitic in composition. Their color ranges from light yellow-green, in the case of altered rocks, to medium- and dark-green in the unaltered rock. Biotite in the altered intrusives has been altered to clay minerals. Most altered material is found in or near faults or shear zones, which may have acted as channels for the altering fluids.

Intrusives have never been observed to cut the veins, except in the case of faulted contacts, and there is no evidence of thermal metamorphism of the veins near plugs, dykes, or sills. Veins do cut the diabase dykes, and these dykes have subsequently been altered to a rock which looks very similar to the altered dolomitic wall rock, though it is less severely jointed and sheared than the dolomite. Diabase dykes cut both intrusives and the Edna dolomite. These dykes bear no obvious structural relationship to the older intrusive bodies, though they may represent the last stages of activity of the intrusive system.

Most of the intrusions are medium grained, but some very fine grained porphyritic sills and dykes are present. These fine grained intrusives, which generally occur as bands within coarser grained sills or dykes, are composed of 1 to 5 mm biotite flakes and 5 to 10 mm green feldspar phenocrysts within a dark green, very fine grained to glassy matrix. Pegmatitic stringers are also present, though these are quite rare.

## C. FAULTS

### Parallel Faults

Two major fault sets are present within the mine (Fig. 3-1). The first set is composed of steeply dipping faults which strike between 30° and 40° E of N, nearly parallel to the strike of bedding. These shall be refered to as the parallel fault set.

The most important parallel fault, the Hoodoo-Madre fault, has a strike of 40° E of N and dips 80° to 85° northwest. Its dip slip motion has displaced the northeast side up 21 meters, its strike slip is right lateral. This fault cuts the Madre vein approximately 30 meters (vein length) above the main Madre haulageway. The Hoodoo mine lies within the upthrown block (Fig. 3-2).

### Cut-Off Faults

Faults of the second set strike 110° to 120° E of N, almost perpendicular to the strike of bedding, and will be referred to as cut-off faults. These faults are near-vertical, dominantly strike slip faults, with right lateral displacement, though an unknown component of dip slip motion has also occurred.

The largest of the cut-off faults is the Deer Trail fault. This fault is actually a system of faults, or a shear zone, with a width of at least 45 meters. The southwest end of the Madre vein is cut by this fault on both the Hoodoo and the Madre levels of the mine (Fig. 3-2). The Deer Trail fault has a right lateral displacement of at least 30 meters, possibly much more. A large vein block within this fault zone has been displaced 10 to 15 meters to the west (right), and has undergone clockwise rotation. The degree of rotation of the block increases with distance into the fault zone, indicating that at least part of the lateral motion was taken up by shearing. A second cut-off fault truncates the vein at the northwest edge of the main Madre stope. It offsets the vein approximately 10 meters right laterally and brings it into contact with an altered granitic body.

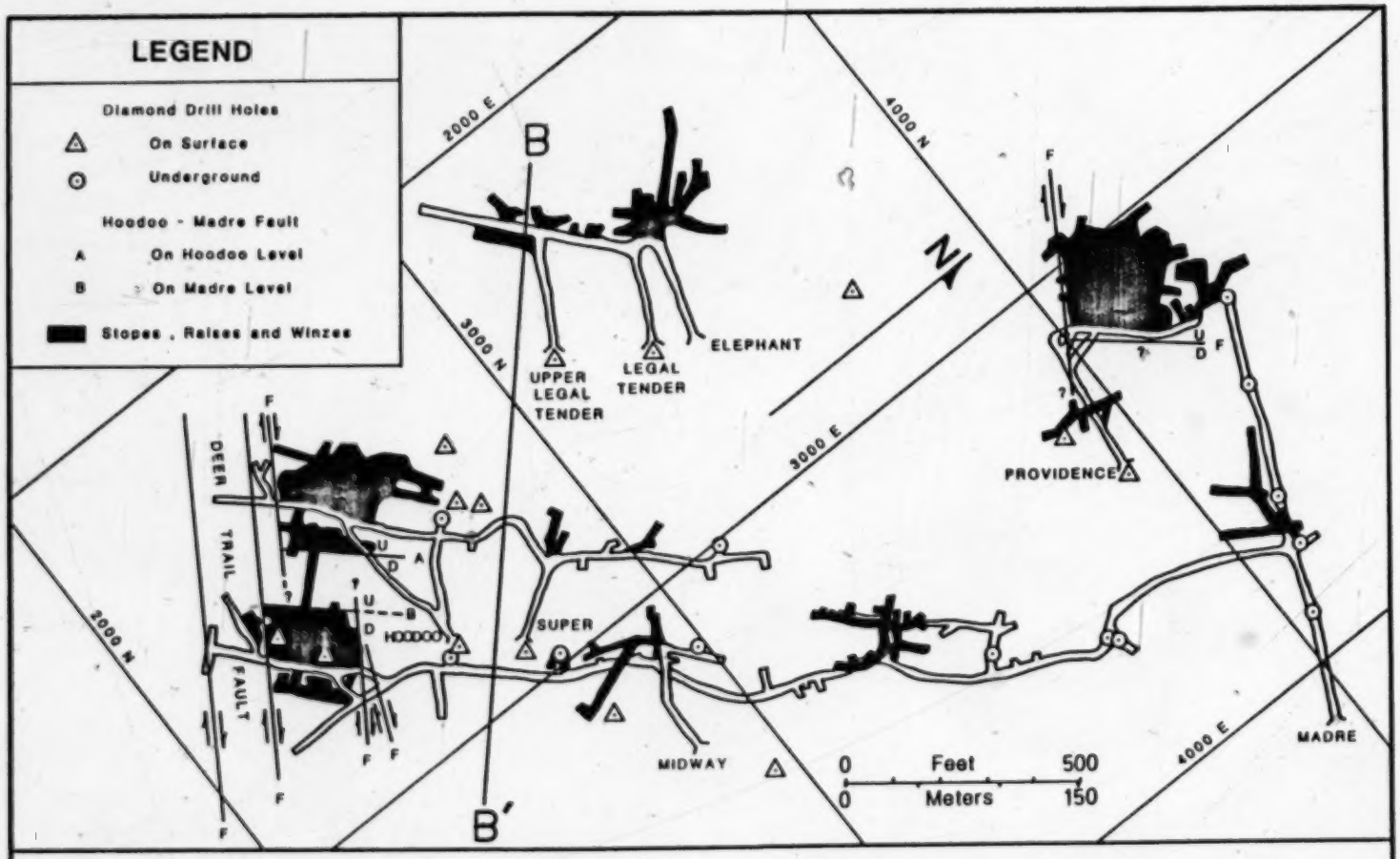


FIG. 3-1 Plan View - Mines Of The Deer Trail District with faults and drill hole locations

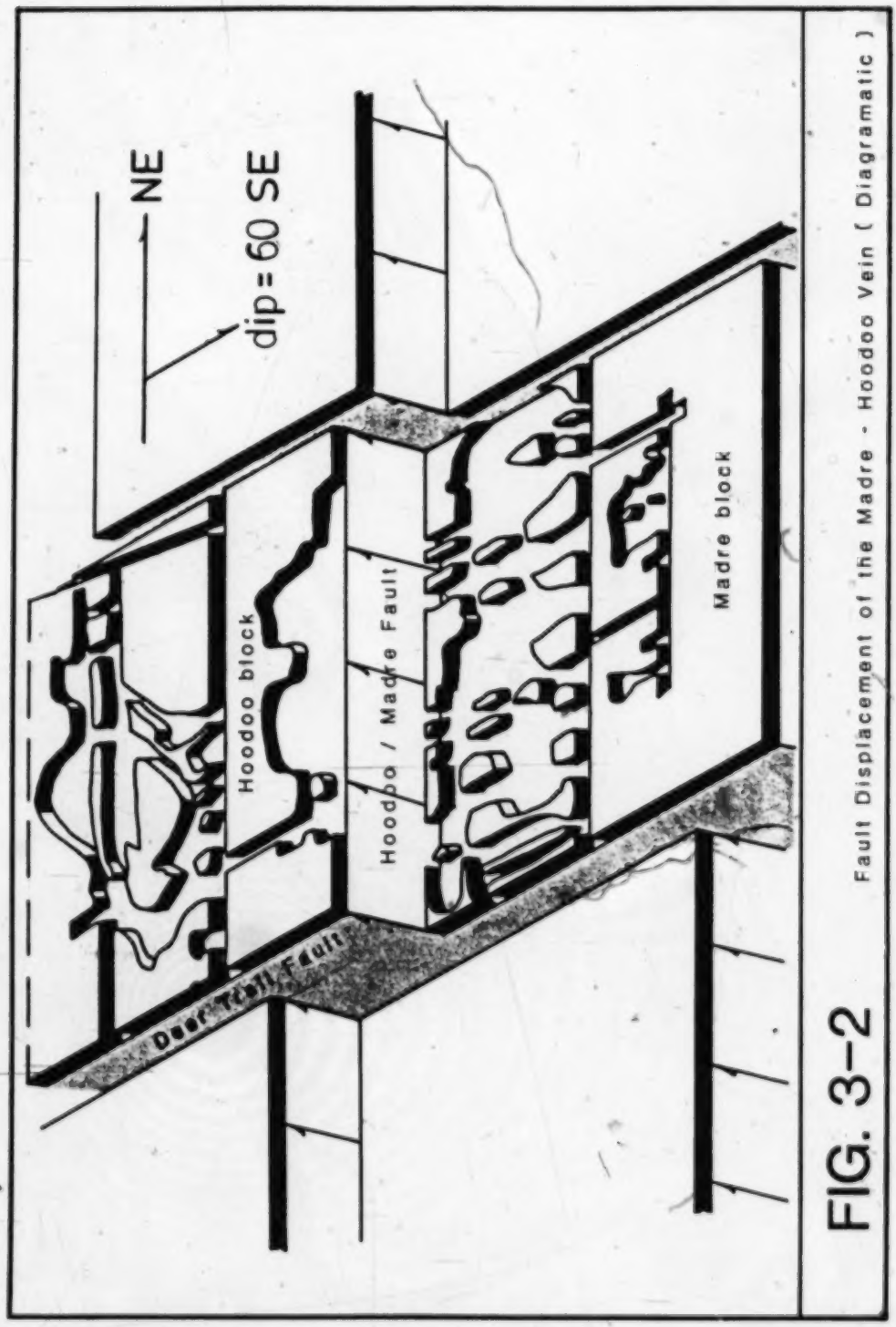


FIG. 3–2 Fault Displacement of the Madre - Hoodoo Vein ( Diagramatic )

The parallel and cut-off fault sets are very nearly parallel to the aforementioned longitudinal and transverse fault sets respectively. They are not, however, members of these two sets. The cut-off and parallel fault sets both cut intrusive bodies, and are therefore much younger than the longitudinal and transverse faults, both of which are truncated by the Loon Lake batholith. The faults present in the mine may be completely unrelated to the two major sets, or they may have formed through reactivation of older faults. This seems more likely to be the case, as it is highly improbable that that two completely unrelated fault sets would have such similar orientations. (Table 3-1)

**Table 3-1**

**Sequence of major events in the development of the Deer Trail district.**

| Event No. | Event | Approximate age of event |
|---|---|---|
| 1 | Deposition of Belt sediments | 1700 to 1400 Ma |
| 2 | Extrusion of Huckleberry lavas | > about 600 Ma |
| 3 | Initial folding event, $F_1$, (and $F_2$?)[1] | 200 Ma |
| 4 | Longitudinal faulting | ----- |
| 5 | Transverse faulting | ----- |
| 6 | Second folding event, $F_3$ | >100 Ma |
| 7 | Emplacement of the Loon Lake batholith | 100 - 80 Ma |
| 8 | Formation of the Deer Trail veins | ----- |
| 9 | Parallel faulting[2] | ----- |
| 10 | Perpendicular faulting[2] | ----- |

[1] - $F_1$ and $F_2$ folds may have formed contemporaneously.

[2] - Parallel and perpendicular faults probably represent reactivated longitudinal and transverse faults.

## D. DEPOSIT DESCRIPTION

There are at least two major Zn-Pb-Ag veins in the Deer Trail mine area, as indicated by both underground exploration and the data from numerous diamond drill holes. Some 56 holes have been drilled in the mine area in recent years, both from the surface and from underground stations. Figure 3-3 was produced from information from 31 of these drill holes. Data from the remaining 25 holes were either unreliable or nonexistant.

### Madre Vein

The Madre vein has been extensively mined on both the Madre and Hoodoo levels. The vein strikes approximately 40° to 50° E of N and dips 55° to 65° to the southeast. The main ore body has a strike length of over 700 meters, a width ranging from 0.2 to 2 meters but averaging approximately 0.7 meters, and a vertical extent of at least 150 meters as measured along the vein from the top of the Hoodoo stopes to the lowest diamond drill hole intersection. Its average Ag grade is 300 to 600 g/t ( 10 to 20 oz./ton), and may reach 6000 to 9000 g/t (200-300 oz/ton) in rich pods and shoots.

### The Elephant Vein

The second major ore body is hosted within the Elephant vein, which may represent a faulted-off section of the Madre vein or an entirely separate entity. It was developed at the turn of the century by the Elephant and Legal Tender mines, along with numerous smaller mines. It strikes parallel to the Madre vein but dips only 25° to 30° southeast, much shallower than the Madre vein. Its average width is approximately 0.3 meters, though pods with widths of up to 2.5 meters have been reported (Thurmond 1928). The lateral extent of the Elephant vein ore body is over 500 meters and it extends to a depth of approximately 125 meters, as measured along the vein.

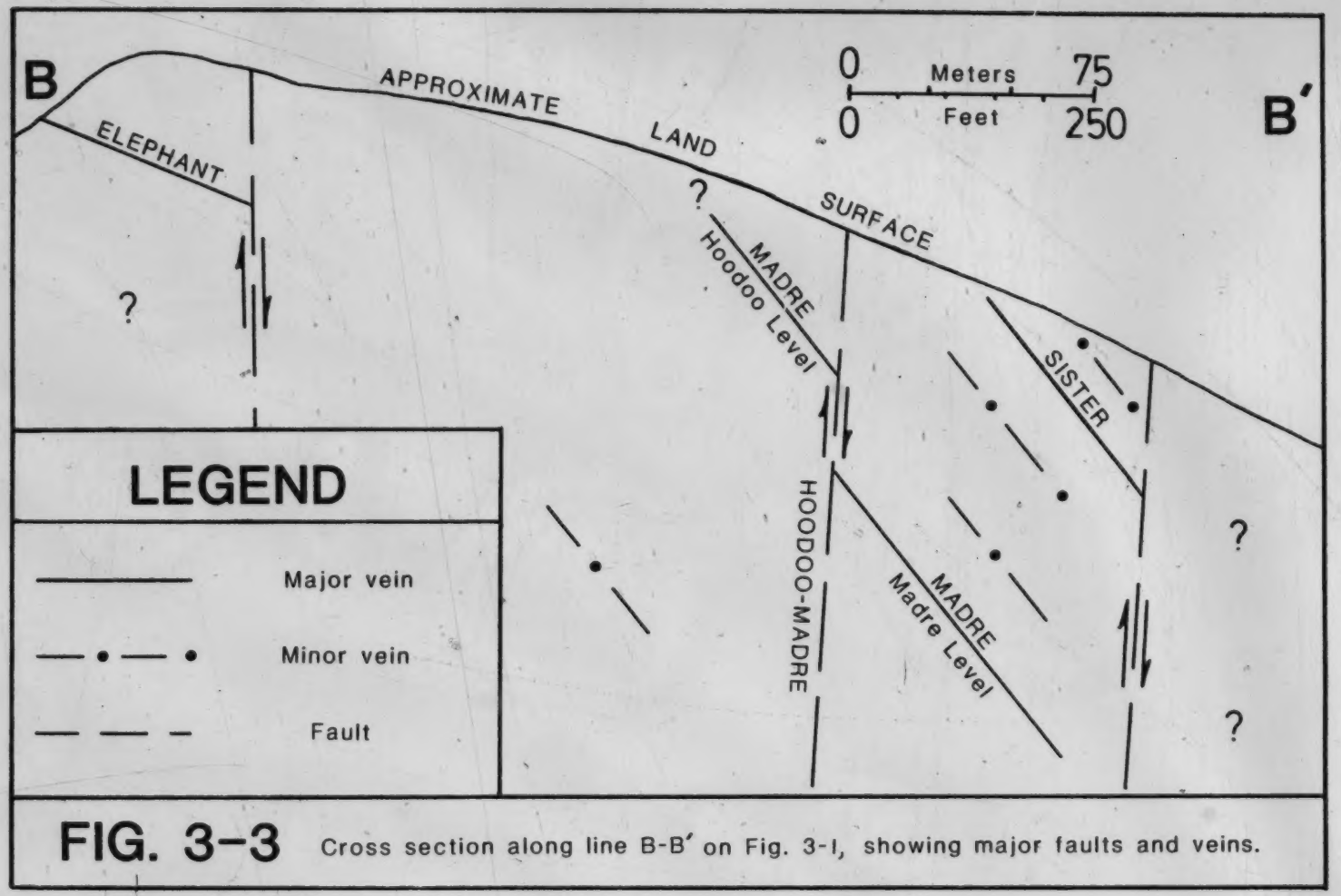


**FIG. 3-3** Cross section along line B-B′ on Fig. 3-1, showing major faults and veins.

Due to its proximity to the surface, the vein has been extensively weathered, resulting in the formation of Ag-rich supergene deposits. These deposits usually occurred as pods or stringers containing native silver, chlorargyrite and acanthite, as well as azurite, malachite, galena and sphalerite. The Ag grades of these pods were very high, probably averaging almost 3000 to 6000 g/t (100-200 oz/ton). Some pods had grades of up to 150000 g/t (5000 oz/ton).

For economic reasons only the very Ag-rich vein material was hand cobbed and shipped to the smelter by mule train. The mine cut off grade was approximately 1500 to 2400 g/t (50 to 80 oz/ton) and old dumps may contain up to 450 g/t (15 oz/ton) Ag.

**Sister Vein**

A third vein, called the Sister Vein, has also been discovered (Fig. 3-3). It may actually be a faulted off section of the Madre vein which has been displaced by a perpendicular fault. This vein is parallel to the other veins in the area and, like the Madre vein, appears to dip southeast at approximately 60°. It has been intersected in two diamond drill holes where grades of 1100 g/t and 126 g/t (36.7 oz/t and 4.2 oz/t) over 30 cm were found. Some exploration of this vein was done, but the drift driven to intersect the vein encountered only small veinlets with slight mineralization and low silver values. The main mineralized zone of the Sister Vein may lie above the explored area, but no work has been done to investigate this possibility.

**Replacement bodies**

Limestone and dolomite adjacent to the veins sometimes hosts small sulfide replacement bodies. These replacement bodies contain disseminated sphalerite, galena, quartz, pyrite and chalcopyrite, but their low silver grade and small size makes it impractical to mine them.

## IV. VEIN PETROGENESIS, MINERALOGY AND PARAGENESIS

### A. BACKGROUND AND METHODS

Each depositional stage in the formation of the Deer Trail veins has a distinct mineralogy. Quartz is always the dominant mineral, comprising 80-100 modal% of the pre-ore stage, 30-70% of the ore stage and 80-95% of the post-ore stage material.

A study, involving 26 polished sections of vein material, was done in order to identify the opaque minerals and to determine the paragenetic sequence of each stage and the veins as a whole. Opaque mineral identification was accomplished through observation of the reflected light characteristics of each mineral, including its color, bireflectance, anisotropy and percent reflectance at 547 angstroms. In addition, a Nomarsky phase interference contrast filter was used to determine the relative polishing hardnesses of adjacent minerals. Transparent minerals were identified in thin section and, to a limited extent, through analysis with the electron microprobe.

Many of the sulfosalts were susceptible to light etching and could thus be roughly identified. As all sulfosalts have very similar optical properties, however, it was sometimes impossible to identify the specific sulfosalt species by simple microscopic methods. To ensure proper identification of the sulfosalts, and other minerals of interest, they were analysed with the energy dispersive analysis system on an EEDS-II electron microprobe. The inhouse software program, EDATA2, was used to calculate the composition of each mineral from its X-ray spectrum. In cases were the analysis was the sole method of mineral identification only those analyses with element totals between 96% and 104% were used, to ensure proper identification. These rather large errors were deemed acceptable as the soft sulfosalts, often in the form of inclusions or grains within harder sulfides, polished down excessively and often had non-planar surfaces with the result that analytical results were often less than perfect.

## B. VEIN PETROGENESIS AND MINERALOGY

All veins in the Deer Trail district appear to have formed through the filling of dilatent fractures by quartz, sulfides and other hydrothermal minerals. This vein filling took place in three stages; the pre-ore stage, the ore stage and the post-ore stage. The pre-ore stage was typified by the deposition of quartz and pyrite at the outer edges of the veins. During the ore stage quartz and the major sulfide minerals were deposited, and the post ore stage was dominated by fracture infilling and overgrowths. A study of the vein mineralogy provided details concerning the depositional sequence and mineralogy of each stage. Little variation in the mineral content of the vein takes place with varying depth of formation. Depositional conditions thus seem to have been stable over a significant vertical column, at least 200 meters, indicating that all deposition took place in a deep portion of the vein system.

Vein fill may be broken down into three major, and one minor, catagories; gangue minerals, non-Ag bearing opaque minerals, Ag-bearing opaque minerals and minor native elements.

### Gangue Minerals

In the following sections the term 'major' is used to describe a mineral comprising over 5% of the material deposited during a stage. 'Minor' refers to a mineral comprising less than 5% of the material deposited during any stage.

#### Quartz

Quartz was deposited throughout all stages of vein formation and is the dominant gangue mineral in all veins. In the pre-ore stage it formed cockscomb quartz of clear to milky crystals up to 10 cm in length. Ore stage quartz is massive milky material which is commonly intergrown with sulfides. Post-ore stage quartz is in the form of thin overgrowths and fracture infill. Most of the quartz contains abundant, though small, fluid inclusions.

**Calcite**

Calcite is a minor gangue mineral. It is present in pre-ore stage material where it is found intergrown with quartz. In ore stage material it occurs as small inclusions, usually less than one mm in diameter, in quartz and sulfides. During the post-ore stage, where it was most common, it was deposited as fracture infill or as a light pink, coarse grained, cavity fill.

**Barite**

Barite is found only in material deposited during the later part of the ore stage. It occurs as tiny inclusions, generally less than 50 $\mu$m in diameter, within sulfides and is associated with calcite blebs and small quartz crystal inclusions.

**Adularia**

This mineral is rare and is found intergrown with quartz in pre-ore stage material. It is also present as fracture infill deposited during the post-ore stage.

**Opaque Minerals : Non Silver-Bearing**

**Sphalerite**

The most common sulfide in the Deer Trail veins is sphalerite. Its color ranges from medium- to light-brown with the lighter material often exhibiting tints of yellow, red and green. Sphalerite composition is very consistent throughout the veins. Microprobe analysis indicates the presence of less than 0.8 wt.% Fe in all sphalerite samples analysed, while cadmium is present in concentrations of up to 0.5 wt.%, but is usually less than 0.2 wt.%. Sphalerite is commonly intergrown with galena, freibergite and quartz, but may also form distinct monomineralic bands. Early sphalerite was in equilibrium with pyrite but replaced quartz, while later sphalerite has often partially replaced pyrite. Sphalerite is rare in weathered sections of the vein as it has been nearly completely altered to smithsonite and hydrozincite, both of which are also present in deeper sections of the vein in the form of fracture filling or as coatings on broken surfaces.

**Galena**

The second most common sulfide in the veins is galena. It has a close association with sphalerite and generally forms coarse grained intergrowths along with sphalerite and, less commonly, freibergite. Galena may also occcur as monomineralic bands. It has often replaced pyrite, and occasionally sphalerite, though it generally appears to have been co-deposited with the sphalerite. Though galena is not a silver bearing mineral it often contains blebs of freibergite or other silver sulfides.

In weathered portions of the veins galena has been extensively altered to cerussite and little of the original galena remains.

**Pyrite**

Pyrite is a relatively rare mineral in the Deer Trail veins. It occurs as small cubes up to 3 mm across which are intergrown with pre-ore stage quartz, or as veinlets in ore stage sphalerite. It is also present as a fracture infill and as crustiform overgrowths associated with quartz, both of which were deposited during the post-ore stage. Early pyrite cubes are often partially or completely replaced by galena and/or sphalerite and may only remain as rounded cores within grains of these two minerals.

**Chalcopyrite**

This mineral is even rarer than pyrite and is closly associated with freibergite and other silver sulfides. It generally occurs as rims between quartz and freibergite or as inclusions within freibergite and galena. Very rarely it also occurs as late fracture filling veinlets within sphalerite and galena. In weathered zones all the chalcopyrite has been altered to malachite and azurite.

**Opaque Minerals : Silver-Bearing**

Silver in the Deer Trail veins is generally contained in sulfosalt minerals. The antimony and arsenic in these minerals act as metals, not as replacements for sulfur as they do in other minerals. In sulfosalts from the Deer Trail veins antimony is by far the more dominant of the two elements. The maximum arsenic content in any of the sulfosalts is approximately 3.0 wt.%.

**Tetrahedrite** ($(Fe,Cu)_{12}Sb_4S_{13}$)

**Freibergite** ($(Ag,Cu)_{12}Sb_4S_{13}$

Freibergite is the main silver-bearing mineral in the Deer Trail veins. It is distributed throughout the deposit as blebs within galena and sphalerite and as individual grains and bodies associated with galena and medium brown sphalerite. It also occurs as monomineralic bands in banded sections of the vein, where it has sometimes been observed to replace galena.

Microprobe analysis of the freibergite indicates that the As content is never greater than 3.3 wt.%. Zn content may reach up to 7.5 wt.% while the Fe content is generally less than 1.0 wt.%. The silver content is generally between 16 and 20 wt.%, though two grains had values of over 24 wt.%. As freibergite can only accomodate approximately 18 wt.% Ag into its lattice without distortion (Hurlbut and Klein 1977) these high values may reflect poor sample polish or the presence of silver-rich inclusions. Table 4-1 shows the variations in element content of several representative freibergite samples.

In weathered sections of the vein the freibergite has been extensively altered to malachite and azurite. In one case the only remaining freibergite was in the form of tiny spheres, 1 mm or less in diameter, within a matrix of altered material. Weathering of the freibergite had lowered the Cu content, and raised the Sb, Ag and Zn content of the alteration product, which may have been the Zn-bearing equivalent of samsonite, i.e., ($Ag_4ZnSb_2S_6$) as opposed to $Ag_4MnSb_2S_6$. No mention of such a mineral has been found in the literature, although Ramdhor (1980) does mention a similar weathering phenomenon in freibergite where the freibergite spheres were surrounded by an unknown material.

**Table 4-1**

**Electron microprobe analyses of freibergite from the Deer Trail Mine, Washington, U.S.A.**

| Sample No. | 14 | 15 | 45 | 45 | 54 | 59 | 65 | 69 | 69 |
|---|---|---|---|---|---|---|---|---|---|
| Wt% Ag | 24.51 | 24.10 | 18.35 | 18.56 | 20.38 | 19.37 | 16.59 | 19.00 | 17.53 |
| " Cu | 20.40 | 19.00 | 21.30 | 19.81 | 23.94 | 24.16 | 26.09 | 24.19 | 25.21 |
| " Fe | 0.66 | 2.97 | 0.88 | 1.83 | 0.99 | 0.45 | 0.59 | 1.12 | 1.19 |
| " Zn | 7.34 | 6.15 | 4.65 | 4.42 | 5.87 | 6.60 | 6.79 | 6.04 | 6.30 |
| " Mg | --- | --- | 0.07 | 0.38 | --- | --- | --- | --- | --- |
| " Sb | 22.17 | 23.18 | 28.91 | 27.48 | 24.71 | 26.76 | 27.19 | 26.59 | 26.78 |
| " As | 3.24 | 1.92 | 1.37 | 2.28 | 1.83 | 0.91 | 0.40 | 0.85 | 0.65 |
| " S | 21.69 | 22.69 | 24.48 | 25.26 | 22.27 | 21.74 | 22.34 | 22.22 | 22.34 |
| Recalculated Total | 100.01 | 100.01 | 100.01 | 100.02 | 99.99 | 99.99 | 99.98 | 100.01 | 100.00 |
| Original Sum | 103.68 | 100.67 | 100.16 | 99.18 | 97.38 | 101.77 | 100.68 | 98.37 | 100.21 |

--- = Less than 0.05 Wt%. Original sums outside the 100.0 ± 1.50 range probably caused by poorly polished sample surfaces. Ag values greater than approximately 20% probably also reflect poor sample finish.

**Polybasite** ($(Ag,Cu)_{16}Sb_2S_{11}$)

Polybasite is the second most abundant silver mineral in the deposit and occurs as blebs within freibergite or as individual grains up to 200$\mu$m in diameter. Its elemental content ranges between 69.7 and 73.5 wt.% Ag; 3.4 to 5.9 wt.% Cu; 0 to 2.3 wt.% As; 6.4 to 9.7 wt.% Sb; and 0 to 1.0 wt.% Zn.

**Acanthite** ($Ag_2S$)

Acanthite is present as separate grains or in the form of intergrown interlocking laths along with quartz and freibergite. It may contain up to 5.0 wt.% Zn and 1.0 wt.% Cu, with traces of Fe. Acanthite is intimately associated with the other silver minerals and, like freibergite, has occasionally replaced galena.

Acanthite is also present in weathered vein material, both as a primary mineral and as an alteration product of freibergite. The acanthite produced by weathering has a lower copper and zinc content than does primary acanthite and occurs as rims around weathered freibergite grains.

**Stephanite** ($Ag_5SbS_4$)

Stephanite is a minor silver phase which occurs as small blebs within freibergite, or as a separate phase associated with acanthite and freibergite. It contains less than 0.5 wt.% Cu and less than 1.0 wt.% Zn.

**Native Elements**

Though very rare, native silver is present in a few of the polished sections of vein material. It occurs as tiny irregular masses in unaltered material and is closely associated with acanthite. In altered material it occurs as separate blebs and as rims around altered freibergite, and other sulfosalt, grains.

Native copper is rare and present only as rims around weathered freibergite grains. It is often associated with native silver.

A single grain of native gold (electrum) was found in a polished section of weathered vein material. It was hosted in an altered freibergite matrix and may have been the product of supergene enrichment. Its composition was approximately 65% gold, 30% silver and 5% copper.

## C. PARAGENETIC SEQUENCE AND DISCUSSION

An idealized paragenetic sequence of the formation the minerals of the Deer Trail vein is given in Figure 4-1. Major mineral deposition is indicated by solid lines, while dashed lines indicate the deposition of minor minerals. The diagram is intended to show only the relative timing and importance of each mineral, not the absolute timing of events. Alteration products of earlier species have been placed in the last column of the diagram, those labeled with a '*' were not observed in this study but were listed in earlier reports and have been included for the sake of completeness.

The three stages of vein formation, defined by mineralogy and form, are as follows:

1. Pre-ore stage ; saw the deposition of quartz, calcite, adularia and pyrite. Cockscomb quartz crystals up to 10 cm in length are often present along the outer edges of the vein. Approximately 15% of the total vein material was deposited during this stage, which probably represents the first activity within the hydrothermal system. The large size of the quartz crystals formed during this stage may indicate that deposition of material was slow and that faults were inactive, allowing the crystals to grow undamaged.

2. Ore stage ; was typified by the deposition of abundant milky quartz, sphalerite and galena, along with freibergite, other sulfosalts, acanthite, and minor chalcopyrite, pyrite, calcite and barite. Ore stage material occurs in three basic forms and textures, making up approximately 80% of the all vein material.

   The first form is massive quartz with knots of sulfides suspended within it. This material is usually found in sections of the vein with widths greater than 1.0 m, and may contain small vugs, usually less than 0.3 mm in diameter.

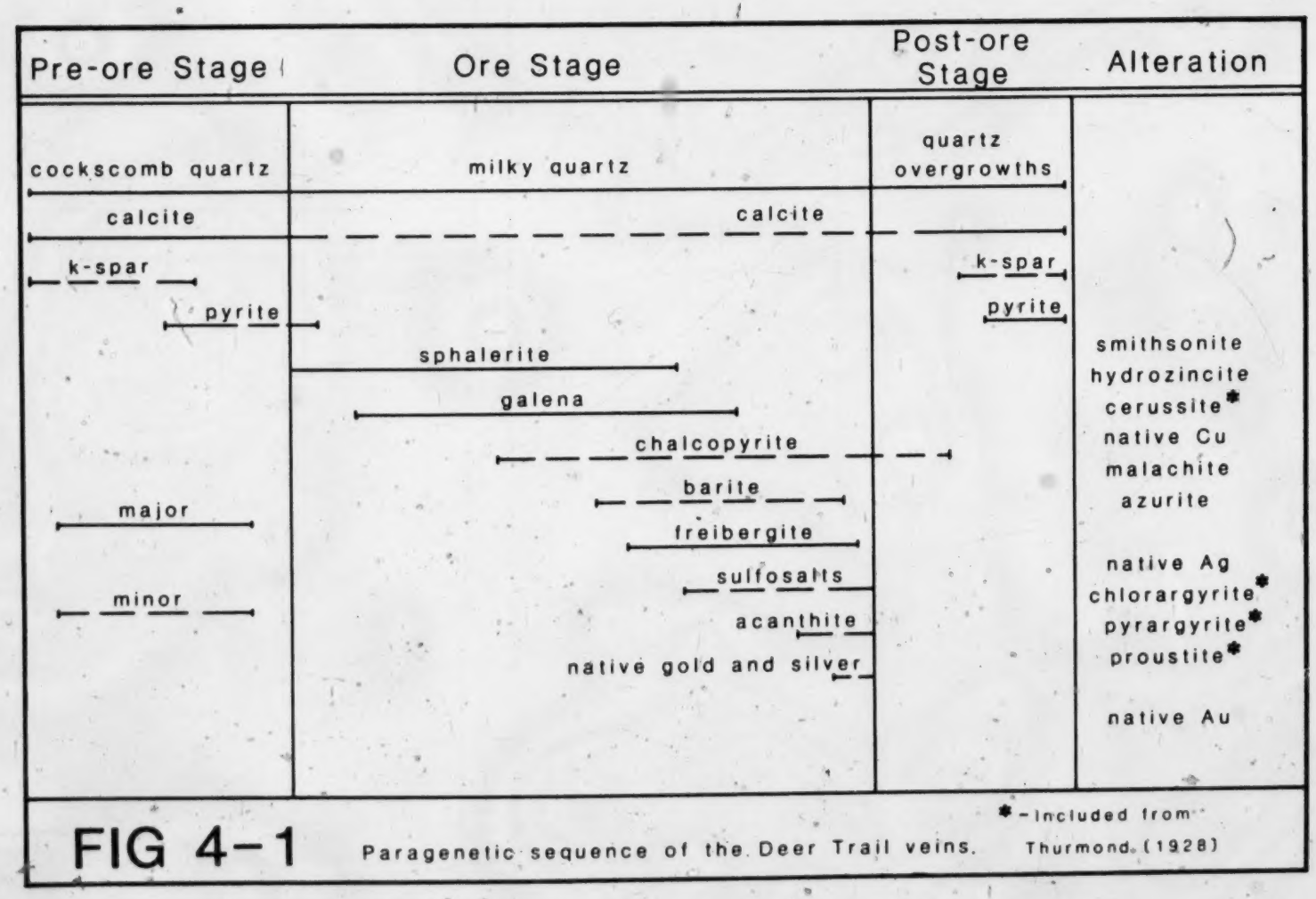


**FIG 4-1** Paragenetic sequence of the Deer Trail veins.

The second major form is intermixed quartz and sulfides in approximately equal amounts. This material seems to be a mass of intergrown plates of different minerals with no continuous bands or mineral zones and is found throughout the vein system.

The third major type is banded vein material which exhibits a crustiform texture and contains separate bands of quartz and sulfides. These bands may range from less than 1.0 cm to over 5.0 cm in width. Sulfide bands may be either monomineralic or composed of intergrowths of sphalerite, galena and freibergite, which are in turn interlayered with quartz bands. This material is generally found in sections of the veins which are less than 0.5 m wide, though it is also present in wider sections. Although ore stage material shows distinct banding no depositional event or band of the minerals was continuous throughout the vein system. It is therefore impossible to correlate any band of sphalerite, for instance, with a corresponding band in the other side of a stope and correlation within the ore stage is impossible.

Some fault motion during this stage is indicated by the presence of breccias composed of wall rock and sulfide clasts, which have been cemented by later vein material. Free-floating wall rock fragments within the vein also indicate fault activity.

3. Post-ore stage ; was a volumetrically minor stage in which quartz and pyrite overgrowths were deposited on earlier quartz and sulfides. Also during this stage fractures in earlier material were filled with quartz, calcite and adularia. The post-ore stage deposited only approximately 5% of the total vein material.

It is impossible to discern how much time elapsed between the end of one depositional stage and the beginning of another, but it appears that the pre-ore and ore stage represent a continuous depositional sequence, while post-ore stage material was deposited at some later time.

# V. FLUID INCLUSION STUDIES

## A. INTRODUCTION

Fluid inclusions are present in nearly all crystals deposited within a hydrothermal medium. During crystal growth minute droplets of the parent medium are trapped within the crystal, thus producing fluid inclusions. This trapping may occur through several mechanisms, including the capture of the parent fluid in surface irregularities and the healing of fluid-filled fractures. Inclusions are generally less than 1 mm in diameter, with the majority of them in the .001 - .01 mm range. They may contain a large variety of fluids depending solely upon the composition of the fluid from which the host was grown. Most inclusions are filled with a saline brine ranging anywhere from 0.1 to 50 wt.% NaCl equivalent (Roedder 1984). Inclusions may also contain liquid or gaseous $CO_2$, liquid or gaseous hydrocarbons, nitrogen gas or any combination of these, as well as NaCl-, KCl-, $MgCl_2$-, and $CaCl_2$-brines.

Several assumptions must be made if fluid inclusion data are to be used in any geothermometric, geobarometric or geochemical study. These are (Roedder 1979);

1. The fluid trapped upon sealing of the inclusion was a single, homogeneous phase.
2. The cavity in which the fluid is trapped does not change in volume after sealing.
3. Nothing is added to or lost from the inclusion after sealing.
4. The effects of pressure are insignificant or are known.
5. The origin of the inclusion is known.

If these assumptions are valid a fluid inclusion is, in effect, a time capsule which has preserved a sample of the host crystal's parent fluid. As such it may provide many clues about conditions during crystal growth, and the formation of any associated mineral deposit.

**Inclusion types and their recognition**

Fluid inclusions may be trapped through several mechanisms, including physical fracturing of the crystal during or after growth, chemical etching of the crystal, or simple overgrowth of material around a droplet on the surface of the crystal. Three main divisions are used in the classification of fluid inclusions.

1. **Primary Inclusions** - Primary inclusions are trapped during initial crystal growth, often along grain boundaries or in hopper-shaped faces. They are usually relatively large and occur as isolated sets or planar arrays outlining former crystal faces. Such inclusions provide information about conditions during initial crystal growth.
2. **Pseudo-secondary inclusions** - These inclusions form during the healing of cracks which develope during crystal growth. Pseudo-secondary inclusions generally occur as curved arrays and may be difficult to distinguish from secondary inclusions. If the array terminates at a former growth face within the crystal, it is of pseudo-secondary origin. These inclusions, like primary inclusions, provide data concerning the conditions and fluids present during initial crystal growth.
3. **Secondary inclusions** - These, like pseudo-secondary inclusions, form during the healing of fractures within the host crystal. They occur as curved arrays which reach the crystal surfaces, and transgress crystal boundaries, indicating that the fracture formed after crystal growth was complete. Such inclusions supply information about conditions after the crystal was formed and are of little use in studies whose purpose is to determine primary depositional conditions.

Roedder (1979) gives an exhaustive list of criteria which may be used to identify and segregate the three types of inclusions.

**Information available from fluid inclusion studies**

Fluid inclusion studies, such as heating and freezing tests, crushing tests and microscopic examination of daughter minerals, may provide important information concerning conditions and fluids present during crystal growth.

**Fluid Composition - Solvents, Solutes and Concentrations**

By finding the eutectic, or temperature of first melting, of the fluid in a brine-filled inclusion the nature of the solute in solution may be determined. The brine may contain NaCl, KCl, $MgCl_2$, or $CaCl_2$, each of which has its own unique eutectic. It may also contain a mixture of two or more salts, thus making salinity and composition determinations more complex.

Freezing-point depression studies provide the temperature of final melting, or initial freezing, which allows the calculation of fluid salinity in wt.% NaCl equivalent. Freezing point studies are also used to determine the presence of $CO_2$, $CH_4$, $N_2$ and other gaseous or liquid substances.

**Temperature and Pressure of Trapping**

By heating the fluid inclusion until it has homogenized to a single phase and applying an appropriate pressure correction, the original trapping temperature of the fluid may be calculated. If the system was boiling at the time of trapping no temperature correction is necesary. The determination of an appropriate pressure correction is often difficult and very rarely precise. This problem is avoided if two sets of primary inclusions, each filled with fluids of different compressibility but trapped under identical conditions, are present.

Separate $CO_2$ and water (brine) inclusions are often used in this situation. They allow the simultaneous calculation of the temperature and pressure at which the inclusion was trapped. The accuracy of this calculation depends upon the slope difference between the $CO_2$ and $H_2O$ isochors and the accuracy of fluid inclusion homogenization temperature determinations of the inclusion homogenization temperatures.

## B. FLUID INCLUSIONS IN THE DEER TRAIL VEINS

Inclusions from the Madre vein (lower set) were studied along with inclusions from the Elephant vein (upper set). Madre and Elephant vein inclusions are segregated in tables and diagrams but not in the text. Inclusions from both veins are generally small, rarely exceeding 20 $\mu$m in diameter. The largest primary inclusions found were 50-70 $\mu$m in diameter and were hosted in light-colored sphalerite and this made it very difficult to find inclusions which were suitable for testing. As a result the number of inclusions studied, 49, was not great.

Three major types of inclusions were recognized in this study (Fig. 5-1). All vapor data herein are given in volume percent at 23°C, the ambient laboratory temperature.

1. Simple liquid - rich brine inclusions:

   a) Primary inclusions with 10-20% vapor.

   b) Pseudo-secondary inclusions and secondary inclusions with 5-15% vapor.

   c) Late secondary inclusions with 1-5% vapor (Formed after the post-ore stage of deposition).

2. Liquid - rich brine inclusions with up to 15 volume% $CO_2$, or up to 20 wt.%$CO_2$.

   These inclusions include primaries, pseudo-secondaries, and secondaries. The $CO_2/H_2O$ ratio was variable within the system but is consistent within single arrays or groups of inclusions. This indicates that $CO_2$ was dissolved in the brine and became immiscible on cooling, producing two phase inclusions from an originally homogeneous fluid.

3. $CO_2$ inclusions with approximately 20% vapor.

   These inclusions are a statistically minor phase in the system. Only two usable $CO_2$ inclusions were found, both from the upper vein. They are primary and were trapped coincidentally with liquid-rich (type 1) brine inclusions.

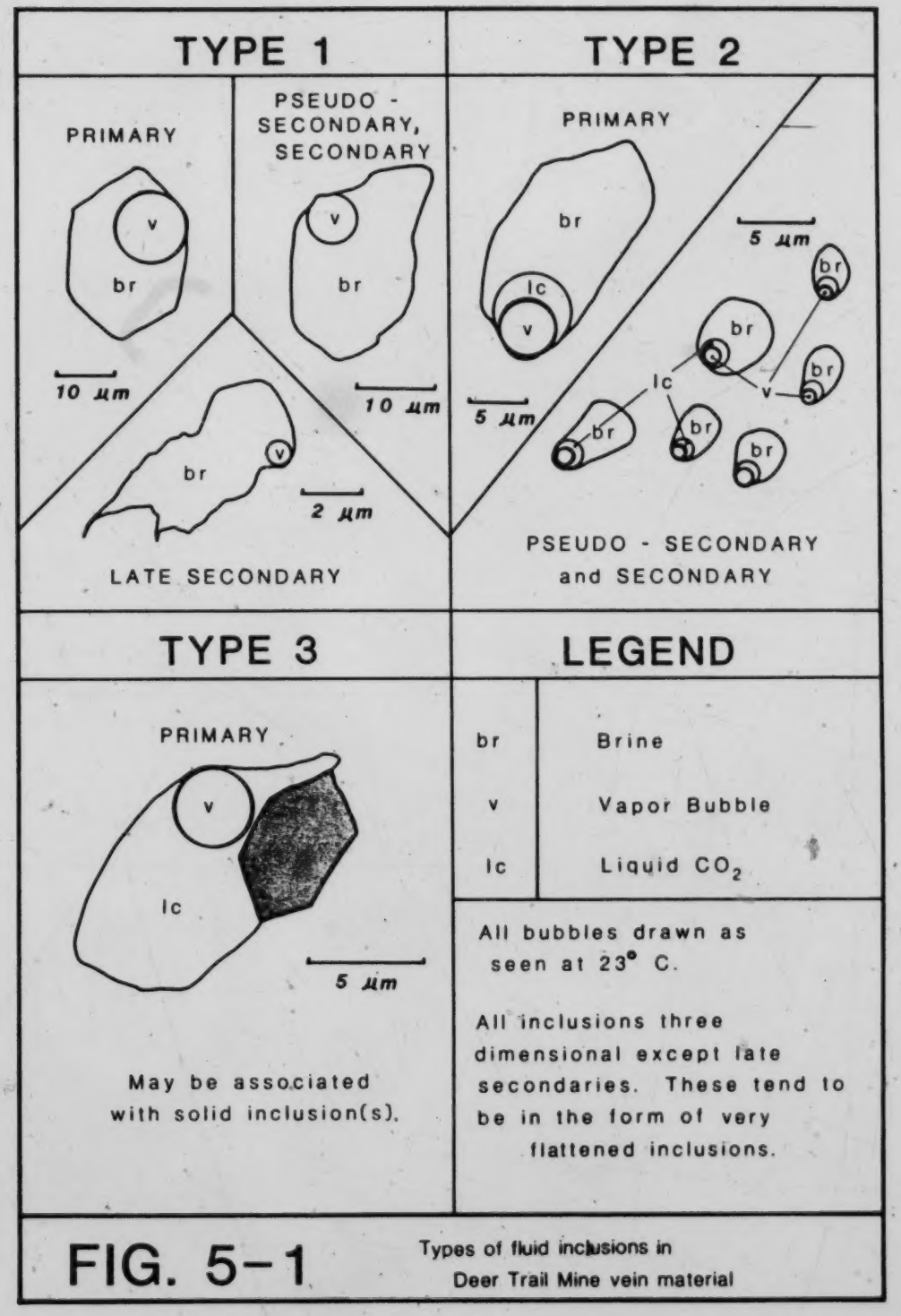


**FIG. 5-1** Types of fluid inclusions in Deer Trail Mine vein material

## C. TESTING METHODS AND RESULTS

### Freezing Tests

All inclusions were examined using a Chaixmeca model VT2-120 heating- and cooling-stage. Homogenization and salinity data are listed in Table 5-1.

**Eutectic** - The eutectic was measured by freezing the inclusion to approximately -60°C, then allowing it to warm until most of the ice had remelted. The inclusion was then slowly cooled to allow water ice to form around the remaining ice nucleus. This concentrated the salt from the original fluid into the remaining fluid and produced a brine whose salinity was high enough to measure the system's eutectic. The inclusion was then warmed at 0.3 to 0.4°C/minute until the first melt (eutectic) was reached. Recognizing this point was difficult at times and the data are scattered from -21°C to -14°C. The main group falls between -21°C and -18°C, which includes the eutectic for an NaCl solution at -20.9°C.

The mixed NaCl-KCl eutectic is -22.9°C and the other mixed and pure salt eutectics are well below this temperature. Since no eutectics below -21°C were observed, all inclusions were assumed to contain pure NaCl brines ± $CO_2$. This holds true for all primary, pseudo-secondary and secondary inclusions.

**Freezing point depression** - The degree of freezing point depression was determined by warming inclusions at 0.3 - 0.4°C per minute within 10°C of the freezing point, until all solids had been melted. The freezing point (last melt) was more easily recognized than the eutectic as it was often signaled by an abrupt rounding of the vapor bubble.

In a simple NaCl-$H_2O$ system the freezing point is controlled only by the salinity of the fluid. The higher the salinity of the fluid the greater the degree of freezing point depression. Knowing the freezing point of a fluid allows the calculation of its salinity by the equation:

$FP = .581855\ ws + 3.48896 \times 10^{-3}\ ws^2 + 4.314 \times 10^{-4}\ ws^3$ (Potter *et al.* 1978).

**Table 5-1**

**Results of freezing and heating tests on fluid inclusions from the Deer Trail Mine, Washington, U.S.A.**

| Inclusion No. | Host Mineral | Paragenetic Stage and location | Inclusion Type | Inclusion Content | Homogenization Temperature | Freezing Temperature | Wt.% NaCl equivalent |
|---|---|---|---|---|---|---|---|
| 10-1-1 | Quartz | O (L) | P | W-C | 209.1 | +7.7 c | 4.6 |
| -2 | " | " | PS | W | 202.3 | --- | --- |
| -3 | " | " | PS | W | 187.6 | --- | --- |
| -4 | " | " | PS | W | 196.6 | --- | --- |
| 12-1-1 | Quartz | O (L) | PS | W | 207.7 | --- | --- |
| -1a | " | " | PS | W | 210.7 | --- | --- |
| -2 | " | " | S | W | 120.2 | -0.8 i | 1.3 |
| 27-1-1 | Quartz | Pr (U) | P | W-C | 205.9 | +6.5 c | 6.9 |
| -1a | " | " | P | W | 203.0 | -4.7 i | 7.4 |
| -1b | " | " | P | W | 201.4 | -4.5 i | 7.2 |
| -1c | " | " | P | W | 204.8 | -4.3 i | 6.9 |
| -2 | " | " | P | C | 24.3 | --- | --- |
| -2a | " | " | P | C | 24.4 | --- | --- |
| 48-2-1 | Quartz | O (U) | P | W | 184.1 | --- | --- |
| -2 | " | " | PS | W | 160.2 | --- | --- |
| -3 | " | " | P | W | 162.0 | -2.9 i | 4.8 |

| | | | | | | | |
|---|---|---|---|---|---|---|---|
| -4 | " | " | PS | W | 157.4 | --- | --- |
| -5 | " | " | P | W | 185.0 | --- | --- |
| -6 | " | " | P | W-C | 186.5 | +7.1 c | 5.6 |
| | | | | | | | |
| 59-7-1 | Quartz | O (U) | P | W-C | 204.4 | +6.5 c | 6.9 |
| -2 | " | " | P | W-C | 201.1 | +7.3 c | 5.2 |
| -3 | " | " | P | W-C | 210.2 | +6.6 c | 6.4 |
| | | | | | | | |
| 60-1-1 | Sphalerite | O (L) | P | W-C | 192.9 | +5.8 c | 7.8 |
| -2 | " | " | S | W | 172.1 | --- | --- |
| | | | | | | | |
| 60-2-1 | Quartz | Pr (L) | P | W | 279.2 | -5.2 i | 8.2 |
| -2 | " | " | S | W | 170.1 | --- | --- |
| -2a | " | " | S | W | 164.4 | --- | --- |
| -5 | Sphalerite | O (L) | P | W | 196.7 | --- | --- |
| -6 | " | " | P | W | 194.5 | --- | --- |
| -7 | " | " | P | W | 206.1 | -3.5 i | 5.7 |
| | | | | | | | |
| 60-3-1 | Sphalerite | O (L) | PS | W-C | 175.8 | +7.0 c | 5.7 |
| -2 | " | " | PS | W-C | 175.2 | +6.6 c | 6.4 |
| | | | | | | | |
| 61-1-1 | Quartz | O (L) | PS | W-C | 205.5 | +7.5 c | 5.0 |
| -2 | " | " | P | W-C | 216.4 | +6.7 c | 6.2 |

| | | | | | | | |
|---|---|---|---|---|---|---|---|
| 62-3-1 | Quartz | Pr (L) | P | W | 285.0 | --- | --- |
| -2 | " | " | P | W | 297.4 | -5.1 i | 8.1 |
| -3 | " | " | S | W | 250.3 | -4.6 i | 7.3 |
| -4 | " | " | S | W | 129.6 | --- | --- |
| -5 | " | " | S | W | 134.1 | --- | --- |
| 63-2-1 | Quartz | O (L) | P | W-C | 244.5 | +5.9 c | 7.7 |
| -2 | " | " | PS | W-C | 234.2 | --- | --- |
| 65-1-1 | Quartz | PO (L) | P | W | 141.7 | -1.8 i | 3.0 |
| -2 | " | " | P | W | 144.1 | --- | --- |
| 66-3-1 | Quartz | O (U) | P | W-C | 196.1 | +7.7 c | 4.6 |
| -2 | " | " | PS | W | 150.1 | --- | --- |
| -3 | " | " | PS | W | 154.4 | --- | --- |
| -4 | " | " | S | W | 125.7 | -0.9 i | 1.5 |
| -5 | " | " | S | W | 122.3 | -0.6 i | 1.0 |
| -6 | " | " | S | W | 134.2 | --- | --- |

Pre-ore stage, Pr; ore stage, O; Post ore stage, PO. Primary inclusion, P; Pseudo-secondary inclusion, PS; Secondary inclusion, S.

**Lower vein set, (L); Upper vein set, (U). **Brine filled inclusion, W; Liquid $CO_2$ filled inclusion, C; Brine and liquid $CO_2$ filled inclusion, W-C.

Melting temperature of $CO_2$ clathrate, c; melting temperature of ice, i.

Where:

FP = Freezing point depression in degrees C

ws = the salinity of the fluid in wt.% NaCl equivalent.

This relatively simple relationship does not apply in the case of saturated or near-saturated brines. Cooling such a brine will result in the formation of $NaCl{\cdot}2H_2O$ (hydrohalite). Any inclusion containing hydrohalite will not melt completely until it has been warmed to -0.1°C, thus making it impossible to calculate salinity through this method. No hydrohalite was detected in any of the inclusions used in this study.

As stated above, this method is only applicable to a pure $NaCl{\cdot}H_2O$ system. Calculated salinities for type 1 and 2 inclusions which contained no visible $CO_2$ and exhibited no clathrate formation are listed in Table 5-1. The values range from approximately 1.0 to 1.5 wt.% for late secondary inclusions, and between approximately 4.5 and 8.5 wt.% NaCl equivalent for primary and pseudo-secondary inclusions from pre-ore and ore stage inclusions.

Fluid inclusions from the Deer Trail veins, however, did not generally contain pure NaCl brines. $CO_2$ was found in nearly 70% of the inclusions, either by direct observation of a separate liquid $CO_2$ phase or through detection of the $CO_2$ clathrate. This clathrate, $CO_2{\cdot}(5.75)H_2O$, forms upon cooling of inclusions containing both $CO_2$ and brine, usually at about -30°C (Collins 1979). During clathrate formation $CO_2$ molecules are trapped within an $H_2O$ lattice. No salt ions are tolerated within the clathrate matrix so any residual brine has a higher salinity than that of the original fluid. For example: An inclusion containing a brine with 5 mole% $CO_2$ and 10 wt.% NaCl will, upon formation of the $CO_2$ clathrate, contain a residual brine with 14.9 wt.% NaCl, i.e., an increase in salinity of almost 50% (Collins 1979 ; Hedenquist and Henley 1985).

Though such a high $CO_2$ content is unlikely to occur in natural fluid inclusion brines at room temperature or below, Malinin and Kurovskaya (1975) estimate that up to 2 mole% $CO_2$ may be present in 5-6wt.% NaCl brines at 25°C and 50 bars. If these data are correct, freezing point depression measurements on such inclusions would indicate salinities of 15-25% higher than was actually the case (Collins 1979).

As long as a brine is $CO_2$ saturated, the degree of freezing point depression is independant of the percentage of liquid $CO_2$ within the inclusion. Only the $CO_2$ in solution takes part in clathrate formation and no appreciable $CO_2$ goes into solution after the clathrate has formed, possibly because the clathrate acts as a barrier to the remaining $CO_2$ (Collins 1979). Formation of the $CO_2$ clathrate is to be expected in all inclusions containing water (brine) and $CO_2$. Detection of the $CO_2$ clathrate can be very difficult, especially in small inclusions with no daughter crystals. No direct observation of the clathrate was made during this study, but its presence was detected by a slight shift of the vapor bubble upon final melting of many of the type 1 and 2 inclusions. The vapor bubble shift and associated smoothing of the bubble meniscus, generally took place between 5.5°C and 8°C (Table 5-1).

The salinity of a $CO_2$ rich inclusion cannot be determined by simple freezing point depression measurements of ice. If the inclusion contains separate liquid $CO_2$, gaseous $CO_2$ and brine phases, however, the brine salinity may be estimated by measuring the freezing point of the $CO_2$ clathrate. This is possible because the clathrate freezing point, like that of ice, is depressed with increasing salinity (Fig. 5-2). Knowing the degree of freezing point depression of the clathrate and using the upper line of Figure 5-3, allows a graphical determination of the NaCl content of the brine at the time of melting, i.e., the salinity of the fluid, not the residual brine (Collins 1979). In cases where such a salinity determination was possible they ranged from 4 to 8 wt.% NaCl equivalent, with the majority at approximately 5 wt.% NaCl equivalent.

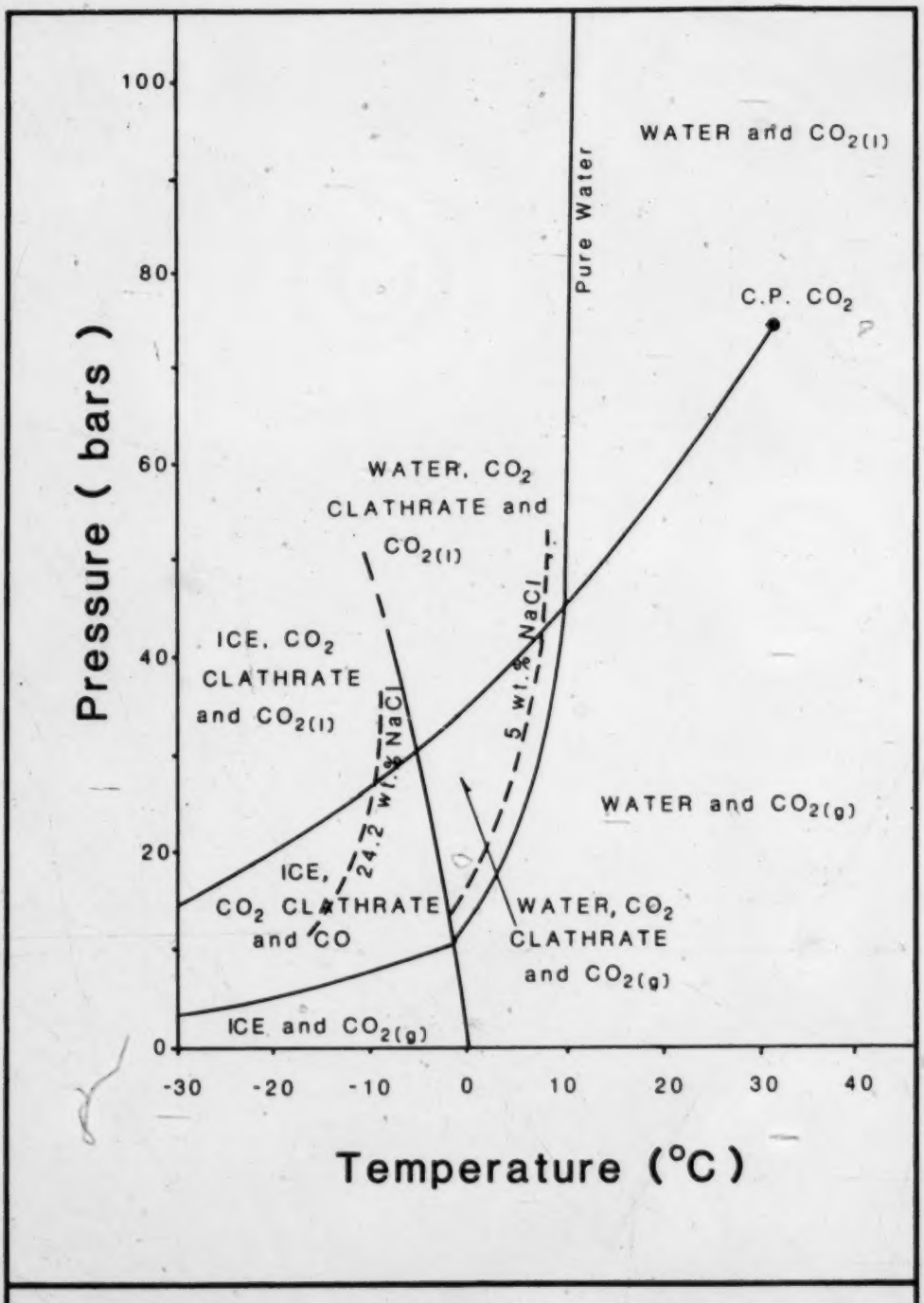


**FIG. 5-2** Phase diagram for the $H_2O$ - $CO_2$ system. Modified from Collins (1979).

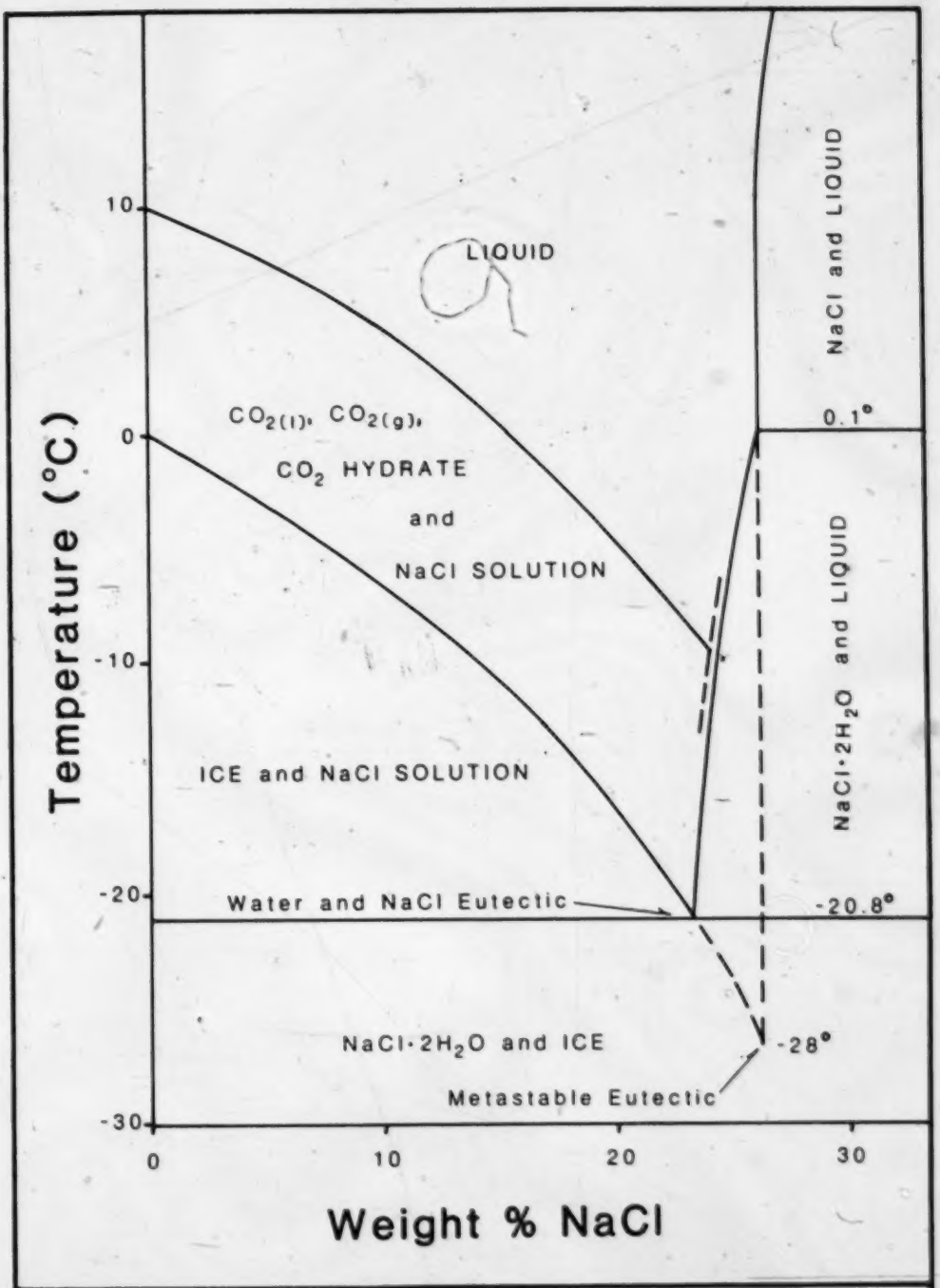


**FIG. 5-3** Melting curves for ice and the $CO_2$ clathrate. Modified from Roedder (1984)

Salinities calculated from the freezing point depression of ice were, as mentioned above, between 4.5 and 8.5 wt.% NaCl equivalent, quite comparable to those found by clathrate freezing point depression measurements. Over-all fluid salinities for each stage of vein formation were:

Pre-ore stage fluids - approximately 6.5-8.5 wt.% NaCl equivalent.

Ore stage fluids - approximately 4-7.5 wt.% NaCl equivalent.

Post-ore stage fluids - approximately 3 wt.% NaCl equivalent.

**Heating Tests - homogenization**

All homogenization temperatures are shown in Figure 5-4a and 5-4b. These values are not pressure corrected.

Homogenization tests were done in order to find the minimum trapping temperature of the inclusions. Measured homogenization temperatures equal actual trapping temperatures only if the fluid was boiling at the time of trapping. If the fluid was not boiling, as was the case in this study, a temperature correction for pressure must be applied to the homogenization temperature to find the actual temperature of trapping.

Uncorrected homogenization temperatures range from 298°C, for a pre-ore stage primary brine inclusion in quartz, to 24.3°C for a pre-ore stage primary $CO_2$ inclusion, also in quartz. The lowest homogenization temperature for a brine-filled inclusion was found in a late stage secondary, measured at 120°C.

Homogenization temperatures for the primary fluid inclusions in ore stage vein material fell between 160°C and 245°C. Only three primary inclusions had homogenization temperatures of over 250°C, and only two below 150°C. All of the high temperature inclusions were hosted in pre-ore stage quartz and homogenized at 279°C, 285°C, and 297°C. The low temperature inclusions, homogenizing at 142°C and 144°C, were in post-ore stage material and probably represent the beginning of the post-ore stage of vein formation.

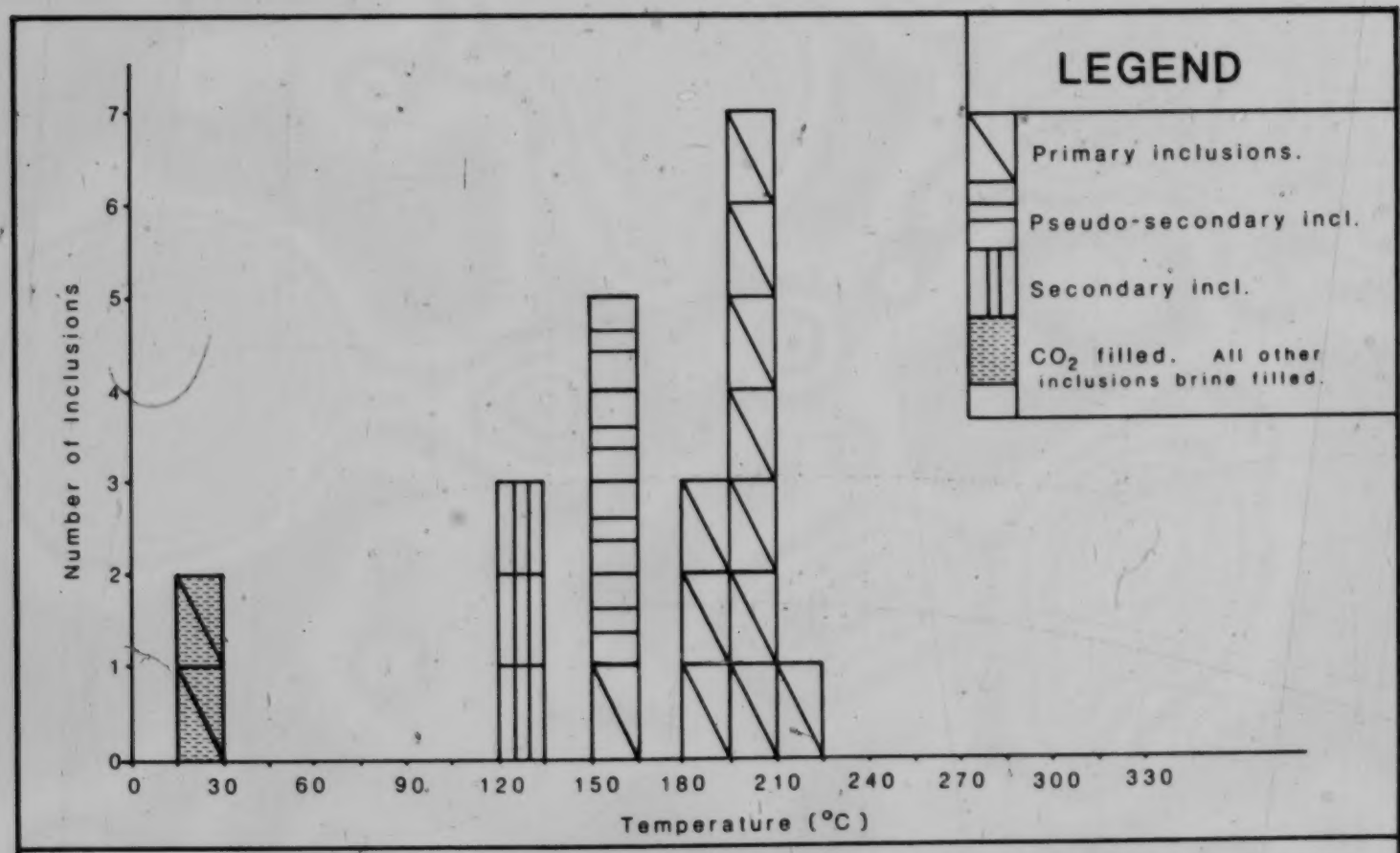


FIG. 5-4a Uncorrected homogenization temperatures for inclusions from the upper vein set.

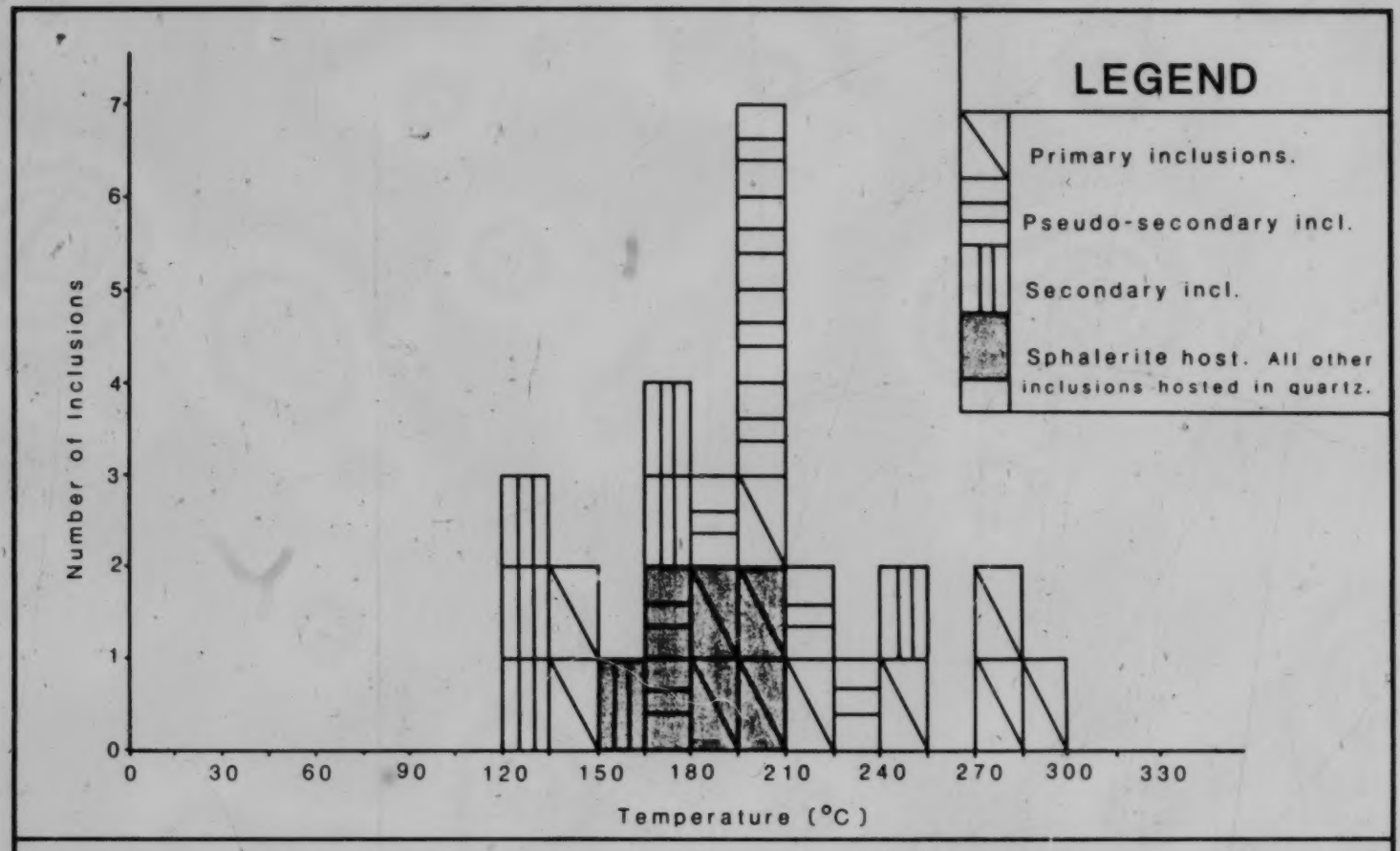


FIG. 5-4b Uncorrected homogenization temperatures for inclusions from the lower vein set.

Pseudo-secondary inclusions homogenized at temperatures ranging from approximately 150°C to 234°C, reflecting the greater part of the temperature range seen by the system during the ore stage. The pseudo-secondary inclusions which homogenized at approximately 230°C or higher probably represent the beginning of the ore stage of vein formation.

A large group of secondaries homogenized at 120°C to 135°C. These may have been formed by a late stage event, such as fracturing caused by renewed fault motion, which was unrelated to the main depositional sequence.

The only $CO_2$ inclusions found homogenized at 24.3°C and 24.4°C and contained no detectable water, either as water ice or as a clathrate. They occurred with three brine inclusions which contained no detectable $CO_2$, had salinities of 7-8 wt.% NaCl equivalent and homogenized at an average of 203°C. Both the $CO_2$ and brine inclusions were primary and, as they were found in the same quartz crystal chip, presumably formed under very similar or identical conditions.

**Crushing Stage**

Crushing of pre-ore stage quartz in immersion oil revealed the presence of high pressure inclusions. Crushing this same material in a $BaCl_2$ solution indicated that the inclusions were dominantly water filled, but that some contained appreciable amounts of $CO_2$, as was found in microscopic examination of the inclusions. Ore stage and post-ore stage material contained no high-pressure inclusions.

## D. INTERPRETATION AND DATA CORRECTIONS

The set of brine filled pre-ore stage primary inclusions which homogenized at an average of 203°C were associated with two separate $CO_2$ inclusions, which homogenized at approximately 24.3°C. When used together in the Kalyuzhnyi and Kolten (1953), crossing $CO_2$ and brine isochors, method of geobarometry/geothermometry, a coincident trapping temperature of 273°C at 975 bars is indicated (Fig. 5-5). This result is valid if the $CO_2$ and brine were trapped at the same pressure and temperature and the inclusions contained pure, or nearly so, water and $CO_2$. This seems rather unlikely considering the miscibility of water and $CO_2$ at elevated temperatures, though freezing tests seemed to indicate that the inclusion sets were relatively free of the other component. The NaCl in the water may be partly responsible for this in that any salt in solution markedly reduces the miscibility of $CO_2$ in that solution.

Repeat tests of homogenization temperatures varied by a maximum of ±4°C. This variation produces a ±2.5 to ±3.5 bar change in the calculated trapping pressure. Salinity variations of ± 10 wt.% NaCl would change the pressure value by ±7 bars at 300°C, or ±3 bars at 250°C. Repeat salinity determinations indicated an accuracy of ±2 wt.% NaCl, so salinity errors probably resulted in only a ±1 to ±2 bar error. Other salts in the solution have a negligable effect on the results as they behave in a manner very similar to pure NaCl in solution (Roedder 1984). If a total combined error of ±10% is assumed, the possible range of coincident trapping pressures and temperatures are 975±100 bars and 273±25°C respectively. This range is indicated by the dashed circle in Fig. 5-5. This pressure regime is extreme and indicates that vein formation took place at some considerable depth.

The calculated temperature of trapping correlates with the 279°C to 297°C range of homogenization temperatures found for pre-ore stage primary inclusions, implying that the temperature correction for pressure which is required for the fluid inclusion homogenization temperatures is small.

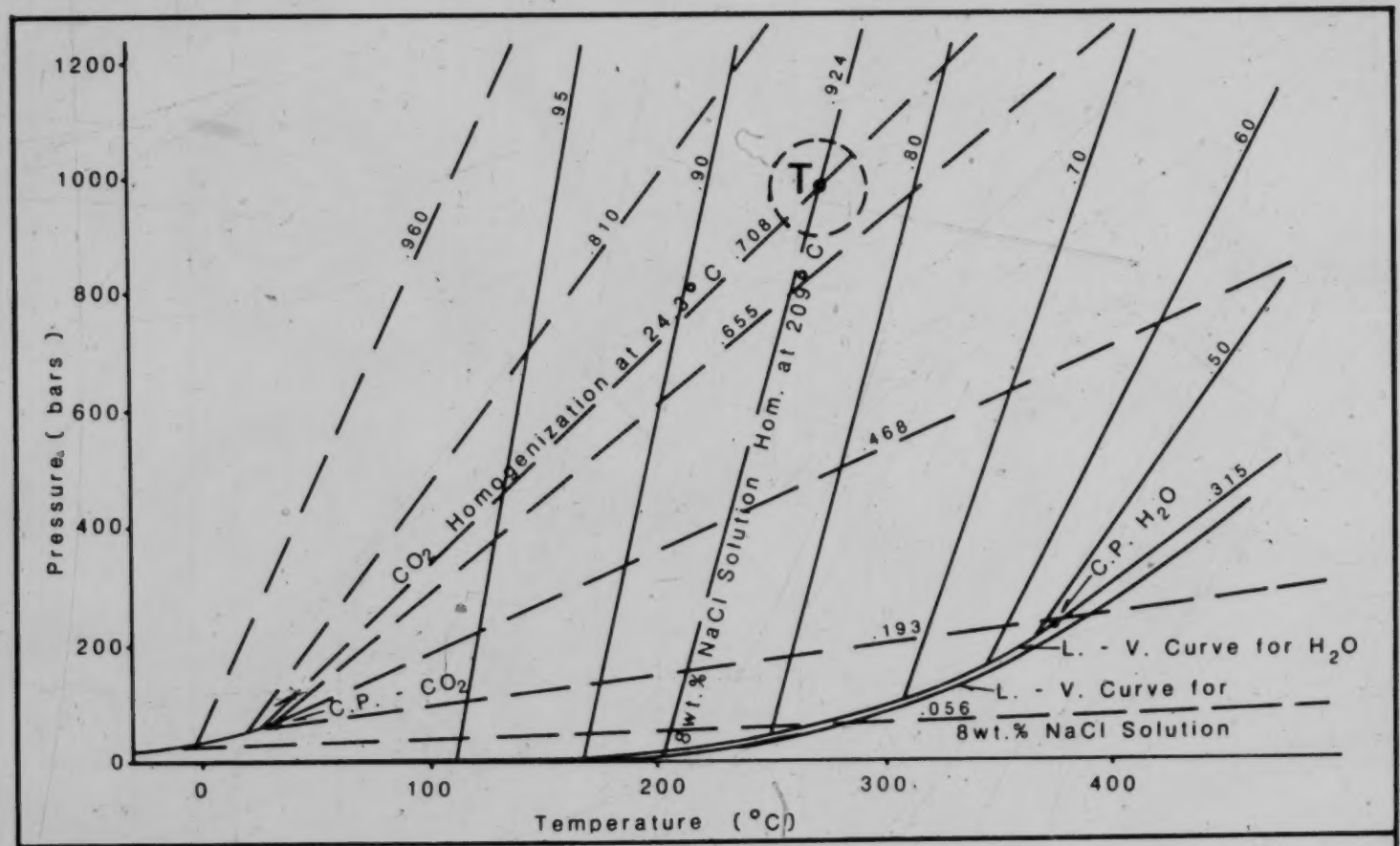


**FIG. 5-5** Plot of Intersecting $H_2O$-$CO_2$ Isochors.
Data from Angus et al (1973), Keenan et al (1969) and Haas (1976).

Minimum pressure during the pre-ore stage may be estimated from fluid inclusion homogenization data. The maximum homogenization temperature measured for a primary inclusion, containing an 8 wt.% equivalent brine, was 297°C. No evidence of boiling was found in this or any other stage of vein development. Pressure at the time of trapping must therefore have exceeded the vapor pressure of the fluid at the temperature of trapping. Haas (1976) constructed several steam tables for $NaCl-H_2O$ solutions of varying salinities and from these the vapor pressure at any given temperature may be found. The vapor pressure of an 8 wt.% NaCl solution boiling at 297°C is approximately 80 bars so that was the minimum pressure during the pre-ore stage of vein formation. Barring pressure surges or drastic changes in fluid density or in overburden thickness, this minimum pressure is probably applicable to all stages of vein formation.

The minimum pressure of 80 bars is just that, a minimum pressure. The minimum trapping pressure required to produce a fluid inclusion with approximately 4 mole% $CO_2$ at room temperature is about 500 bars (Gehrig 1979). Thus, vein formation probably took place at a pressure between 500 and 1000 bars. The formation of inclusions at such pressures, without invoking an overpressure situation, requires a formation depth of at least 2 km at lithostatic loads, or over 5 km at hydrostatic loads if a water density of of 1 g/mL is assumed. Crushing stage experiments which indicate the presence of high pressure inclusions in the pre-ore stage quartz, and a lack of such inclusions in ore stage and post-ore stage material, may be explained because if the $CO_2$ content of an inclusion is low, as it was in ore stage and later inclusions, the coefficient of expansion of the fluid is quite small so no dramatic bubble expansion will occur on crushing.

Potter (1977) produced graphs of the temperature corrections for pressure which must be applied to inclusions of given salinities which were trapped at various pressures. These graphs apply only to the pure $NaCl-H_2O$ system and are thus not directly applicable to most of the inclusions used in this study, as they contain $CO_2$. The graphs show that, for a 5 wt.% NaCl equivelant solution, at pressures less than 40 MPa (400 bars) and homogenization temperatures above 200°C, the necessary temperature corrections are generally less than +30°C. In general, the higher the temperature of trapping, the smaller the temperature correction will be.

The temperature correction for pressure for this studies inclusions may thus be in the +10 to +30°C range however, since it is impossible to accurately determine its true value, it must be ignored. Homogenization temperatures are thus assumed to approximate the trapping temperature, except in the case of inclusions in the $CO_2$/brine set, for which an estimate of the temperature correction for pressure may be made.

Overall homogenization temperatures and salinities for the upper and lower vein inclusions are very similar, making it possible to treat all data as a single group. Figure 5-6a shows the combined results of homogenization tests on both the upper and lower vein inclusions. The lower part of the diagram (Fig. 5-6b) shows the temperature ranges for the three main stages of vein formation.

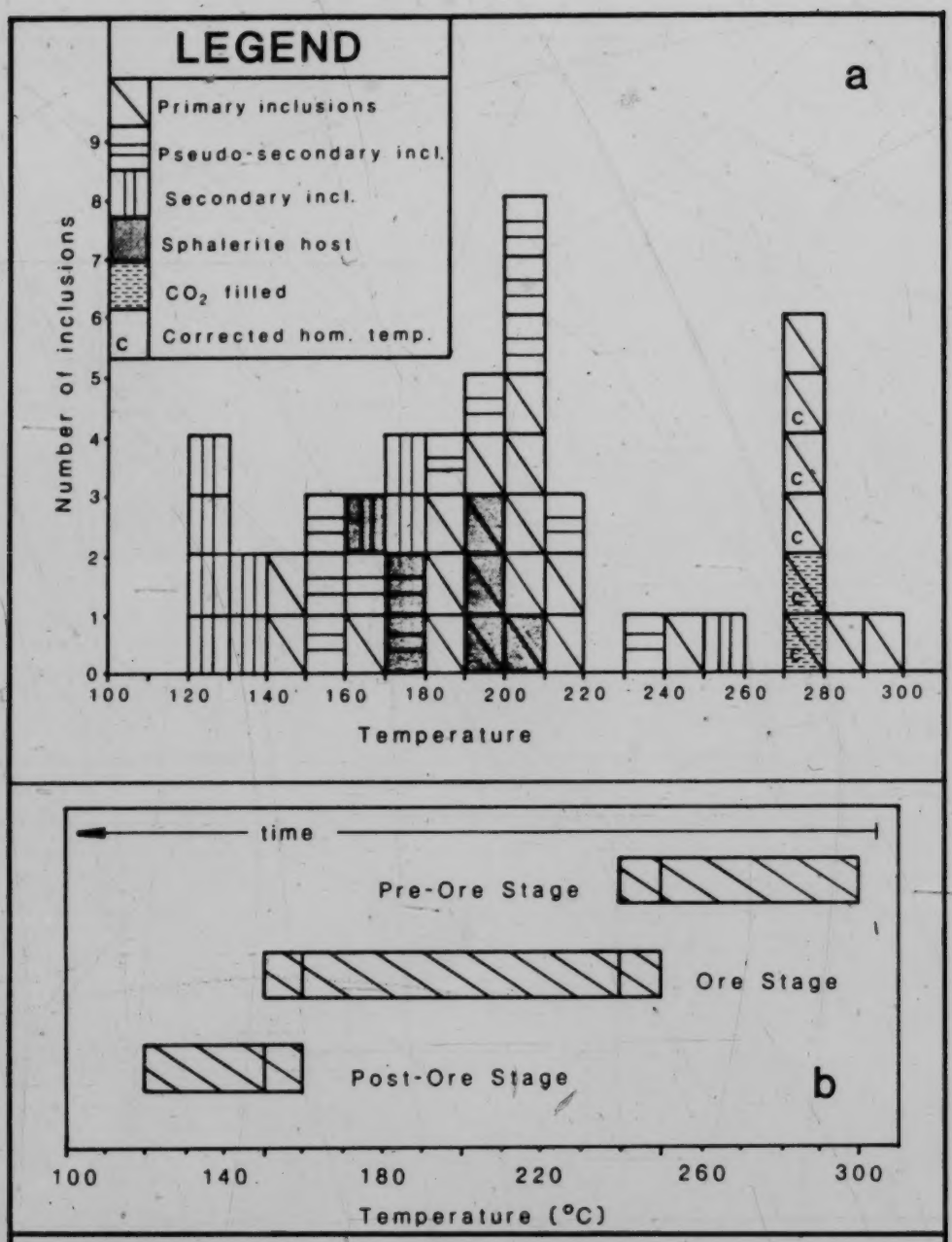


**FIG 5-6** a - Compilation of homogenization temperatures for fluid inclusions from the upper and lower vein sets.

b - Diagram of probable temperature ranges of stages in vein formation. (from fluid inclusion study)

## E. CONCLUSIONS

The Deer Trail veins were formed within a hydrothermal system which cooled from a maximum temperature of approximately 300°C to less than 150°C. The hydrothermal fluids had a variable $CO_2$ content, which seems to have been highest in the pre-ore and early ore stages. The $CO_2$ content fell during the ore stage and was probably negligable by the post-ore stage. This may reflect the contribution of $CO_2$ to the system by reactions taking place in the carbonate host rocks as a result of their thermal metamorphism by the intruding batholith. As the batholith cooled the rate of $CO_2$ production dropped, resulting in a decline of the fluids $CO_2$ content.

Fluid salinity had a maximum value of about 8 wt.% NaCl equivalent during the pre-ore stage and fell with time; the salt in solution seems to have been nearly pure NaCl. Salinity values and high pressures similar to those noted in this deposit have been reported for other deposits. Salinities were in the 8 to 12 wt.% NaCl equivalent range and pressures reached up to 1 Kbar in the early stages of formation of the tin-tungsten deposits of Panasqueira, Portugal (Kelly and Rye 1979). Many other base metal dominated deposits also seem to have formed at pressures above 400 bars.

Post-ore stage fluids seem to have had lower salinities than the the ore stage fluids, only approximately 3 wt.% NaCl equivalent, and post-ore stage inclusions homogenized at only 140°C to 150°C, much cooler than the other two stages. Very late stage secondary fluid inclusions homogenized at approximately 120°C to 130°C. These inclusions formed after the post-ore stage and may have been caused by the fracturing of quartz and other minerals as a result of renewed fault motion. They are probably unrelated to the actual formation of the veins.

# VI. OXYGEN AND HYDROGEN ISOTOPE STUDIES

## A. INTRODUCTION TO OXYGEN AND HYDROGEN ISOTOPES

Three stable isotopes of oxygen exist in nature: $^{16}O$, 99.765%; $^{17}O$, 0.039%; and $^{18}O$, 0.205%. The abundance and relatively large mass difference between $^{16}O$ and $^{18}O$ make them the most suitable pair for use in oxygen isotope studies. Only two stable isotopes of hydrogen exist: $^{1}H$, 99.985% and $^{2}H$ (deuterium, D), 0.015%. The standard for oxygen and hydrogen isotope work is SMOW, or Standard Mean Ocean Water, whose $\delta^{18}O$ and $\delta D$ values are both defined as 0‰ (Craig 1961). The relative $^{18}O$ enrichment in parts per thousand of any material with respect to the standard is calculated by the equation:

$$\delta^{18}O‰ sample = [\{ (^{18}O/^{16}O)sample / (^{18}O/^{16}O)standard \} -1 ] \times 1000$$

The behaviour of oxygen isotopes and hydrogen isotopes, like those of sulfur, depends upon the temperature at which a reaction takes place; the lower the temperature the greater the variation in their behaviour or fractionation. An example of low temperature oxygen and hydrogen fractionation is the variation in the $\delta^{18}O$ value of rainwater. Water vapor in the atmosphere undergoes progressive condensation fractionation as it moves inland, thus coastal rain is isotopically similar to SMOW, while that which falls inland is significantly depleted in $^{18}O$ and D.

Minerals also show variations in their $\delta^{18}O$ values, though the variation is usually not as extreme as that seen in meteoric water. (The $\delta D$ values of minerals are useful only in cases where the mineral contains significant amounts of chemically bound water.) If conditions allow, a mineral will have a $\delta^{18}O$ value which is in equilibrium with that of its parent fluid. This equilibrium, or degree of oxygen isotope fractionation, is dependent upon the temperature of formation of the mineral. Quartz, for example, is always enriched in $^{18}O$ with respect to its parent fluid and the lower the temperature of formation the greater the degree of enrichment. This enrichment, at equilibrium, may be calculated using the equation:

$1000ln\alpha = 3.38(10^6T^{-2}) - 3.40$ (Clayton and O'neil 1972)

where:

$1000ln\alpha = \delta^{18}O(quartz) - \delta^{18}O(fluid)$

T = the temperature of formation in degrees Kelvin.

For calcite the equation is; $1000ln\alpha = 2.78(10^6T^{-2}) - 2.89$ (Bottinga and Javoy 1973)

From the above discussion it follows that if either the temperature of deposition of a mineral or the degree of oxygen fractionation between the parent fluid and mineral are known, the other may be calculated. In geological studies the parent fluid is generally unavailable for study, thus the $\delta^{18}O$ values of minerals deposited at known temperatures are used to calculate the $\delta^{18}O$ value of the parent fluid. The most reliable method of determining the depositional temperature of these minerals is by testing their fluid inclusions, as was done in this study.

Four main types of water are involved in the formation of ore deposits, namely:

1. **Meteoric water**

The $\delta^{18}O$ values of meteoric waters lie between approximately 0‰ and -25‰,(lower in Arctic and Antarctic precipitation and ice sheets). The $\delta D$ values range from approximately 0‰ to -200‰ or lower, again in high latitude precipitation and the polar ice sheets (Taylor 1974). The $\delta D$ and $\delta^{18}O$ values of meteoric waters are related by the equation ; $\delta D‰ = 8\delta^{18}O‰ + 10‰$. Only very slight variations from this 'meteoric water line' have been observed in nature.

Meteoric waters trapped in rocks for great lengths of time may, through isotopic exchange with the rocks and salinity increases, become what are referred to as 'connate' waters. The $\delta D$ values of these connate waters remain essentially unaltered, as there are relatively few H-bearing minerals available for exchange. Slight increases in the $\delta D$ values of these waters may occur as a result of low temperature evaporation in hot spring type environments.

2. **Ocean water**

The average $\delta^{18}O$ and $\delta D$ values of SMOW (Standard Mean Ocean Water) are defined as 0‰ but oceanic $\delta^{18}O$ values may vary between about 2‰, in highly evaporitic areas like the Red Sea, and -1‰ in areas with high influxes of meteoric water such as the Arctic ocean. Similarly, $\delta D$ values may reach 11‰ in evaporitic areas and fall to less than 0‰ in the Arctic ocean (Taylor 1979). The isotopic composition of the oceans has probably remained quite close to its present value for the last 150 Ma (Taylor 1979), and probably throughout most of its history, at least during the time that spreading ridges have been active. The $\delta^{18}O$ value seems to be buffered at approximately 0‰ by water/rock reactions which take place at and around these spreading ridges (Muehlenbachs and Clayton 1972). Variations in the oceans isotopic composition may have occurred as a result of the growth and retreat of glaciers, and from changes in mid-ocean ridge activity levels.

Ocean water, like meteoric water, may be trapped in sediments and become connate water. Oceanic and meteoric connate waters may be distinguished by their $\delta D$ values, and sometimes by their $\delta^{18}O$ values, depending upon the degree of oxygen exchange which has taken place between the fluid and the wall rock.

3. **Metamorphic water**

Metamorphic water is produced by the breakdown of hydrous minerals at elevated temperatures and pressures during regional metamorphism and rarely, if ever, makes its way to the surface. Thus, all isotope values must be calculated from the isotope values of metamorphic minerals. The $\delta^{18}O$ value of metamorphic water probably ranges from 5‰ to 25‰, reflecting the fact that the fluids are derived from many different types of source rocks with widely varying $\delta^{18}O$ values. Metamorphosed sediments, especially carbonates, tend to produce waters with high $\delta^{18}O$ values, while metamorphosed volcanics and greywackes produce waters at the lower end of the scale. The $\delta D$ values of metamorphic waters range from approximately -20‰ to

-65‰.

Metamorphic water is probably also produced during thermal metamorphism of sediments, especially shales, during igneous intrusive events, though the volume would be much less than that produced during regional metamorphism. Their very similar δD values may indicate that primary magmatic waters are sometimes incorporated into metamorphic fluids.

4. **Primary Magmatic water**

Primary magmatic waters seem to have a narrow range of $\delta^{18}O$ values from approximately 5‰ to 10‰, and a δD value range from -50‰ to -85‰. It is difficult, if not impossible, to get a sample of pure magmatic water from which to determine the δD and $\delta^{18}O$ values directly and the fluid isotope values must again be calculated from the δD and $\delta^{18}O$ values of associated minerals.

Interestingly, the δD range of -50‰ to -85‰ correlates closely with that of normal OH-bearing authigenic minerals deposited in equilibrium with ocean water. Taylor (1979) proposed a theory which may explain why this is so: When oceanic sediments containing OH-bearing minerals are carried down along subduction zones, they undergo partial melting and dehydration. Water released from the hydrous minerals is added to the pre-existing magma along with the new melt. As most magmas contain relatively little water, the addition of the newly released water will have a large influence, and may in fact be the controlling factor, on the composition of the magmatic fluids. Such magmatic fluids should thus reflect the $\delta^{18}O$ values of the original authogenic minerals, as appears to be the case.

In any geothermal system one or more of these types of waters may make up the hydrothermal fluid. Studying the $\delta^{18}O$ values of minerals deposited in such a system allows the calculation of the $\delta^{18}O$ value of the original fluid, though this calculated value may not unequivocally identify the source of this fluid.

If the fluid was unreacted meteoric or ocean water, the $\delta^{18}O$ values would identify it as such, being some value below 0‰, or approximately equal to 0‰, respectively. However, fluids in such systems often undergo oxygen exchange with the wall rocks or mixing with other fluids, which alters their original $\delta^{18}O$ values. Reaction with wall rock will generally raise the fluid's $\delta^{18}O$ value, and in these cases the $\delta D$ value of the water may be of great assistance in identifying the type or types of water present in the hydrothermal fluid. An example of such oxygen exchange is found in the Salton Sea of California, where meteoric water held in a reservoir of deltaic sediments has undergone an $\delta^{18}O$ shift of approximately positive 15‰. Even larger changes may be expected in fluids which pass through highly reactive carbonate sediments. Mixing, alternately, will produce a fluid with a $\delta^{18}O$ and $\delta D$ value somewhere between the two original values. Both of these processes make the source of the fluid much more difficult to determine.

## B. OXYGEN ISOTOPE STUDY

### Method

Eleven samples of quartz from all three stages of vein formation, along with two post-ore stage calcites, a very late calcite, and three altered carbonate wall rock samples, were analysed to determine their $\delta^{18}O$ values.

All samples were hand crushed to approximately -100 mesh. Quartz samples were then leached in aqua regia for 24 hours to remove all soluble foreign matter, particularly any carbonates. The clean samples were then reacted with bromine pentafluoride, $BrF_5$, for 12 hours at approximately 650°C. All derived oxygen was frozen out and reacted with a platinum treated carbon rod at approximately 850°C to produce $CO_2$ gas. This $CO_2$ was analysed by mass spectrometry to determine its $\delta^{18}O$ value. Carbonates were used 'as is' because only the mineral of interest reacted with the acid over the leaching times used. Calcite and dolomite were reacted with phosphoric acid for 1.5 to 2.5 hours and one week respectively. The evolved $CO_2$ was analysed by mass spectrometry to determine the $\delta^{18}O$ value of the samples. All analyses were performed in Dr. K. Muehlenbachs laboratory in the geology department at the University of Alberta, by Mrs. Toth.

### Analytical Results

The raw quartz analyses results are given in Table 6-1, while raw carbonate analyses results are given in Table 6-2.

All 10 pre-ore and ore stage quartz samples had $\delta^{18}O$ (SMOW) values between 16‰ and 19‰. The fact that pre-ore and ore stage quartz samples all had very similar $\delta^{18}O$ values is probably not a coincidence as they were deposited at similar temperatures, probably by similar fluids. The two post-ore stage calcite samples and one post-ore stage quartz sample had $\delta^{18}O$ values of between 11‰ and 14‰, while the very late calcite sample had a $\delta^{18}O$ value of 16‰. All wall rock calcite and dolomite $\delta^{18}O$ values ranged between 14‰ and 16‰.

**Table 6-1**

**$\delta^{18}O$ values for quartz and the calculated parent fluid $\delta^{18}O$ values for samples from the Deer Trail Mine, Washington, U.S.A.**

| Sample No. | Depositional Stage | Raw $\delta^{18}O$ value and error $^{o}/_{oo}$ | $\delta^{18}O$ value (SMOW) | Maximum parent fluid $\delta^{18}O$ value | Minimum parent fluid $\delta^{18}O$ value | Mean parent fluid $\delta^{18}O$ value |
|---|---|---|---|---|---|---|
| DTM -11 | pre-ore | -1.33 ± 0.02 | 17.04 | 10.15 | 8.08 | 9.12 |
| DTM - 12 | ore | -0.99 ± 0.04 | 17.38 | 8.42 | 1.88 | 5.15 |
| DTM - 20 | post-ore | -4.80 ± 0.03 | 13.57 | -1.93 | -4.91 | -3.42 |
| DTM - 24 | pre-ore | -1.05 ± 0.04 | 17.32 | 10.43 | 8.36 | 9.40 |
| DTM - 30 | ore | -0.87 ± 0.05 | 17.50 | 8.54 | 2.00 | 5.27 |
| DTM - 54 | ore | +0.13 ± 0.02 | 18.50 | 9.54 | 3.00 | 6.27 |
| DTM - 57 | ore | -1.44 ± 0.05 | 16.93 | 7.97 | 1.43 | 4.70 |
| DTM - 59 | ore | -0.71 ± 0.04 | 17.66 | 8.70 | 2.16 | 5.43 |
| DTM - 62 | pre-ore | -0.46 ± 0.06 | 17.91 | 11.02 | 8.95 | 9.99 |
| DTM - 67 | ore | -0.60 ± 0.04 | 17.77 | 8.81 | 2.27 | 5.54 |
| DTM - 95 | ore | -2.64 ± 0.04 | 15.73 | 6.77 | 0.23 | 3.50 |

Pre-ore stage temperatures = 300°C to 250°C, Ore stage temperatures = 250°C to 150 °C, Post-ore stage temperatures = 150°C to 120°C.

$\delta^{18}O^{o}/_{oo}$(SMOW) = raw$\delta^{18}O$ value +18.37

$1000ln\alpha = 3.38 \times (10^{6}T^{-2}) - 3.40$

**Table 6-2**

**$\delta^{18}O$ values for calcite and dolomite and the calculated parent fluid $\delta^{18}O$ values for hydrothermal calcites from the Deer Trail Mine, Washington, U.S.A.**

| Sample No. | Depositional Stage | Raw $\delta^{18}O$ value and error ‰ | Raw $\delta^{13}C$ value and error ‰ | $\delta^{18}O$ ‰ value (SMOW) | Maximum parent fluid $\delta^{18}O$ value | Minimum parent fluid $\delta^{18}O$ value | Mean parent fluid $\delta^{18}O$ value |
|---|---|---|---|---|---|---|---|
| DTM - 20C | (Po)calcite | 3.80 ± 0.04 | -4.82 ± 0.03 | 12.39 | -0.26 | -2.54 | -1.45 |
| DTM - 28C | limestone wallrock | 5.91 ± 0.05 | -4.05 ± 0.06 | 14.50 | ---- | ---- | ---- |
| DTM - 59C | (Po) calcite | 2.55 ± 0.07 | -3.03 ± 0.08 | 11.13 | -1.43 | -3.98 | -2.71 |
| DTM - 73D | dolomitic wallrock | 6.49 ± 0.02 | -0.43 ± 0.05 | 14.82 | ---- | ---- | --- |
| DTM - 73C | calcite from DTM - 73 | 5.64 ± 0.02 | -1.26 ± 0.04 | 14.20 | ---- | ---- | --- |
| DTM - 91C | very late calcite | 6.82 ± 0.03 | -0.54 ± 0.02 | 15.46 | -8.29 | -14.00 | -11.15 |
| DTM - 94D | dolomitic wallrock | 7.80 ± 0.04 | -3.01 ± 0.02 | 16.09 | ---- | ---- | ---- |
| DTM - 94C | calcite from DTM - 94 | 5.98 ± 0.06 | -2.86 ± 0.02 | 14.56 | ---- | ---- | ---- |

(Po) = post-ore stage. Post-ore stage temperatures = 150°C to 120°C.

Very late calcite temperatures = 20°C to 50°C.

Calcite $\delta^{18}O$‰(SMOW) = raw$\delta^{18}O$ value +8.63 - 0.009 $\delta C^{13}$(raw).

Dolomite $\delta^{18}O$‰(SMOW) = raw$\delta^{18}O$ value + 7.75 - 0.009 $\delta C^{13}$(raw).

$1000 ln\alpha = 2.78 \times (10^6 T^{-2}) - 2.89$ (Sharma and Clayton 1965).

To calculate the $\delta^{18}O$ value of the parent fluid of each stage, the temperature of deposition of the quartz or calcite analysed must be known. Fluid inclusion studies indicate that these temperatures, or rather range of possible temperatures, are;

Pre-ore ; 300°C to 250°C

Ore ; 250°C to 150°C

Post-ore ; 150°C to 120°C

Very late calcite ; 20°C to 50°C (assumed)

Using the high and low temperatures of deposition of each quartz/calcite sample, and knowing the degree of oxygen fractionation between a fluid and the deposited mineral at any given temperature (Clayton and O'neil 1972; Bottinga and Javoy 1973), allowed the calculation of the maximum and minimum $\delta^{18}O$ values of the parent fluid of each sample. These values are listed in Tables 6-1 and 6-2.

The mean $\delta^{18}O$ values of the parent fluid of each sample are plotted along the abscissa of Figure 6-1. The mean $\delta^{18}O$ values for the pre-ore, ore, and post-ore stage fluids form three separate and distinct groups, though their error ranges do show some overlap, especially in the case of the ore and pre-ore stage fluids.

Pre-ore stage fluids had a possible range of $\delta^{18}O$ values from 8‰ to 11‰. This range lies within the fields of both primary magmatic water and of metamorphic waters. Because of their large range of possible formation temperatures, ore stage fluid $\delta^{18}O$ values may have ranged between 0‰ and 10‰, partially within the fields of primary magmatic water, metamorphic water, meteoric water and ocean water. Post-ore stage fluids had a total possible $\delta^{18}O$ value range of 0‰ to -5‰, and the very late calcite parent fluids had $\delta^{18}O$ values of approximately -11‰, both lie below the fields of primary magmatic waters and must therefore have been dominantly meteoric waters.

In the cases of the post-ore stage fluids and the very late calcite the $\delta^{18}O$ values are sufficient to define the type of water which made up the hydrothermal fluid. Determination

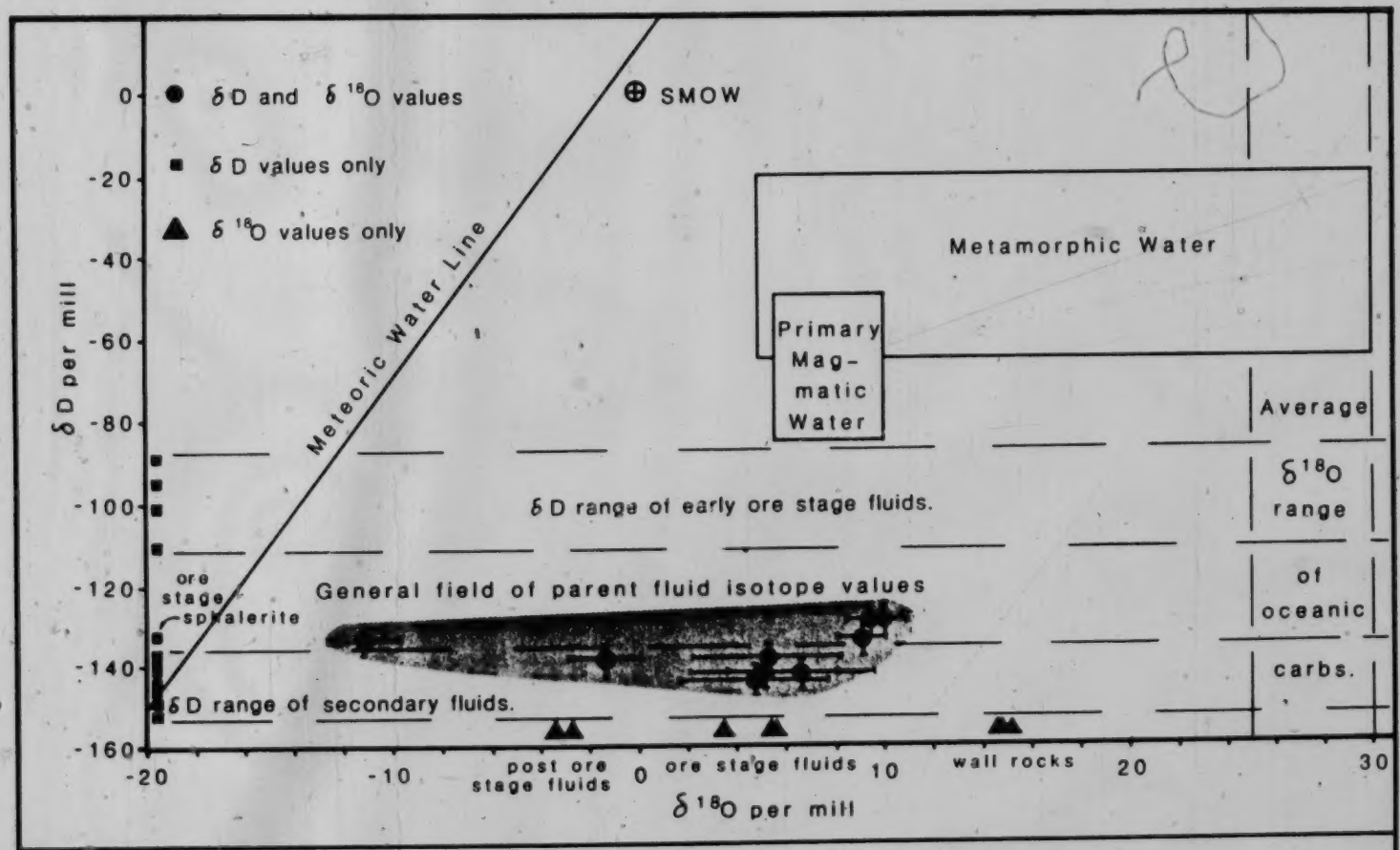


FIG. 6-1 Results of O and D isotope study on inclusion fluids and O-bearing minerals from the Deer Trail mine, Washington.

of the δD values of fluids in fluid inclusions from both pre-ore and ore stage material may also allow the identification of these waters.

## C. HYDROGEN ISOTOPE STUDY

### Method

Four ore stage sphalerite, two post-ore stage calcite and nine pre-ore and ore-stage quartz samples were used in this study. Two methods of collecting water from fluid inclusions were used;

1. Physical crushing of the sample under vacuum at approximately 80°C.
2. Heating induced decrepitation at 300°C and 700, under vacuum.°C

Of these the decrepitation method was found to give better water yields and sample control. (See Appendix)

Water collected by both methods was passed over uranium metal which was heated to approximately 800°C, resulting in the production of clean hydrogen gas. This gas was collected and analysed by mass spectrometry to determine its D/H ratio, and thus the D/H ratio of the inclusion water. Errors for $\delta D$ values were determined to be $\pm 4‰$ from repeat measurements. The errors are shown as error bars in figure 6-1, as are the possible ranges of $\delta^{18}O$ values. Errors for the $\delta^{18}O$ values cover a 2 sigma range of the total possible range of values calculated for each sample; i.e., $\pm 1‰$ for pre-ore values, $\pm 3‰$ for ore values and $\pm 1.5‰$ in the case of post-ore sample values.

All analyses were performed by the author in Dr. John Grays laboratory, in the University of Alberta physics department.

**Analytical Results**

All measured values fall into one of three groups, two of which have very similar δD ranges (Table 6-3).

The first group contains the parent fluids of three early ore stage sphalerite samples and one early ore stage quartz sample. Their δD values fall between -89 and -111‰ and are plotted on the 'Y' axis of Fig. 6-1 as no calculated or measured $\delta^{18}O$ values were available for these fluids. Sphalerite formed during this phase was generally massive and clean, making it perfect for analysis. Quartz was less common and rarely pure, thus the presence of only one quartz sample.

The second group contains the parent fluids of three pre-ore and four ore stage quartz samples, one post-ore stage calcite and one very late calcite sample. Oxygen analyses of these specimens was also done and the combined δD vs. $\delta^{18}O$ values are plotted and form the stippled area on Fig. 7-1. All δD values fall within the range of -127 to -143‰, while $\delta^{18}O$ values range from -11 in the case of the very late calcite, to 10 in the case of a pre-ore stage quartz sample. Also included in this group is an ore stage sphalerite whose primary inclusion fluids have a δD value of -132‰ and an unknown parent fluid $\delta^{18}O$ value.

The third group is composed of the fluids from the secondary inclusions of all analysed samples. δD values range from -137 to -152‰ with the main range centered at approximately -140‰. This group shows significant overlap onto the δD values of the second group, indicating that the fluids which deposited the pre-ore, most of the ore, and the post-ore material were very similar to those found in the secondary inclusions of all samples.

**Table 6-3**

**$\delta D$ ‰ values for fluids from primary and secondary inclusions in quartz, calcite, and sphalerite from the Deer Trail veins, Washington, U. S. A.**

| Sample No. | Depositional stage and type | Extraction Method | Fluid type | Raw $\delta D$ value and error ‰ | $\delta D$ (SMOW) value | $\delta^{18}O$ (SMOW) (mean value) |
|---|---|---|---|---|---|---|
| DTM - 11 | (Pr) quartz | D | P | -86.162 ± 1.21 | -134 | 9.21 |
| DTM - 12 | (O) quartz | C | - | -104.200 ± 0.59 | -151 | --- |
| DTM - 12(a) | (O) quartz | D | S | -104.589 ± 0.34 | -152 | --- |
| DTM - 12(b) | (O) quartz | D | P | -94.133 ± 0.81 | -142 | 5.15 |
| DTM - 20C | (Po) calcite | C | - | -75.823 ± 1.85 | -125 | --- |
| DTM - 20C(a) | (Po) calcite | D | P | -91.165 ± 0.26 | -139 | -1.37 |
| DTM - 24(a) | (Pr) quartz | D | S | -89.696 ± 0.46 | -137 | --- |
| DTM - 24(b) | (Pr) quartz | D | P | -80.214 ± 0.56 | -128 | 9.40 |
| DTM - 24(b)(rep) | (Pr) quartz | D | P | -74.472 ± 0.58 | -123 | --- |
| DTM - 30 | (O) quartz | C | - | -98.818 ± 0.42 | -146 | --- |
| DTM - 30(b) | (O) quartz | D | P | -90.183 ± 0.76 | -138 | 5.27 |
| DTM - 30S | (O) sphalerite | C | - | -69.298 ± 1.30 | -118 | --- |
| DTM - 30S(a) | (O) sphalerite | D | S | -91.862 ± 1.42 | -139 | --- |
| DTM - 30S(b) | (O) sphalerite | D | P | -44.756 ± 1.26 | -95 | --- |
| DTM - 45(b) | (O) quartz | D | P | -51.702 ± 1.00 | -102 | --- |
| DTM - 54(a) | (O) quartz | D | S | -101.930 ± 1.38 | -149 | --- |
| DTM - 54(b) | (O) quartz | D | P | -94.294 ± 0.52 | -142 | 6.27 |
| DTM - 54S | (O) sphalerite | C | - | -51.261 ± 0.55 | -101 | --- |

| | | | | | | |
|---|---|---|---|---|---|---|
| DTM - 54S(a) | (O) sphalerite | D | S | -98.136 ± 0.82 | -146 | --- |
| DTM - 54S(b) | (O) sphalerite | D | P | -61.687 ± 0.23 | -111 | --- |
| DTM - 56S | (O) sphalerite | C | - | -68.131 ± 0.95 | -117 | --- |
| DTM - 56S(a) | (O) sphalerite | D | S | -92.591 ± 0.76 | -140 | --- |
| DTM - 56S(a)(rep) | (O) sphalerite | D | S | -96.381 ± 0.73 | -144 | --- |
| DTM - 56S(b) | (O) sphalerite | D | P | -38.251 ± 1.09 | -89 | --- |
| DTM - 57(a) | (O) quartz | D | S | -92.912 ± 0.72 | -141 | --- |
| DTM - 57(b) | (O) quartz | D | P | -95.797 ± 0.53 | -143 | 4.70 |
| DTM - 57(b)(rep) | (O) quartz | D | P | -92.806 ± 1.25 | -140 | --- |
| DTM - 57S(b) | (O) sphalerite | D | P | -84.216 ± 1.43 | -132 | --- |
| DTM - 62(a) | (Pr) quartz | D | S | -96.814 ± 1.21 | -144 | --- |
| DTM - 62(b) | (Pr) quartz | D | P | -80.238 ± 0.59 | -129 | 9.99 |
| DTM - 91C(b) | very late calcite | D | P | -78.812 ± 1.41 | -127 | -11.15 |

$\delta D(SMOW) = \{[(\{ \delta D(raw) \times 10^{-3} + 1 \} / 1.006) \times 0.953] + 1\} \times 10^{3}$

(rep) = repeat sample

(Pr) = pre-ore stage, (O) = ore stage, (Po) = post-ore stage

C = crushing, D = decrepitation

P = primary fluids, S = secondary fluids (i.e., Fluids from primary and secondary inclusions separated by heating to different temperatures, the actual temperature used being dependant upon the type and mineral host of each sample.)

**Discussion**

All δD values are equal to or less than -89‰(SMOW) indicating that the hydrothermal fluid was dominated at all times by meteoric water. Pre-ore stage parent fluids had δD values of between -128‰ and -134‰ indicating, within error limits, a single fluid. The calculated parent fluid $\delta^{18}O$ values, however, do not correspond to the δD values if initial $\delta D/\delta^{18}O$ ratios are assumed to have been those of meteoric water. This may be the result of an increase in the $\delta^{18}O$ value of the fluid, probably caused by oxygen exchange between the fluid and the wall rock at elevated temperatures. The degree to which the $\delta^{18}O$ value of the fluid was raised may be calculated. With a δD value of -130‰ the equilibrium $\delta^{18}O$ value is -17.5‰. As the $\delta^{18}O$ value calculated from oxygen analyses of the host quartz is approximately 10‰, the $\delta^{18}O$ value of the fluid must have been raised by nearly 27‰. This is a very large change but it may be reasonable as the water was hot, approximately 300°C, and exchanging with very reactive carbonate rocks which had very high initial, 20‰ to 25‰, $\delta^{18}O$ values.

Analysis of calcite and dolomite in altered wall rock from the Deer Trail mine shows that calcite now has $\delta^{18}O$ values between 14‰ and 15‰ and dolomite has $\delta^{18}O$ values between 15‰ and 16‰.

As mentioned above, the δD values of the ore stage fluids range from -89 to -143‰. The parent fluids of early ore stage sphalerite and quartz make up the part of the group from -89 to -111‰. These values indicate that the fluid was not pure meteoric water, assuming that pure meteoric water had a δD value of approximately -130 to -135‰, and that a D rich fluid, such as primary magmatic water or thermal metamorphic water, was mixed with the meteoric water. These values may also indicate very low water/rock ratios and progressive equilibration of meteoric waters with the Loon Lake batholith.

The parent fluids of later ore stage quartz and sphalerite had δD values of between -132 and -143‰, indicating that the fluid was probably nearly pure meteoric water. According to the calculated parent fluid $\delta^{18}O$ values, this fluid had also undergone oxygen exchange with the wall rocks, which raised its $\delta^{18}O$ value by approximately 23‰.

Fluid from the one post-ore stage calcite tested had a δD value of -139‰, again indicating meteoric water. The calculated $\delta^{18}O$ value of the parent fluid is -1‰, indicating that the fluid had undergone oxygen exchange with the wall rocks, this time raising its $\delta^{18}O$ value by approximately 17‰. The parent fluid of the very late calcite had a δD value of -127‰ and a calculated $\delta^{18}O$ value of -11‰ so its $\delta^{18}O$ value was raised by 6‰. Fluids from all secondary inclusions have δD values which are compatable with meteoric water.

All samples for which both δD and $\delta^{18}O$ values are available fall within the narrow δD range of -127 to -143‰. While there is a slight separation between the δD values of the parent fluids of the pre-ore and ore stage minerals, the error bars of these two groups - as well as those of the post-ore and very late calcite - overlap, and may thus represent a single δD value. Alternatively, the pre-ore stage fluids may actually have had a slightly higher δD value than the ore stage fluids, possibly reflecting a change in the δD value of the areas rain water with time. δD variations within the parent fluid may have been caused by low temperature evaporation, fluid mixing or by incomplete separation of the primary and secondary fluids during decrepitation. This seems to be the case as secondary fluid δD values generally fall on, or slightly below, the main range of the primary fluids

The $\delta^{18}O$ values of these samples range from -11‰ to 10‰, probably reflecting varying degrees of oxygen exchange with varying temperature, residence time and water to rock ratios. If this is the case a line drawn at the average δD value, approximately -135‰, should intersect the meteoric water line at the fluid's original $\delta^{18}O$ value, i.e., approximately -18‰(SMOW).

The measured δD values of the parent fluids correlate closely with those of present-day surface waters in the mine area which, according to Taylor (1979), have δD values of between -125‰ and -140‰. This is not surprising as the δD values of rainwater seem to have remained fairly constant for the last 150 my (Taylor 1979).

## VII. SULFUR ISOTOPES

### A. INTRODUCTION TO SULFUR ISOTOPES

Sulfur isotope studies make use of the fact that there are four naturally occuring stable isotopes of sulfur ; $^{32}S$, 95.02%; $^{33}S$, 0.75%; $^{34}S$, 4.21%; and $^{36}S$, 0.02%. Due to their abundance and relatively large mass difference, $^{32}S$ and $^{34}S$ are the most commonly used isotopes in sulfur isotope studies. The standard used in sulfur isotope studies is troilite from the Canyon Diablo meteorite, the $^{34}S/^{32}S$ ratio of which is approximately 0.0450045, and whose $\delta^{34}S$ value is defined as 0.0‰. This value is almost exactly the same as that of terrestrial igneous sulfur, making it a reasonable standard to use. The relative $^{34}S$ enrichment is calculated in a manner identical to that described for the oxygen isotopes.

Because of their mass differences, the behaviour of the sulfur isotopes differ during chemical and physical reactions. For example ; During biological reactions in which sulfur is converted to $H_2S$, the $H_2S$ is depleted in $^{34}S$ with respect to the parent sulfur. Conversly, during sulfur equilibrated precipitation of sulfide minerals, elements such as iron which have high bond strengths form sulfides which are enriched in $^{34}S$ with respect to the sulfides of elements with lower bond strengths, such as lead. Thus, pyrite in a given deposit is generally richer in $^{34}S$ than galena from the same deposit.

The degree of $^{34}S$ enrichment of pyrite over galena is a linear pressure independent function controlled by the temperature at which the minerals are deposited. The lower the temperature of formation the larger the $\Delta\delta^{34}S$ value, or difference between the $\delta^{34}S$ values of the two minerals. It is thus possible to use the $\Delta\delta^{34}S$ between two coeval/cogenetic minerals to determine their temperature of formation (Tatsumi 1965). Any sulfide mineral pair may be used for such a determination, but sphalerite/galena pairs generally seem to give the best results. All proceeding references to '$\Delta^{34}S$' will refer to $\Delta\delta^{34}S$(sphalerite-galena) unless otherwise specified.

The temperature of formation of a sphalerite/galena pair may be calculated using the equation:

$$T = [(0.89)^{*} \times 10^{3}] / \Delta^{34}S^{5}$$ (Ohmoto and Rye 1979).

Where:

T = temperature of formation in degrees Kelvin.

$\Delta^{34}S$ = absolute difference between the $\delta^{34}S$ values of the sphalerite and galena.

* - this is not the value quoted in the Ohmoto paper. The value varies widely between different authors and experiments, ranging from approximately 0.963 (Sakai 1968) to 0.62 (Grootenboer 1969). A value of 0.89 was used in this study. This value is slightly higher than that recommended by Ohmoto and Rye (1979) and slightly lower than that used by Dr. H. Krouse. It also gives formation temperatures which agree fairly closely with those found during the fluid inclusion study.

In addition to their usefulness in determining depositional temperatures, $\delta^{34}S$ values of sulfides may be used to calculate the initial sulfur isotope composition of their parent fluid. This calculation is complex and because the $\delta^{34}S$ value of any sulfide is controlled not only by the temperature at which it was deposited but also by the sulfur isotope composition of the parent fluid and the relative abundances of the sulfur species $H_2S$, $HS^-$, $S^{2-}$ and $SO_4^{2-}$ in solution, its accuracy is dependent upon many factors. $H_2S$ and $SO_4^{2-}$, stable in low $fO_2$ / acidic-to-neutral environments, and high $fO_2$ / basic-to-neutral environments respectively, are the most important of the four. This is because the $\Delta\delta^{34}S$ between $H_2S$, $HS^-$ and $S^{2-}$ is minor, approximately 1‰ at 200°C, compared to that between $H_2S$ and $SO_4^{2-}$, which is nearly 32‰ at 200°C (Ohmoto 1972).

The ratio of $H_2S$ to $SO_4^{2-}$ in solution is controlled by the pH, $fO_2$, $fS_2$ and ionic strength of the parent fluid. Therefore, in order to calculate the sulfur isotope composition of the parent fluid its physico-chemical makeup must be defined. A fluid with a high $fO_2$ will favor the stability of $SO_4^{2-}$ over $H_2S$ and, because the $SO_4^{2-}$ ion concentrates $^{34}S$, the $\delta^{34}S$ value of any $H_2S$ present would be lowered. Sulfides precipitated by such a fluid would have lower $\delta^{34}S$ values than would those precipitated by a low $fO_2$, $H_2S$-rich fluid because the $\delta^{34}S$ values of sulfides are similar to those of the $H_2S$ in solution. Sulfides with high $\delta^{34}S$ values were therefore probably deposited by a fluid with either a low $fO_2$, a high initial $\delta^{34}S$ value, or both.

## B. SULFUR ISOTOPE STUDY

### Method

Fourteen sulfide mineral separates were obtained from ore stage vein material from both the Madre and Hoodoo levels. Six of the separates were sphalerite, six were galena and two were freibergite. Lack of suitable sample material precluded the use of pyrite or barite.

In the case of galena and sphalerite only samples that appeared to be in equilibrium were used. This allowed not only the determination of the absolute $\delta^{34}S$ vaue of each sulfide but also the $\Delta\delta^{34}S$(sphalerite-galena) value and the calculation of the temperature at which the sphalerite/galena pairs were deposited. As freibergite was generally deposited late in the vein sequence it was rarely in equilibrium with either sphalerite or galena.

Sulfide samples were separated, crushed and picked to ensure sample purity. The crushed and cleaned samples were sent to Dr. H. Krouse's lab in the University of Calgary where they were reacted under vacuum with a half-and-half $Cu_2O$-CuO mixture at approximately 1000°C for one half hour. $SO_2$ derived from this reaction was frozen off and purified, then analysed by mass spectrometry to determine the sulfur $^{34}S/^{32}S$ ratio of each separate.

### Analytical Results

All the sphalerite $\delta^{34}S$ values lie between 9.3‰ and 11.9‰, a range of only 2.6‰. The galena $\delta^{34}S$ values lie between 4.5‰ and 7.9‰, for a total range of only 3.4‰. The complete separation of the $\delta^{34}S$ values for sphalerite and galena seems to indicate that the minerals are in equilibrium with respect to $^{34}S$ (Table 7-1). The $\delta^{34}S$ values of the freibergite separates are 8.9‰ and 10.3‰, well within the $\delta^{34}S$ range of the sphalerite and galena. All sulfides are thus enriched in $^{34}S$ and fall within the narrow range of $8.2 \pm 3.7$‰.

**Table 7-1**

**Sulfide $S^{34}$ values and sulfur isotope geothermometry results for sphalerite and galena from the Deer Trail Mine, Washington, U. S. A.**

| Sample No. | Location | galena $\delta^{34}S$ value ± 0.1‰ | sphalerite $\delta^{34}S$ value ± 0.1‰ | tetrahedrite $\delta^{34}S$ value ± 0.1‰ | Δ (sphalerite - galena) ± 0.2‰ | Depositional temperature °C |
|---|---|---|---|---|---|---|
| DTM - 14 | Main Madre stope | 7.9 | 11.9 | ---- | 4.0 | 172 ± 24 |
| DTM - 30 | Madre haulageway | 7.5 | 11.0 | ---- | 3.5 | 203 ± 28 |
| DTM - 54 | Madre winze | 5.7 | 11.1 | 8.9 | 5.4 | 110 ± 17 |
| DTM - 57 | Madre winze | 6.6 | 11.3 | 10.3 | 4.8 | 133 ± 20 |
| DTM - 63 | Hoodoo winze | 4.5 | 9.3 | ---- | 4.8 | 133 ± 20 |
| DTM - 67 | Hoodoo haulageway | 7.3 | 10.0 | ---- | 2.7 | 269 ± 38 |

Rye (1974) tested numerous sphalerite/galena pairs and compared the calculated $\Delta\delta^{34}S$ depositional temperatures to those determined by fluid inclusion homogenization tests. Even within single sphalerite samples the $\delta^{34}S$ value varied up to 0.8‰. $\delta^{34}S$ variations were also noted in galena samples, though the maximum range was only 0.6‰. Considering such intrasample ranges, it is remarkable that the total variation of $\delta^{34}S$ values for sphalerite was only 2.6‰, and only 3.4‰ in the case of galena. This seems to indicate that conditions during the ore stage were quite stable with respect to pH, salinity and sulfur speciation within the hydrothermal fluid.

**Sulfur Isotope Geothermometry**

Temperature determinations based on $\Delta^{34}S$ measurements are rarely as precise as assumed. Even if the sphalerite/galena pair were in equilibrium, and the mineral separates were absolutely pure there would still be a large error in the calculated temperature. This error is caused by uncertainties from two separate sources.

The first source of uncertainty is the equation representing the degree of fractionation between sphalerite and galena at any given temperature. In the equation ; $T = [(0.89) \times 10^3] / \Delta^{34}S^{\cdot 5}$, the actual value of the constant is $0.89 \pm 0.03$. This $\pm 0.03$ range represents a possible temperature variation of $\pm 16$°C at 200°C.

The second source of uncertainty is the fact that any $\delta^{34}S$ determination is accurate to only $\pm 0.1$‰. When a pair of $\delta^{34}S$ values are used, as in a temperature calculation, the error rises to $\pm 0.2$‰, representing a temperature range of $\pm 12$°C at 200°C. Taken together these uncertainties produce a total temperature error of approximately $\pm 28$°C at 200°C. The errors listed in Table 7-1 have been calculated for each sample, as the size of the error varies with temperature.

Sample DTM-54 has a calculated temperature of formation of 112°C, well below the temperature of ore stage deposition as indicated by fluid inclusion studies. This low temperature is indicated by a large $\Delta^{34}S$ value, and may be in error partly due to an impure sphalerite separate. The sphalerite contained tiny veinlets of pyrite which were very difficult to remove from the crushed sample. Such contamination would probably have raised the apparent $\delta^{34}S$ value of the sphalerite, thus increasing the $\Delta^{34}S$ value and lowering the apparent temperature of co-precipitation. Even if the 11‰ sphalerite contained 10 volume% of pyrite with an assumed value of 14‰, however, this effect alone could not have produced such a low apparent temperature; it requires that the galena and sphalerite be in disequilibrium with respect to $^{34}S$. Evidence that the indicated temperature is incorrect is the fact that pseudo-secondary inclusions in this sample homogenized at approximately 200°C, so the material was probably deposited at even higher temperatures.

The calculated temperatures of formation for the other five sphalerite/galena pairs range from 133±20°C to 269±38°C. Within their errors, all values fall within the temperature limits of the ore stage of deposition, 150°C to 250°C as determined in the fluid inclusion study. A larger number of sphalerite/galena pairs may have provided a more complete and reliable statistical range of formation temperatures, unfortunately very few such pairs were available for study.

The two lowest temperature values, both 153°C (calculated by adding the maximum error to the temperature value), were determined for samples containing abundant freibergite and other sulfosalts which were intergrown with the sphalerite and galena. These other sulfosalts were not present in the other three samples. Freibergite was also very rare in these samples and was present only as fracture-fill or overgrowths. Since most sulfosalts were deposited in the later part of the ore stage the sulfide/sulfosalt intergrowth probably indicates that the two low temperature samples were formed then. If so it seems reasonable that they reflect the relatively low temperatures present at that time, while other sphalerite/galena pairs reflect depositional temperatures at various points throughout the ore stage.

## VIII. FLUID CHEMISTRY

### A. METHOD

The $\delta^{34}S$ value of a sulfide mineral is controlled by the temperature at which it is deposited, the $\delta^{34}S$ value of the parent fluid, and the relative abundances of sulfur species in solution (Rye and Ohmoto 1974). The relative abundances of the sulfur species are controlled by the temperature, $fO_2$, and pH of the solution so, if the chemistry of the fluid can be approximated, and the $\delta^{34}S$ values of sulfides deposited by it are known, it is possible to determine the dominant sulfur species at the time of mineral deposition. Once this is known the $\delta^{34}S$ value of the parent fluid may be calculated. This value may indicate the source of the sulfur in the fluid. Their are four major sources of sulfur for such fluids;

1. Sulfides in nearby intrusions, or sulfur in fluids originating from these intrusions.
2. Syngenetic or diagenetic sulfides/sulfates within the host rocks.
3. Sulfates in separate evaporitic units within or near the host rocks of the deposit.
4. Sea water sulfate or sulfate in connate brines or formation waters.

The temperature, salinity, and approximate pressure on the hydrothermal fluid during the ore stage have been previously determined through the study of fluid inclusions. To determine which sulfur species was dominant, the pH and $fO_2$ of the fluid must now be calculated.

Holland (1965) suggests that in low- to medium-temperature hydrothermal deposits the fugacity of $CO_2$ probably ranges between approximately .01 and 100 atmospheres, log $fCO_2$ values would thus range from about -2 to +2. Deposits hosted in carbonates should have $fCO_2$ values in the upper part of this range. This is relevant as the location of the boundary between the calcite and anhydrite dominated fields, plotted on an $fS_2$ vs. $fO_2$ diagram, is partially controlled by the $fCO_2$ in the system. The higher the $fCO_2$, the higher the $fO_2$

necessary to stabilize anhydrite, or $CO_2$ in the case of the graphite/$CO_2$ boundary. As calcite and $CO_2$ are usually dominant over graphite and anhydrite in this type of deposit, these two boundaries are useful in delimiting the possible range of fluid chemistry with respect to $fO_2$, $fS_2$, and pH.

At $\log fCO_2$ values greater than or equal to +2, separate $CO_2$ inclusions should be formed (Holland 1965). The $fCO_2$ during the ore stage was probably fairly high, as indicated by the presence of abundant $CO_2$/brine inclusions and by the presence of rare pure $CO_2$ inclusions in pre-ore stage material. Such $CO_2$ inclusions are not found in ore stage material, so the $\log fCO_2$ during the ore stage is assumed to have had a maximum value of approximately +1.5. A minimum $\log fCO_2$ value of -0.5 was chosen, which is somewhat lower than that indicated by Holland (1965).

The pH of a solution which contains $CO_2$ in equilibrium with calcite, such as the Deer Trail veins, should be buffered by reactions involving calcite and $CO_2$. The following expression includes terms for the dissociation of calcite to $Ca^{+2}$ and $CO_3^{-2}$ ions, as well as $H_2CO_3$ to $H^+$ and $CO_3^{-2}$ ions, and may be used to calculate the pH of a solution in terms of its physico-chemical parameters at given pressures and temperatures;

$$(3)\log\alpha H^+ = (2)\log\alpha Ka + \log\alpha Kb + (2)\log B + (2)\log fCO_2 + \log\alpha Ca^{+2} - \log Kc - \log 2 - \log\alpha HCO_3^-$$ (Robinson 1971; see Appendix)

Where;

Ka = Kequilibrium of the reaction ; $H_2CO_3 \rightarrow H^+ + HCO_3^-$, at temperature T.

Kb = Kequilibrium of the reaction ; $HCO_3^- \rightarrow H^+ + CO_3^{-2}$, at temperature T.

B = 55.5 ÷ Henry's Law constant for $CO_2$, at temperature T.

$fCO_2$ = the fugacity of $CO_2$ in the system

$\alpha Ca^{+2}$ = the activity of the $Ca^{+2}$ ion in solution.

Kc = Kequilibrium of the reaction ; $CaCO_3$ (min) $\rightarrow Ca^{+2} + CO_3^{-2}$, at temperature T.

$\alpha HCO_3^-$ = the activity of the $HCO_3^-$ ion in solution.

This, and all subsequent diagrams were calculated at 80 bars, as this was the absolute minimum pressure of formation of the veins. Higher pressures shift the boundaries of the gas controlled phases but have little effect on the stability fields of the solid phases. Increased pressure does not alter the dominant sulfur species in solution, as determined later in this chapter.

The calcite/$CO_2$ buffered pH of a system may be calculated at any temperature and $f$ $CO_2$ value. Figure 8-1 is a graph of this relationship with buffered pH lines drawn for log$f$ $CO_2$ values of -2, 0, and +2. It shows that at 250°C a solution with a log$f$ $CO_2$ value of between -0.5 and +1.5 will have a buffered pH of between 5.2 and 6.2. This is a reasonable range as neutral pH at this temperature is 5.57. A near neutral pH is indicated because even though the veins are hosted in carbonate rocks, very little dissolution of the wall rocks is evident.

An $fO_2$ vs. $fS_2$ diagram of the stable mineral phases at the temperature and pressure of interest may now be used to determine the approximately fugacity of oxygen in the hydrothermal system. Vein minerals deposited during the early ore stage include calcite, quartz, sphalerite, galena, chalcopyrite, and pyrite. Of these calcite, chalcopyrite, and pyrite have useful ranges and limits of stability, while the others are stable over very wide ranges of $fO_2$ and $fS_2$. Wall rocks adjacent to ore stage vein material contain calcite, quartz, pyrite, hematite, kaolinite and muscovite. Again, the useful minerals include calcite and pyrite, but this time with the addition of hematite. Combining these two assemblages requires that pyrite, hematite, calcite, and chalcopyrite all be stable at the $fO_2$, $fS_2$, pressure and temperature conditions prevalent at the time of deposition. $CO_2$ must also be stable as it was present in the hydrothermal fluid.

Figure 8-2 is an $fO_2$ vs. $fS_2$ diagram of the iron-sulfur-oxygen system at 250°C and 80 bars. The activity of FeS is assumed to be .55 in the pyrite and magnetite fields (Barton and Skinner 1979). Problems related to the monoclinic pyrrhotite field have been ignored as they do not effect the area of interest. The pyrrhotite, pyrite, hematite and magnetite fields are plotted, along with the chalcopyrite + (pyrite / hematite / magnetite) vs. bornite +

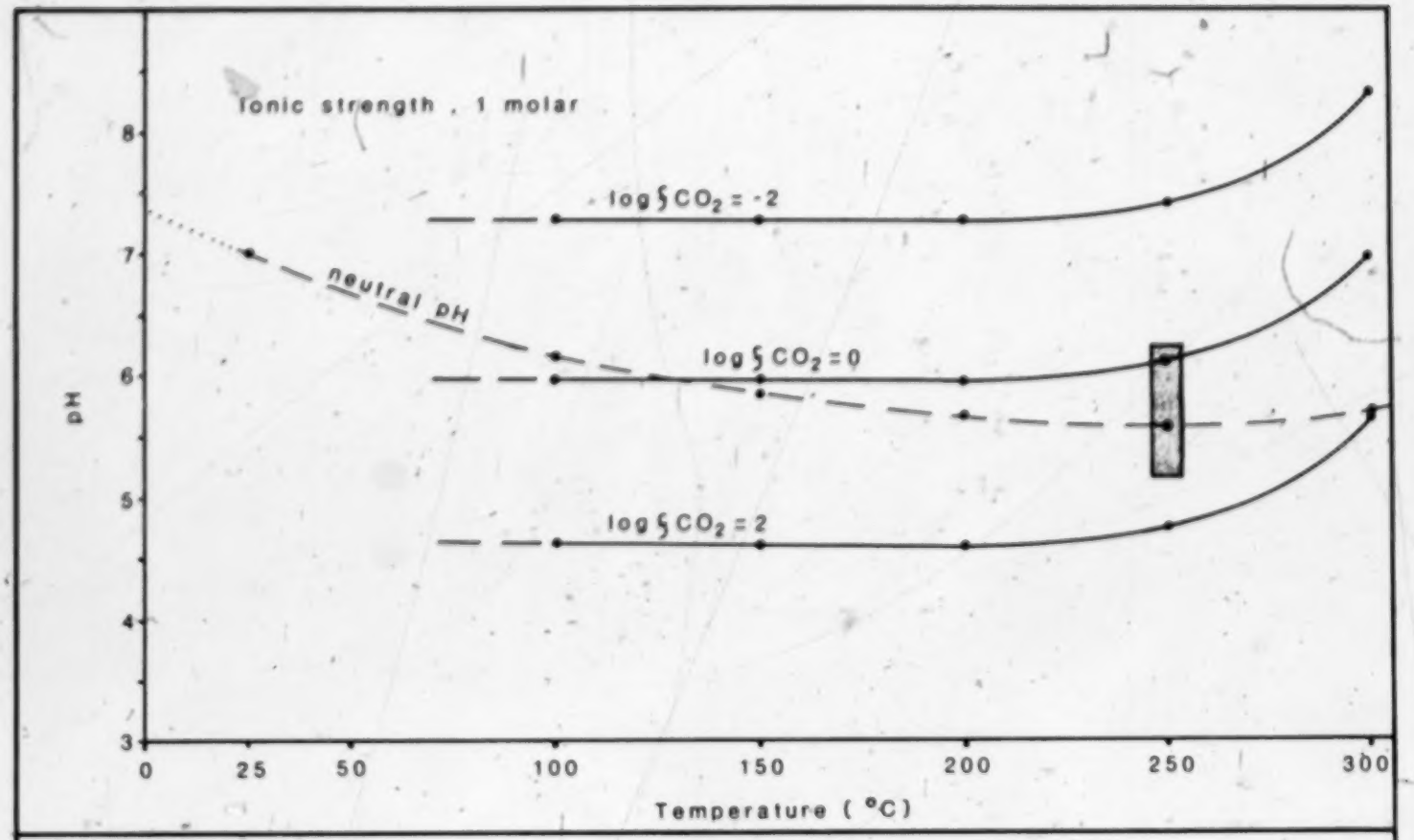


FIG. 8–1 Temperature vs. pH at given $CO_2$ fugacities.

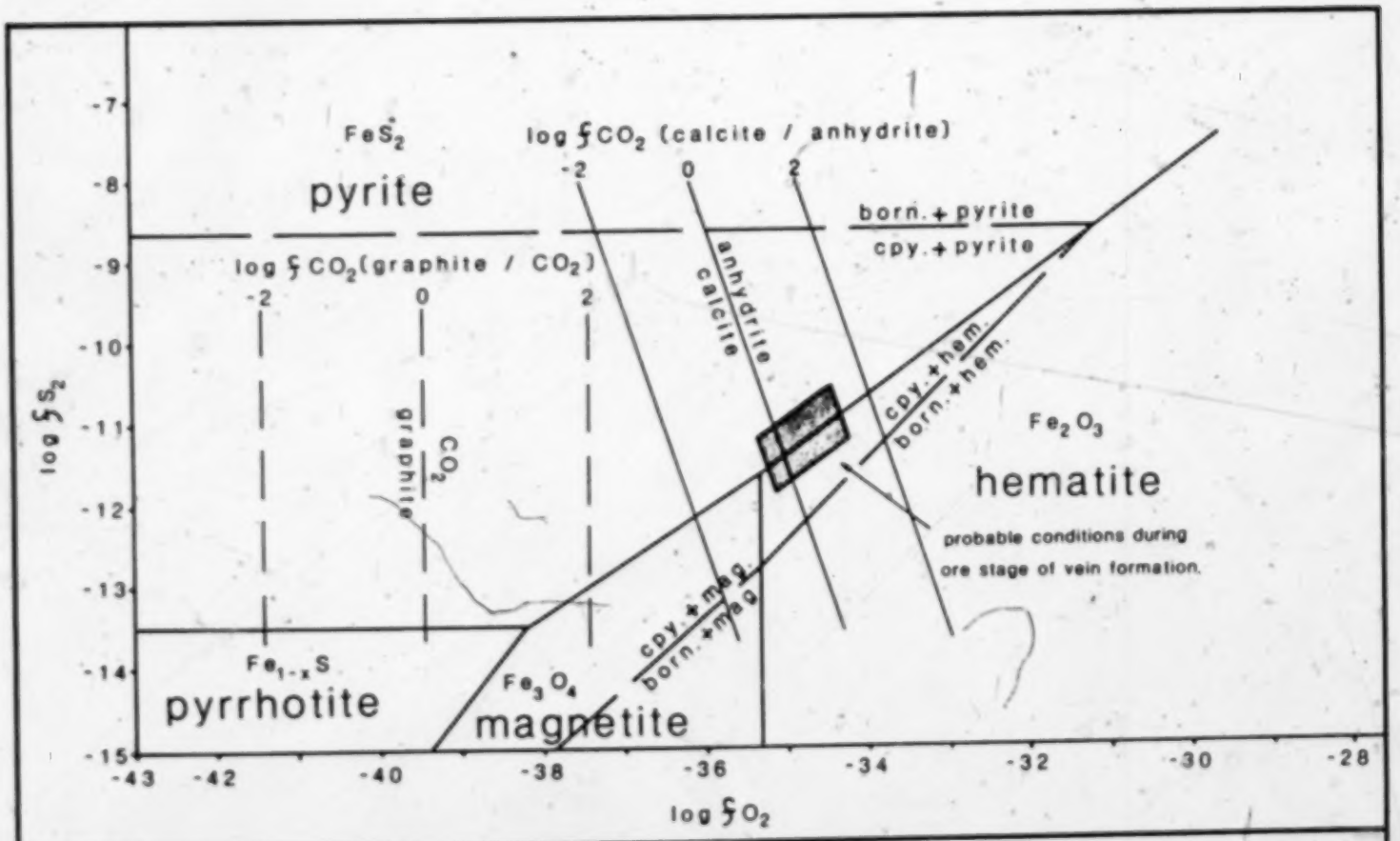


**FIG. 8–2** Log$fS_2$ vs. log $fO_2$ diagram : Fe, O, S system with calcite, anhydrite, graphite and $CO_2$ fields at 250°C and 80 bars.

(pyrite / hematite / magnetite) boundaries. Also plotted are the calcite vs. anhydrite and graphite vs. $CO_2$ boundaries at $\log f CO_2$ values of -2, 0, and +2. The shaded area indicates probable conditions during the early ore stage of vein formation. The area is limited to the left and right by the calcite vs. anhydrite line at $fCO_2$ values of -0.5 and +1.5 respectively. The top and bottom limits are drawn where the alternate mineral (i.e., hematite in the pyrite field or pyrite in the hematite field) has an activity of 0.1, or 10% that of the dominant mineral. This limit was chosen because the pyrite and hematite abundances in the wall rock are of the same order of magnitude, neither being obviously dominant over the other. This area includes $\log f S_2$ values between approximately -10.4 and -11.8, and $\log f O_2$ values from approximately -34.2 to -35.3.

Now that the appropriate ranges of $\log f O_2$ and pH have been determined, they may be used to find the dominant sulfur species in the hydrothermal fluid during the early ore stage. Figure 8-3 delineates the stability fields of $HS^-$, $H_2S$, $SO_4^{2-}$, and $HSO_4^-$ at 250°C and 80 bars. Heavy lines outline the fields of dominance of each sulfur species. Light lines represent 90% dominance of the species within whose field it lies, with a 10% contribution from the species in the adjacent field, while light dashed lines represent an activity ratio of 99% vs. 1%. The effects of $S^{2-}$ have been ignored in calculation of the 90% and 99% lines within the $HS^-$ field as the effects are very minor.

The stippled area, bounded by the log $fO_2$ and pH values determined above, lies entirely within the $H_2S$ field, most of it within the 90% activity line, indicating that $H_2S$ was the dominant sulfur species in solution during the early ore stage. The narrow range of $\delta^{34}S$ values for sphalerite and galena indicates that throughout the ore stage of deposition the parent fluid was relatively stable with respect to the dominant sulfur species in solution. Some variation probably occurred but the reduced sulfur species, i.e., $H_2S$ and $HS^-$, were probably always dominant over the oxidized sulfur species, i.e., $SO_4^{2-}$ and $HSO_4^-$. If $SO_4^{2-}$ had become dominant over $H_2S$, sulfur partitioning would have lowered the $\delta^{34}S$ value of the $H_2S$ and produced significant variations in the $\delta^{34}S$ values of any sulfides deposited.

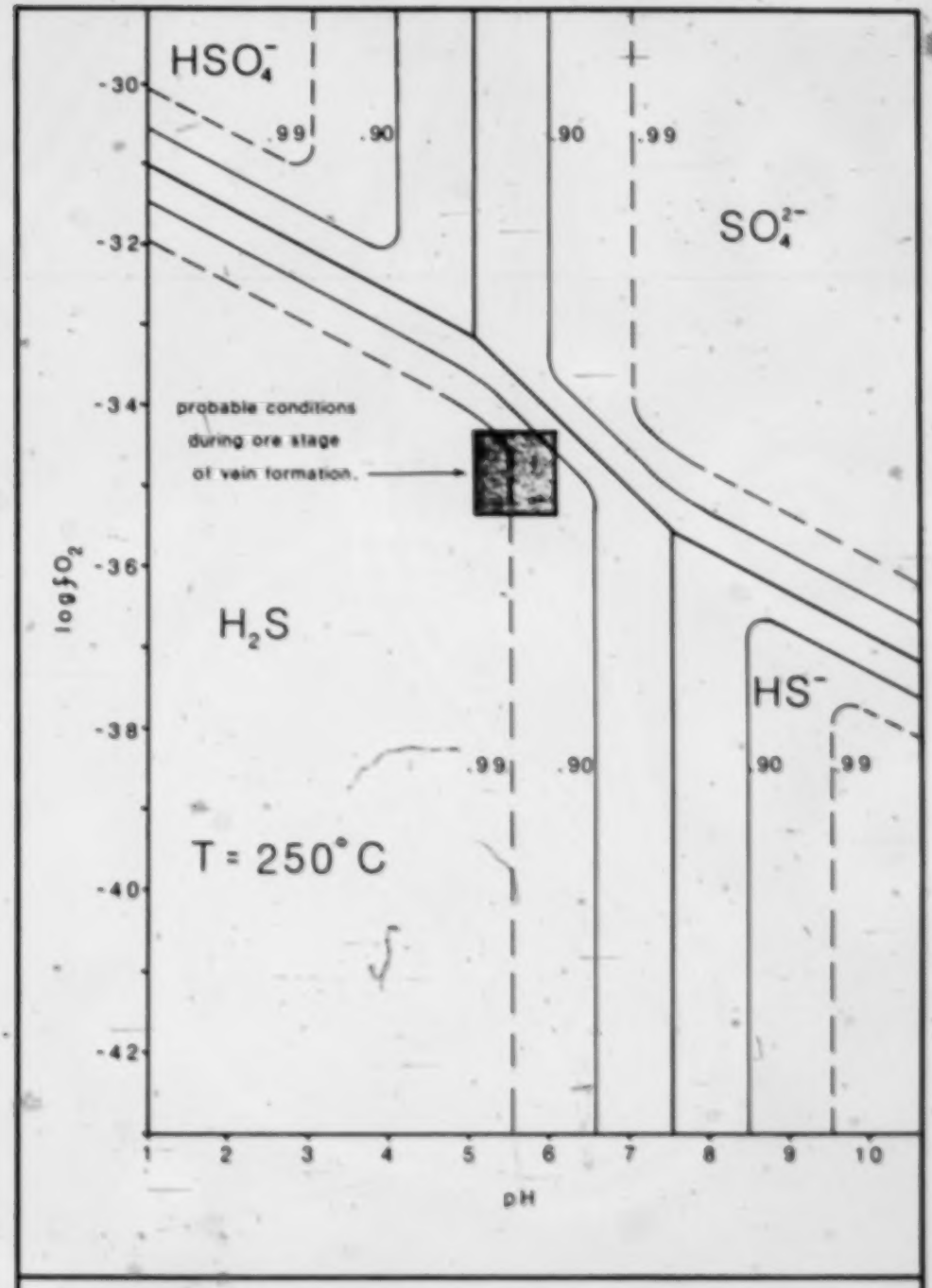


FIG. 8–3 Log $f_{O_2}$ vs. pH diagram of aqueous sulfur species.

The $\delta^{34}S$ value of the hydrothermal fluid may now be calculated through the use of the known $^{34}S$ fractionation values between sulfides and $H_2S$. Equations representing this fractionation are given below.

$$\Delta\delta^{34}S(\text{sphalerite-}H_2S) = [(0.12 / T^2) \times 10^6]$$

$$\Delta\delta^{34}S(\text{galena-}H_2S) = [(-0.67 / T^2) \times 10^6]$$

These values give results that correlate with the sphalerite/galena temperature fractionation used previously, as they must to be internally consistent, and are within the range proposed by Rye and Ohmoto (1979). For example; sphalerite deposited at 200°C will have a $\delta^{34}S$ value which is 0.54‰ higher than that of the $H_2S$ in solution, while galena deposited under identical conditions will have a $\delta^{34}S$ value which is 2.95‰ lower than the $H_2S$. At 250°C the sphalerite will be 0.48‰ greater, and the galena 2.40‰ lower, than the $\delta^{34}S$ value of the $H_2S$

Table 8-1 lists the samples tested, the $\delta^{34}S$ values of each sphalerite and galena sample, the calculated temperature of deposition of each sphalerite/galena pair, and the sulfur fractionation values for sphalerite and galena at the calculated temperature of formation. The formation temperatures are rounded to the nearest 25°C and are constrained to lie between 150°C and 250°C. Also listed are the calculated $\delta^{34}S$ values of the parent fluids of each sphalerite and galena sample, based on the calculated formation temperature for each sphalerite/galena pair.

The calculated $\delta^{34}S$ values for the parent fluid of the sphalerite and galena from each sample pair are very similar, the maximum variation being 0.4‰ in the case of DTM-63. If the calculated $\delta^{34}S$ values for the parent fluids of a sphalerite/galena sample pair were very dissimilar they would have to be disregarded, but the fact that all pairs are internally consistent with respect to $\delta^{34}S$ values, indicates that they are in equilibrium with respect to sulfur.

**Table 8-1**

**Calculation of parent fluid $\delta^{34}S^{o}/_{oo}$ value from $\delta^{34}S^{o}/_{oo}$ values of galena and sphalerite samples from the Deer Trail Mine, Washington, U.S.A.**

| Sample No. | $\delta^{34}S^{o}/_{oo}$ of sphalerite | $\delta^{34}S^{o}/_{oo}$ of galena | Formation Temperature °C (T) | $\Delta^{34}S$ (sphal - $H_2S$) at temp. T. | $\Delta^{34}S$ (gal - $H_2S$) at temp. T. | Calculated $\delta^{34}S^{o}/_{oo}$ value of sphalerite parent fluid. | Calculated $\delta^{34}S^{o}/_{oo}$ value of galena parent fluid. |
|---|---|---|---|---|---|---|---|
| DTM - 14 | 11.9 | 7.9 | 172 | 0.6 | -3.4 | 11.3 | 11.3 |
| DTM - 30 | 11.0 | 7.5 | 203 | 0.5 | -3.0 | 10.5 | 10.5 |
| DTM - 57 | 11.3 | 6.6 | 150 | 0.7 | -3.7 | 10.6 | 10.3 |
| DTM - 63 | 9.3 | 4.5 | 150 | 0.7 | -3.7 | 8.6 | 8.2 |
| DTM - 67 | 10.0 | 7.3 | 250 | 0.4 | -2.4 | 9.6 | 9.7 |
| | | | | | Average value °/oo | 10.1 | 10.0 |

Range of $\Delta^{34}S$ values of parent fluids from 8.2 to 11.3°/oo.

The average calculated $\delta^{34}S$ value of the parent fluids of galena samples is 10.0‰, nearly identical to that of the sphalerite parent fluids at 10.1‰. The fluid from which the sulfides were precipitated probably had an average $\delta^{34}S$ value of about 10.0‰ and may have varied between 8.0‰ and 11.5‰

If the $\delta^{34}S$ value, and the $H_2S/SO_4^{2-}$ ratio of the parental fluid remains constant, and the sulfides are in equilibrium with respect to sulfur, a $\Delta^{34}S$ vs. $\delta^{34}S$(sphalerite, galena) plot of the sulfur isotope data should define two straight lines (Fig. 6-4a). One line is defined by the sphalerite data points, while the other is defined by the galena data points. If the above criteria are met these lines intersect at a point on the Y axis and, because the Y axis corresponds to an infinitely high temperature where there is no $^{34}S/^{32}S$ fractionation, the $\Delta^{34}S$ value of this line is equal to 0.0‰. The point of intersection of these two lines thus represents the $\delta^{34}S$ value of the parent fluid. In Figure 8-4a the $\delta^{34}S$ value of the parent fluid is 10.0‰. This is essentially a graphical extrapolation method of determining the same value as that found in the previous calculations and is only applicable if the sulfides were deposited under the ideal conditions defined above. These conditions do not seem to have been met during the formation of the Deer Trail veins.

Figure 8-4b is a plot of the results of this sulfur isotope study. The sphalerite and galena pairs define two lines which intersect at a point on the Y axis. Values from DTM - 63, labeled 63, are anomalous and do not correspond to the lines defined by the other four pairs of data points. This may be the result of low temperature sulfur disequilibrium or it may have been caused by a fluctuation in the $\delta^{34}S$ value of the parent fluid or a change in its $H_2S/SO_4^{2-}$ ratio. Best fit lines to the two sets of points intersect at a $\delta^{34}S$ value of about 8.5‰. This is in rough agreement with the 10‰ value calculated previously, but the associated $H_2S$ line is non-horizontal. This may indicate that the parent fluid $\delta^{34}S$ value rose with time, possibly because of initial preferential reduction of $^{32}S$ of intersticial sulfates followed by the reduction of $^{34}S$ as the light sulfur was exhausted. Such a sloped line may also have been caused by a rise of the $H_2S/SO_4^{2-}$ ratio of the fluid as deposition continued.

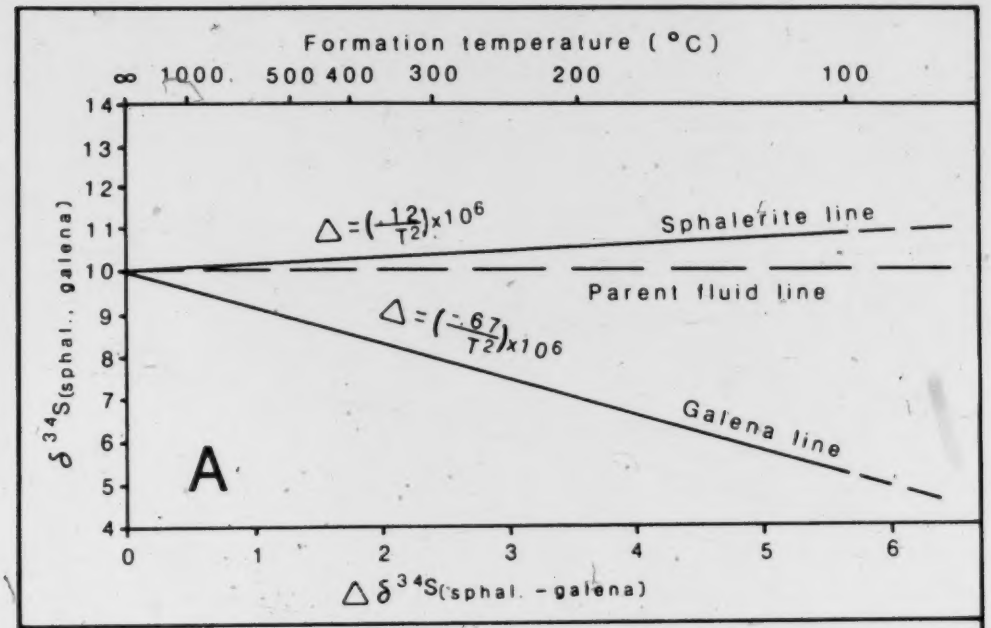


Ideal $\Delta\delta^{34}S$ (sphalerite-galena) vs. $\delta^{34}S$ (sphalerite,galena) diagram at $\delta^{34}\Sigma S = 10‰$

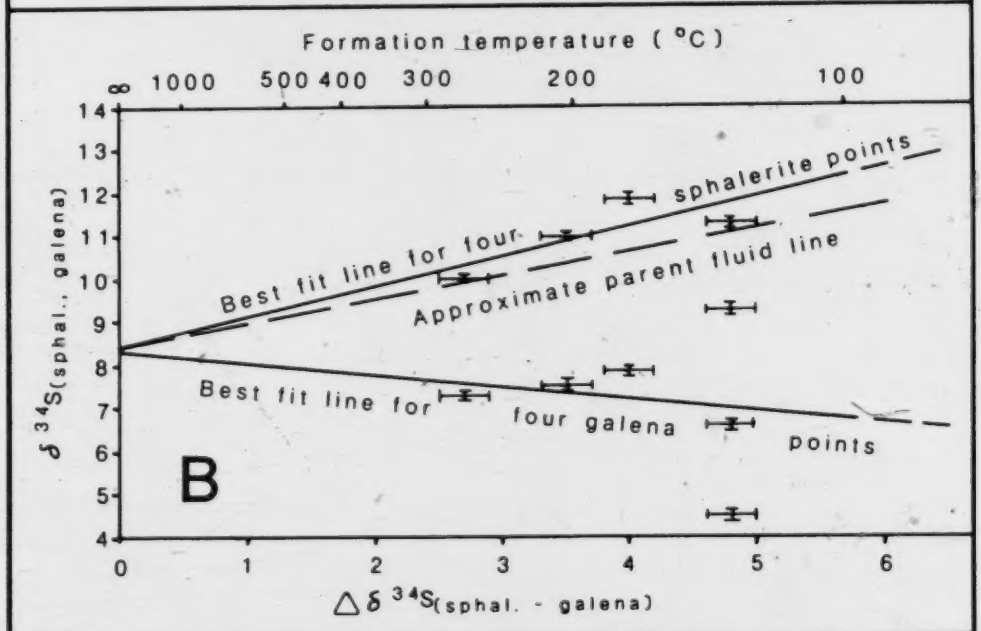
Formation temperature (°C)
∞ 1000 500 400 300 200 100
Best fit line for four sphalerite points
Approximate parent fluid line
Best fit line for four galena points
B
$\delta^{34}S_{(sphal.,\ galena)}$
$\Delta\delta^{34}S_{(sphal.\ -\ galena)}$

**FIG. 8–4** As above with data from this study.

## B. INTERPRETATION

Figure 8-5 shows the $\delta^{34}S$ ranges of the Deer Trail vein minerals, fluids, and possible sulfur sources.

Fluids in a hydrothermal system are often assumed to be driven by a deeply buried heat source. In the case of the system which formed the Deer Trail veins this heat source was probably the Loon Lake batholith. Hydrothermal fluids which penetrated the batholith could have leached sulfur from the sulfides within it and the extracted sulfur would have had a $\delta^{34}S$ value of approximately 0‰. Any sulfides deposited by this fluid, assuming the dominant sulfur species was $H_2S$, would have had $\delta^{34}S$ values of slightly less than 0‰ to approximately -5‰, depending upon the temperature of deposition and the mineral species being precipitated. The same range of $\delta^{34}S$ values would also occur if the sulfur in the fluid was derived from the intrusion in the form of primary magmatic water which contained magmatic sulfur. As the $\delta^{34}S$ values of sulfides from the Deer Trail mine range between 4.5‰ and 11.9‰, the source of sulfur in the hydrothermal fluid was probably not the Loon Lake batholith. Also, sulfides deposited by fluids containing magmatic sulfur generally demonstrate highly variable $\delta^{34}S$ values, which is not the case with the Deer Trail vein sulfides.

Though the Deer Trail series is dominated by dolostone and limestone, substantial volumes of slate, quartzite, and argillite are also present. Many of the slaty and argillic units are goethite stained and, near intrusive bodies, have been highly metamorphosed and now contain large pyrite metacrysts, especially the McHale slate (Campbell and Loofbourow 1962). This, or other sulfide rich units, could have acted as a sulfur source for any fluids circulating through them.

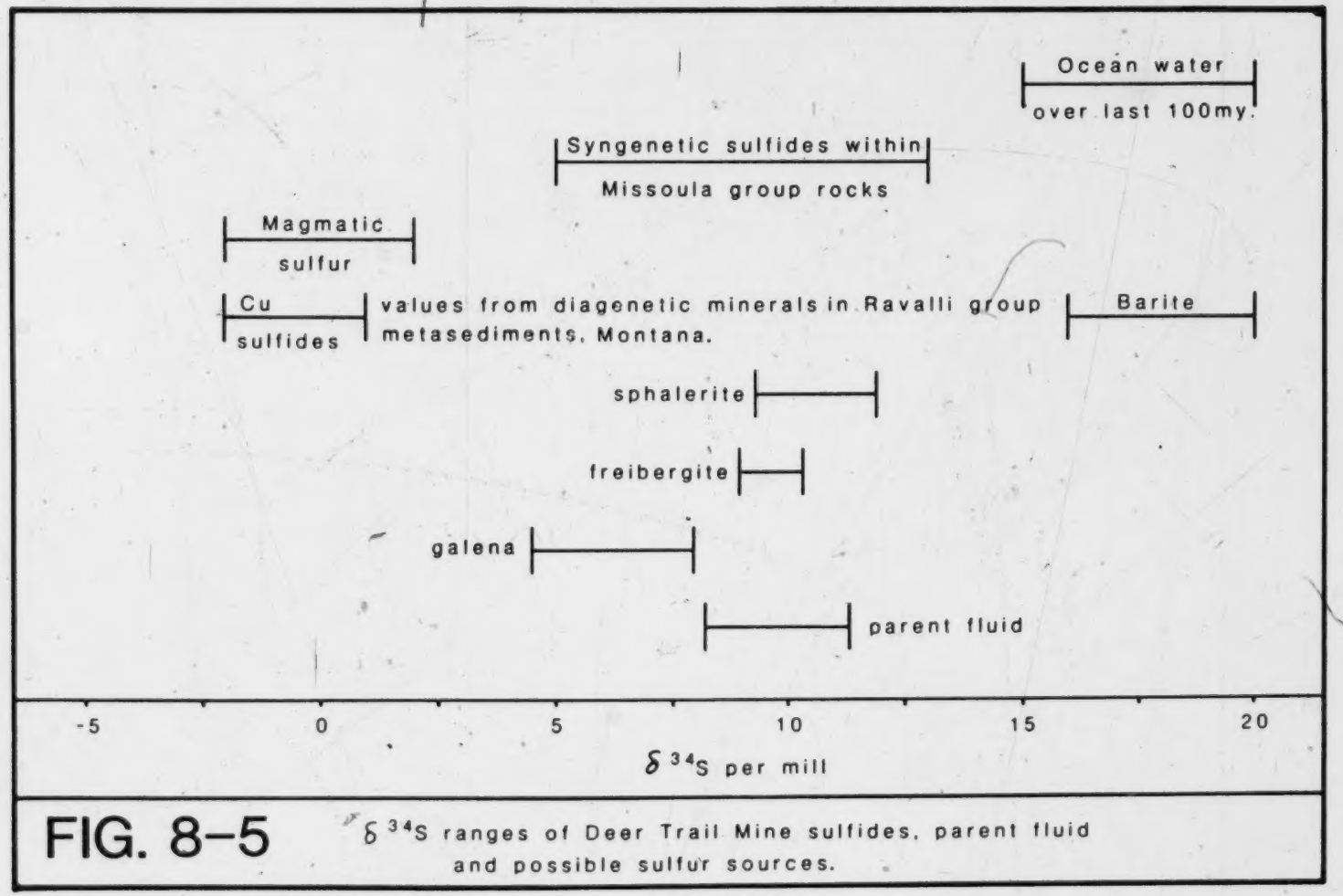


FIG. 8–5 $\delta^{34}S$ ranges of Deer Trail Mine sulfides, parent fluid and possible sulfur sources.

The Deer Trail series was deposited in a very shallow sea, as evidenced by mudcracks and ripple marks on paleosurfaces (Campbell and Loofbourow 1962). Evaporitic sulfur-bearing minerals, while not present as discrete beds, may be included as small grains within the carbonate and silty units. These could also have act as a sulfur source to any fluid circulating through the sequence and, because their volume is so large, their bulk sulfur concentration need not have been very high to supply the volume of sulfur necessary to produce a large sulfide vein deposit.

No isotope analyses of the Deer Trail series metasediments are available but Rye *et al.* (1984) conducted a sulfur isotope analysis of diagenetic barite and copper sulfides which are present in small quantities within Ravalli Group metasediments of Montana. These sediments are older than the Missoula Group but were deposited under very similar conditions so the data should be generally applicable to the Deer Trail series metasediments. The $\delta^{34}S$ values of the barite generally range from 15‰ to 20‰, though a few values fall between -5‰ and 2‰, and one sample had a $\delta^{34}S$ value of 6‰. The low $\delta^{34}S$ value barites were attributed to an influx of meteoric water during barite formation, while high $\delta^{34}S$ value barite was assumed to have formed in a system dominated by sea water. The copper sulfides tested had $\delta^{34}S$ values of between -3‰ and 1‰. If fluids leached this, or a similar, sediment the combined sulfur from copper sulfides and barite could have had an average $\delta^{34}S$ value of approximately 10‰. The barite $SO_4^{2-}$ would have had to have been reduced during or after leaching by the fluids so as to produce a fluid dominated by $H_2S$ and compatable with the results of this study.

Another possibility is that the sulfur was leached from pre-existing sulfide deposits. Numerous stratabound copper-zinc-lead deposits are present the Belt rocks of the northwestern states, southwestern Alberta and southeastern British Columbia (Harrison 1972 ; Clark *et al.* 1971). The Missoula Group hosts such deposits in Stevens county, though no mineable deposits have yet been found. The $\delta^{34}S$ values of sulfides in similar deposits in southwestern Alberta generally fall between 5‰ and 13‰, though a few values do lie well above or below this range (Morton *et al.* 1974).

Any hydrothermal fluids indiscriminatly leaching sulfur from these deposits would have acquired a sulfur isotope 'signature' similar to that of the original sulfides, i.e., $\delta^{34}S$ values between 5‰ and 13‰, which correlates with the calculated $\delta^{34}S$ values of the parent fluids of the Deer Trail veins.

Whether the ultimate sulfur source was the partially evaporitic sequence of Deer Trail series metasediments, stratabound sulfide deposits within these metasediments or a combination of both, the source reservoir volume was large and the parent fluid could have retained a fairly consistant $\delta^{34}S$ value, as seems to have been the case with the sulfides from the Deer Trail veins. Some minor variations in either the $\delta^{34}S$ value or the $H_2S/SO_4^{2-}$ ratio of the parent fluid probably occurred, but the $\delta^{34}S$ values of the Deer Trail vein sulfides still correspond to those of sulfides deposited by fluids containing dominantly sedimentary-derived sulfur.

# IX. SUMMARY AND CONCLUSIONS

All the data gathered during this study indicate that the Deer Trail veins are a fairly typical mesothermal deposit. The veins developed through the infilling of dilatent fractures in a hydrothermal system which was driven by the cooling Loon Lake batholith. The veins, parallel and longitudinal faults, and the $F_1$ and $F_2$ fold axes all have parallel to sub-parallel strikes and trends, so the dilatent fractures may be genetically related to these structures.

The pre-ore stage was dominated by the deposition of quartz with minor pyrite and calcite, between approximately 250°C and 300°C. The hydrothermal fluid was dominated by meteoric water with a $\delta D$ value of approximately -130‰. As the $\delta^{18}O$ value of this fluid was between 8‰ and 10‰ it had probably undergone oxygen exchange with the host rocks, increasing its $\delta^{18}O$ value by about 27‰. Fluid salinity was approximately 8 wt.% NaCl equivalent and it contained substantial $CO_2$, which may have formed during thermal degradation of the carbonate-rich country rocks by the Loon Lake batholith. System pressure was probably between 500 and 1000 bars, and had an absolute minimum value of 80 bars.

Ore stage sulfide deposition took place between 250°C and 150°C. Early ore stage fluids had $\delta D$ values between -89‰ and -111‰, indicating the presence of a D-rich fluid, possibly magmatic water from the batholith or metamorphic water generated in the metamorphic aureole surrounding the batholith. The high D values could also have been caused by re-equilibration of meteoric water with the batholith at low water/rock ratios. Hydrothermal fluids during the rest of the ore stage had $\delta D$ values of approximately -135‰ so were nearly pure meteoric water. As the $\delta^{18}O$ value of the ore stage fluid was between 4‰ and 7‰, oxygen exchange had again raised its $^{18}O$ content, this time by about 23‰. Fluid salinity was generally near 6 wt.% NaCl equivalent, and the $CO_2$ content of the fluid fell from a high initial value to essentially nil by the end of the ore stage.

Sphalerite and galena formed during this stage had $\delta^{34}S$ values of between 4.5‰ and 11.9‰. The hydrothermal fluid therefore had a $\delta^{34}S$ value of about 10‰, indicating a sedimentary sulfur source.

Below 150°C sulfide deposition essentially ceased, barring minor amounts of pyrite associated with post-ore stage quartz. The post-ore stage fluids had a $\delta D$ value of approximately -135‰. The $\delta^{18}O$ value was approximately -4‰, so even at temperatures below 150°C oxygen exchange between the fluid and host rocks was taking place. The salinity of the post-ore stage fluid was approximately 3 wt.% NaCl equivalent, much lower than that of the ore stage.

The Deer Trail veins are very similar to other quartz-Ag-base metal vein deposits in Stevens county in several ways;

1. The deposits are dominated by quartz, sphalerite, galena and freibergite, and also contain pyrite and chalcopyrite.
2. Quartz is the dominant gangue mineral, though calcite and adularia may be present.
3. No Sb, As or Hg sulfides are present though Sb and As are present in other minerals.
4. Wall rocks around the deposits are highly altered and silicified.
5. Silver is present in freibergite and as other silver sulfosalts.

The Deer Trail mine is at the southern end of a linear array of mines which stretches to the northeast of the Deer Trail mine. (Fig 2-1). All deposits are hosted by dolostone or limestone dominated units. No major veins have been found in slaty or other incompetent units, probably because such units are unable to maintain open fractures. All deposits including the Deer Trail were formed after batholith emplacement, late Cretaceous to early Tertiary.

Mills (1977) reported that the average $\delta^{34}S$ value of galena from four discordant vein deposits like the Deer Trail veins was 9.2‰, similar to the 6‰ average value found for Deer Trail mine galena and suggesting a common source of lead for all deposits. Mineralogical and other physical similarities indicate that these deposits are genetically related. Proximity to the Loon Lake batholith, however, seems to have controlled both the density of quartz veins in an area and the silver grade of these veins. Three mines in the Deer Trail district, which is adjacent to a batholith, have produced over 100,000 oz. of silver. Two of these have produced almost, or over, 300,000 oz. of silver. The three large mines to the northeast of the Deer Trail mine; the Nevada, Double Eagle and Cleavland mines, have produced only 100,000 oz. of silver in total. Ore grades in the Deer Trail district were also higher, averaging 1500 to 2400 g/t (50 to 80 oz./t), while the Ag grade of the other three mines was approximately 300 to 600 g/t (10 to 20 oz./t).

Other mines similar to the Deer Trail mine are also present in northern Stevens county. All important silver producers are closely associated with batholithic intrusions resembling, or associated with, the Loon Lake batholith (Mills 1977).

The Coeur d'Alene mining district of Idaho Alies approximately 150 km east of the Deer Trail district. These two districts are similar in many respects. Both are rich silver producers which are hosted in Precambrian Belt metasediments and associated with Jurassic-Cretaceous quartz monzonitic intrusions. Both are probably mesothermal veins with large vertical extents and in both districts silver is present as freibergite along with other lesser sulfosalts.

Fluid inclusions in Coeur d'Alene vein quartz homogenize or decrepitate at approximately 325°C (Yates and Ripley 1985). This is somewhat hotter than the temperatures found for the homogenization of ore stage inclusions from the Deer Trail veins, but comparable to those found for the pre-ore stage. Coeur d'Alene inclusions contain brines with fluid salinities of approximately 11 wt.% NaCl equivalent and appreciable $CO_2$. There is no indication of fluid boiling in either deposit. Coeur d'Alene hydrothermal fluids had $\delta^{18}O$ of

approximately 8.5‰ and δD values of -110‰ to -140‰. The fluids were thus oxygen exchanged meteoric water very similar to those of the Deer Trail system.

Harris *et al.* (1981) analysed several tetrahedrite samples from the Sunshine mine of the Coeur d'Alene district and found that their $\delta^{34}S$ values ranged between 2.9‰ and 5.9‰ with a mean value of 4.4‰. Two galena samples from the Coeur d'Alene district had $\delta^{34}S$ values of approximately 4‰ (Ault 1962). These values are somewhat lower than those of Deer Trail mine sulfides and give a poorer indication of a sedimentary sulfur source.

In many respects the Deer Trail and Coeur d'Alene districts are very similar. Their form and mineralogy differ somewhat but their apparent age, temperature of formation and isotope signatures indicate that they were formed by similar processes. Such processes were probably controlled by large scale geological events which occurred coincidentally in the Deer Trail and Coeur d'Alene districts. These events may have extended to northern Stevens county and into southern British Columbia, though more isotope and mineralogical data are needed before anything can be stated with certainty.

## X. REFERENCES CITED


Akande, S. O., and Zentilli, M. 1984. Geologic, fluid inclusion and stable isotope studies of the Gays River lead - zinc deposit, Nova Scotia, Canada. Economic Geology, **79**, pp. 1187-1211.

Andrew, A., Godwin, C. I., and Sinclair, A. J. 1984. Mixing line isochrons : A new interpretation of galena lead isotope data from southeastern British Columbia. Economic Geology, **79**, pp. 919-932.

Ault, W. U. and Jensen, M. L. 1962. Summary of sulfur isotope standards. *In* Biogeochemistry of sulfur isotopes: National Science Foundation Symposium, Yale university proceedings. *Edited by* M. L. Jensen. pp 16-29.

Angus, S., Armstrong, B., and deReuck, K. M. 1973. International Thermodynamic Tables of the Fluid State, $CO_2$. Pergamon Press, Oxford, England. 385 p.

Bancroft, H. C. 1914. The ore deposits of northeastern Washington. U.S. Geological Survey Bulletin **#550**. 215 p.

Barton, P. B., Bethke, P. M., and Roedder, E. 1977. Environment of ore deposition in the Creede Mining District, San Juan Mountains, Colorado. III Progress toward interpretation of the ore forming fluid for the OH vein. Economic Geology, **72**, pp. 1-24.

----------., and Skinner, B. J. 1979. Sulfide mineral stabilities. *In* Geochemistry of Hydrothermal Ore Deposits. *Edited by* H.L. Barnes, John Wiley & Sons, New York, N.Y. 798 p.

----------., and Toulmin, P. III. 1966. Phase relations involving sphalerite in the Fe-Zn-S system. Economic Geology, **61**, pp. 815-849.

Bennett, E. H., and Vankatakrishman, R. 1982. A palenspastic reconstruction of the Coeur d'Alene mining district based on ore deposits and structural data. Economic Geology, **77**, pp. 1851-1866.

Bethke, P. M. and Rye, R. O. 1979. Environment of ore deposition in the Creede Mining District, San Juan Mountains Colorado: Part IV. Source of fluids from oxygen, hydrogen, and carbon isotope studies. Economic Geology, **74**, pp. 1832-1851.

Bottinga, Y., and Javoy, M. 1973. Comments on oxygen isotope geothermometry. Earth and Planetary Science Letters, **20**, pp. 250-265.

Boyle, R. W. 1968. Chemistry, Mineralogy and Geochemistry of Silver. Geological Survey of Canada Bulletin #160. 264 p.

Bozzo, A. T., Chen, H-S., Kass, J. R., and Barduhn, A. J. 1975. The properties of the hydrates of chlorine and carbon dioxide. Desalination, 16, pp. 303-320.

Brown, J. S. 1965. Oceanic lead isotopes and ore genesis. Economic Geology, 60, pp. 47-68.

Campbell, I., and Loofbourow, J. S. Jr. 1962. Geology of the magnesite belt of Stevens County, Washington. U.S. Geological Survey Bulletin #1142-F. 53 p.

----------., and Raup, O. B. 1964. Preliminary geologic map of the Hunters Quadrangle, Stevens and Ferry Counties, Washington. U.S. Geological Survey Mineral Investigations Field Map MF-276. Scale = 1:48,000.

Chryssoulis, S., and Wilkinson, N. 1983. High silver content of fluid inclusions in quartz from Guadalcazar granite, San Luis Potasi, Mexico : A contribution to ore genesis theory. Economic Geology, 78, pp. 302-318.

Clayton, R. N., O'neil, J. R., and Mayeda, T. K. 1972. Oxygen isotope exchange between quartz and water. Journal of Geophysical Research, 77, pp. 3057-3067.

Collins, P. L. F. 1979. Gas hydrates in $CO_2$ bearing fluid inclusions and the use of freezing data for estimates of salinity. Economic Geology, 74, pp. 1435-1444.

Craig, H. 1961. Standards for reporting concentrations of deuterium and oxygen-18 in natural waters. Science, 133, pp. 1833-1934.

Doe, B. R., and Stacey, J. S. 1974. The application of lead isotopes to the problems of ore genesis and ore prospect evaluation : A review. Economic Geology, 69, pp. 757-776.

Ellis, A. J. 1979. Explored geothermal systems. *In* Geochemistry of Hydrothermal Ore Deposits. *Edited by* H.L. Barnes, John Wiley&Sons, New York, N.Y. 798 p.

Fyles, J. T., and Hewlett, C. G. 1959. Stratigraphy and structure of the Salmo lead - zinc area. British Columbia Department of Mines Bulletin, 41, 162 p.

Garrels, R. M., and Christ, C. L. 1965. Solutions, minerals and equilibria. Freeman, Cooper & Company, San Fransisco. 450 p.

Goldich, S. S., Baadsgaard, Halfdon, Edwards, George, and Weaver. 1959. Investigations in radioactivity - dating of sediments. (Minnesota and Montana). American

Association of Petroleum Geologists Bulletin, **43**, pp. 654-662.

Grootenboer, J., and Schwarcz, H. P. 1969. Experimentally determined sulfur isotope fractionations between sulfide minerals. Earth and Planetary Science Letters, **7**, pp. 162-166.

Haas, J. L. Jr. 1976. Physical properties of the coexisting phases and thermochemical properties of the $H_2O$ component in boiling NaCl solutions. U.S. Geological Survey Bulletin 1421-A. 73 p.

Hackbarth, C. J., and Peterson, U. 1984. A fractionization crystalization model for the deposition of argentian tetrahedrite. Economic Geology, **79**, pp. 448-460.

Harris, R. H., Lange, I. M., and Krouse, H. R. 1981. Major element and sulfur isotopic variations in the Lower Chester vein, Sunshine Mine, Idaho. Economic Geology, **76**, pp. 706-715.

Harrison, J. E. 1972. Precambrian Belt basin of northwestern United States : Its geometry, sedimentation and copper occurances. Geological Society of America Bulletin, **83**, pp. 1215-1240.

----------., and Grimes, D. J. 1970. Mineralogy and geochemistry of some Belt rocks, Montant and Idaho. U.S. Geological Survey Bulletin, **1312**, pp. 1-49.

Hattori, K., and Sakai, H. 1979. D/H ratios, origins, and evolution of the ore-forming fluids for the neogene veins and Kuroko deposits of Japan. Economic Geology, **74**, pp. 535-555.

Hedenquest, J. W., and Henley, R. W. 1985. The importance of $CO_2$ on freezing point measurements of fluid inclusions: Evidence from active geothermal systems and implications for epithermal ore deposits. Economic Geology, **80**, pp. 1379-1406.

Helgeson, H. C. 1969. Thermodynamics of hydrothermal systems at elevated temperatures and pressures. American Journal of Science, **267**, pp. 729-804.

Hobbs, S. W., Griggs, A. B., Wallace, R. E., and Campbell, A. B. 1965. Geology of the Coeur d'Alene district, Shoshone County, Idaho. U.S. Geological Survey Professional Paper #**478**, 139 p.

Holland, H. D. 1965. Some applications of thermochemical data to problems of ore deposits II. Mineral assembleges and the composition of ore forming fluids. Economic Geology, **60**, pp. 1101-1166.

----------. 1973. Granites, solutions and base metal deposits. Economic Geology, **67**, pp. 281-301.

Hollister, L. S., and Burruss, R. C. 1976. Phase equilibria in fluid inclusions from the Khtada Lake metamorphic complex. Geochimica et Cosmochimica Acta, **40**, pp. 163-175.

Hunting, M. J. 1966. Washington mineral deposits. Canadian Institute of Mining and Metallurgy Special Volume, **8**, pp. 209-214.

Hurlbut, C. S., and Klein, C. 1977. Manual of Mineralogy, 19th edition. John Wiley & Sons, New York, N.Y. 532 p.

Ixer, R. A., and Stanley, C. J. 1982. Silver mineralization at Sark's Hope mine, Sark, Channel Islands. Mineralogical Magazine, **47**, pp. 539-545.

Jasinski, A. W. 1982. Some aspects of silver mineralization in the Hallefors region (Bergslagen, Sweden). Mineralogical Magazine, **47**, pp. 507-514.

Jenkens, O. P. 1924. Lead deposits of Pend Oreille and Stevens County, Washington. Washington Division of Geology Bulletin, **31**, 153 p.

Kajiwara, Y., and Krouse, H. R. 1971. Sulfur isotope partitioning in metallic sulfide systems. Canadian Journal of Earth Sciences, **8**, pp. 1397-1408.

Kalyuzhnyi, V. A., and Kolton, L. I. 1953. Some data on pressures and temperatures during formation of minerals in Nagol'nyz Kryozh, Donets Basin. L'vov. Geol. Obshch. Mineral. Sbornik, **7**, pp. 67-74.

Keenan, J. H., Keyes, F. G., Hill, P. G., and Moore, J. G. 1969. Steam Tables; Thermodynamic Properties of Water, Including Vapor, Liquid and Solid Phases. John Wiley & Sons, New York, N.Y., 126 p.

Kelly, W. C., and Rye, R. O. 1979. Geologic, fluid inclusion, and stable isotope studies of the tin-tungsten deposit of Panasquiera, Portugal. Economic Geology, **74**, pp. 1721-1822.

Koopman, H. T., and Binda, P. L. 1985. Preliminary observations on strataform copper occurances in the basal Siyeh Formation of Proterozoic age, southern Alberta. Geological Survey of Canada paper, **85-1B**, pp. 133-140.

Malinin, S. D., and Kurovskaya, N. A. 1975. The Solubility of $CO_2$ in chloride solutions at elevated temperatures and $CO_2$ pressures. Geochemistry International, **12**, pp. 199-201.

McDowell, F. W., and Klup, J. L. 1969. Potassium - argon dating of the Idaho batholith. Geological Society of America Bulletin, **80**, pp. 2379-2382.

Mills, J. W. 1977. Zinc and lead ore deposits in carbonate rocks, Stevens County, Washington. Division of Geology and Earth resources Bulletin, **70**, 171 p.

Moen, W. S. 1976. Silver occurances in Washington. Washington Department of Natural Resources, Division of Geology and Earth Resources Bulletin, **69**, 188 p.

Morton, R. D., Goble, E., and Goble, R. J. 1973. Sulfide deposits associated with Precambrian Belt - Purcell strata in Alberta and British Columbia, Canada. *In*Belt Symposium (Moscow, Idaho), **1**, pp. 159-179.

----------., Goble, R. J., and Fritz, P. 1974. The mineralogy, sulfur-isotope composition, and origin of some copper deposits in the Belt Supergroup, Southeast Alberta, Canada. Mineralium Deposita, **9**, pp. 223-241.

Muehlenbachs, K., and Clayton, R. N. 1972. Oxygen isotope studies of fresh and weathered submarine basalts. Canadian Journal of Earth Sciences, **9**, pp. 172-184.

Nash, T. J. 1973. Geochemical studies in the Park City District I: Ore Fluids in The Mayflower Mine. Economic Geology, **68**, pp. 34-51.

Ohmoto, H. 1972. Systematics of sulfur and carbon isotopes in hydrothermal ore deposits. Economic Geology, **67**, pp. 551-578.

---------., Mizukami, M., Drummond, S. E., Eldridge, C. S. Pisutha-Arnond, V., and Lenagh, T. C. 1983. Chemical processes of Kuroko formation. Economic Geology Monograph, **5**, pp. 570-604.

---------., and Rye, R. O. 1979. Isotopes of sulfur and carbon. *In* Geochemistry of Hydrothermal Ore Deposits. ***Edited by*** H.L. Barnes, John Wiley&Sons, New York, N.Y. 798 p.

O'neil, J. R., Clayton, R. N., and Mayeda, T. 1969. Oxygen isotope fractionation in divalent metal carbonates. Journal of Chemical Physics, **51**, pp. 5547-5558.

----------., and Silberman, M. L. 1974. Stable isotope relations in epithermal Au-Ag deposits. Economic geology, **69**, pp. 902-909.

----------., ----------., Fabbi, B.P., and Chesterman, C. W. 1973. Stable isotope and chemical relations during mineralization in the Bodie mining district, Mono County, California. Economic Geology, **68**, pp. 765-784.

Pattrick, R. A. D., Coleman, M. L., and Russell, M. J. 1983. Sulfur isotopic investigations of vein lead-zinc mineralization at Tyndrum, Scotland. Mineralium Deposita, **18**, pp. 477-485.

Potter, R. W. II. 1977. Pressure corrections for fluid-inclusion homogenization temperatures based on the volumetric properties of the system NaCl-$H_2O$. U.S. Geological Survey Journal of Research, **5**, pp. 603-607.

----------., Clynne, M. A., and Brown, D. L. 1978. Freezing point depression of aqueous sodium chloride solutions. Economic Geology, **73**, pp. 284-285.

----------., and Farrand, M. G. 1982. Sulfur isotopes and the origin of stibnite mineralization in New England, Australia. Mineralium Deposita, **17**, pp. 161-174.

Reeser, J. E. 1984. The Purcell Supergroup in the Purcell Mountains, British Columbia. Montana Bureau of Mines and Geology Special Publication **#90**, pp. 33-35.

Rhamdor, P. 1980. Ore Minerals and their Intergrowths. 2nd. edition. Pergamon Press, Toronto. 1205 p.

Robie, R. A., Hemingway, B. S., and Fisher, J. R. 1978. Thermodynamic properties of minerals and related substances at 298.15 K and 1 bar (105 Pascals) pressure and at higher temperatures. U. S. Geological Survey Bulletin, **1452**. 456 p.

Robinson, B. W. 1971. Studies on the Echo Bay silver deposits, N.W.T., Canada: Unpublished Ph.D. thesis, University of Alberta, Edmonton, Alberta, Canada.

----------., and Ohmoto, H. 1973 Mineralogy, fluid inclusions and stable isotopes of the Echo Bay U-Ni-Ag-Cu deposits, Northwest Territories, Canada. Economic Geology, **68**, pp. 635-656.

Roedder, E. 1979. Fluid Inclusions as samples of ore fluids. *In* Geochemistry of Hydrothermal Ore Deposits. *Edited by* H.L. Barnes, John Wiley & Sons, New York, N.Y. 798 p.

----------. 1984. Fluid Inclusions. *In* Reviews in Mineralogy, **12**, Mineralogical Society of America. *Edited by* Paul H. Ribbe, 594 p.

----------., and Bodnar, R. J. 1980. Geologic pressure determinations from fluid inclusion studies. Annual Review of Earth and Planetary Sciences, **8**, pp. 263-301.

Rye, D. M., and Rye, R. O. 1974. Homestake gold mine, South Dakota: I. Stable isotope

studies. Economic Geology, **69**, pp. 293-317.

Rye, R. O. 1974. A comparison of sphalerite-galena sulfur isotope temperatures with filling temperatures of fluid inclusions. Economic Geology, **69**, pp. 26-32.

----------., Hall, W. E., and Ohmoto, H. 1974. Carbon, hydrogen, oxygen and sulfur isotope study of the Darwin Pb - Ag - Zn deposit, Southern California. Economic Geology, **69**, pp. 468-481.

----------., and Ohmoto, H. 1974. Sulfur and carbon isotopes in ore genesis : A review. Economic Geology, **69**, pp. 826-842.

----------., and Sawkins, F. J. 1974. Fluid inclusion and stable isotope studies on the Casapalca Ag-Pb-Zn-Cu deposit, Central Andes, Peru. Economic Geology, **69**, pp. 181-205.

----------., Whelan, J. F., Harrison, J. E., and Hayes, T. S. 1984. The origin of copper - silver mineralization in the Ravalli group as indicated by preliminary stable isotope studies. *In* The Belt, Montana Bureau of Mines and Geology Special Publication, **90**, *Edited by* S. Warren Hobbs. 117 p.

Sakai, H. 1968. Isotopic properties of sulfur compounds in hydrothermal processes. Geochemical Journal, **2**, pp. 29-49.

Sangameshwar, S. R., and Barnes, H. L. 1983. Supergene processes in zinc - lead - silver sulfide ores in carbonates. Economic Geology, **78**, pp. 1379-1397.

Scott, S. D., and Barnes, H. L. 1971. Sphalerite geothermometry and geobarometry. Economic Geology, **66**, pp. 653-669.

Sharma, T. and Clayton, R. N. 1965. Measyrement of $O^{18}/O^{16}$ ratios of total oxygen of carbonates. Geochimica et Chosmichimica Acta, **29**, pp. 1347-1353.

Sheppard, S. M. F., Nielson, R. L., and Taylor, H. P. J. 1971. Hydrogen and oxygen isotope ratios in minerals from porphyry copper deposits. Economic geology, **66**, pp. 515-542.

----------., and Taylor, H. P. Jr. 1974. Hydrogen and oxygen isotope evidence for the origin of water in the Boulder batholith and the Butte ore deposit, Montana. Economic Geology, **69**, pp. 926-946.

Shikazona, N. 1985. Gangue minerals from neogene vein-type deposits in Japan and an estimate of their $CO_2$ fugacity. Economic Geology, **80**, pp. 754-768.

Skinner, B. J., and Barton, P. B. Jr. 1973. Genesis of mineral deposits. Annual Review of Earth Planet Sciences, **1**, pp. 183-211.

Small, W. D. 1973. Isotope compositions of selected ore leads from northeastern Washington. Canadian Journal of Earth Sciences, **10**, pp. 670-678.

Sourirajan, S., and Kennedy, G. C. 1962. The system $H_2O$-NaCl at elevated temperatures and pressures. American Journal of Science, **260**, pp. 115-141.

Takenouchi, S, and Kennedy, G. C. 1965. The solubility of carbon dioxide in NaCl solutions at high temperatures and pressures. American Journal of Science, **263**, pp. 445-454.

Takeuchi, S. 1971. Study of $CO_2$-bearing fluid inclusions by means of a freezing stage microscope. Mineral Geology, **21**, pp. 186-300. ( English abstract of Japanese paper )

Tatsumi, T. 1965. Sulfur isotopic fractionation between coexisting sulfide minerals from some Japanese ore deposits. Economic Geology, **60**, pp. 1645-1659.

Taylor, H. P. Jr. 1974. The application of oxygen and hydrogen isotope studies to the problem of hydrothermal alteration and ore deposition. Economic Geology, **69**, pp. 843-883.

----------. 1979. Oxygen and hydrogen isotope relationships in hydrothermal mineral deposits. *In* Geochemistry of Hydrothermal Ore Deposits. *Edited by* H.L. Barnes. John Wiley & Sons, New York, N.Y. 798 p.

Thurmond, F. L. R. 1928. Mining Corporation of America Prospectus Report on the Deer Trail Mine. 28 p.

Vikre, P. G. 1985. Precious metal vein systems in the National district, Humboldt County, Nevada. Economic Geology, **80**, pp. 360-393.

Waters, A. C., and Krauskopf, K. 1941. Pyroclastic border of the Colville batholith. Geological Survey of America Bulletin, **59**, pp. 1355-1417.

Weaver, C. E. 1920. The Mineral Resources of Stevens County, Washington. Washington Geological Survey Bulletin, **#20**, 350 p.

White, D. E. 1974. Diverse origins of hydrothermal ore fluids. Economic Geology, **69**, pp. 954-973

----------. 1980. Active geothermal systems and hydrothermal ore deposits. *In* Economic Geology Seventy Fifth Anniversary Volume. *Edited by* Brian J. Skinner. Lancaster Press, Inc., Lancaster, Pennsylvania. 964 p.

Whitwell, G. E., and Patty, E. N. 1921. The Magnesite Deposits of Washington; Their occurance and technology. Washington Geological Survey Bulletin, **25**, 144 p.

Willis, B. 1927. Some geological features of the Washington magnesite deposits. (Discussion) Engineering and Mining Journal, **124**, pp. 858.

Yates, M. G., and Ripley, E. M. 1985. Fluid inclusion and isotopic studies of the galena mine, Coeur d'Alene district, Idaho. Geological Society of Americe, 98th Annual Meeting Abstract with Programs, pp. 756.

Yates, R. G., Becraft, G. E., Campbell, A. B., and Pearson, R. C. 1966. Tectonic Framework of northeastern Washington, northern Idaho, and northwest Montana. Canadian Institute of Mining and Metallurgy Special Volume, **8**, pp. 47-59.

Zartman, R. E. 1978. Lead isotopic provinces in the cordillera of the western United States and their geological significance. Economic Geology, **69**, pp. 792-805.

----------., and Stacey, J. S. 1971. Lead isotopes and mineralization in Belt Supergroup rocks, northwestern Montana and northern Idaho. Economic Geology, **66**, pp. 849-859.

## XI. APPENDIX - TEST, CALCULATION AND CALIBRATION METHODS

### A. ELECTRON MICROPROBE

All samples were analysed with the energy dispersive analysis section of the EEDS-II electron microprobe facilities of the department of geology. All spectra were counted for 240 seconds at an operating voltage of 15 Kv. Standards for all elements were chosen so as to minimize the corrections that were necessary in processing the data. To do this standards with chemical properties and average molecular weights similar to those of the samples were chosen. The standards were also required to contain, where possible, at least twice as much of the element of interest as the sample. The standards used for each element were:

silver metal (Ag) - silver

chalcopyrite ($CuFeS_2$) - copper

pyrite ($FeS_2$) - iron, sulfur

stibnite ($Sb_2S_3$) - antimony

willemite ($Zn_2SiO_4$) - zinc, manganese

Default standards were used in the processing of arsenic and cadmium data.

## B. STAGE CALIBRATION

All fluid inclusion heating and freezing tests were performed with a Chaixmeca model VT2 120 microthermometry apparatus. Cooling was accomplished by circulating a liquid nitrogen cooled gaseous nitrogen stream through the sample stage. Heat was supplied by an electrical resistance circuit within the stage. The stage temperature was measured by a platinum resistance sensor within the stage, the readout for which has a resolution of 0.1°C.

To determine the accuracy and precision of the indicated temperature under actual test conditions, it was necessary to calibrate the stage. Calibration was done by testing several standards which melt at known temperatures, or over very small temperature ranges. Each standard was placed between two cover-slip fragments, the thermal mass of which approximated that of the fluid inclusion chips used in actual runs.

Six standards were chosen to cover the probable range of interest, i.e., -60°C to +400°C. They were;

A) Pure $CO_2$; m.p. = -56.6°C. ( In quartz from Bitsch, Switzerland.)

B) Pure water; m.p. = +0.01°C.

C) Merck 9700; m.p. = +100.0°C.

D) Ammonium nitrate; $NH_4NO_3$; m.p. = +169.6°C.

E) Sodium nitrate; $NaNO_3$; m.p. = +306.8°C.

F) Potassium dichromate; $Kr_2Cr_2O_7$; m.p. = +398.0°C.

Each standard was tested seven times. Heating rates were held to 0.3°C to 0.4°C per minute within 10°C of the melting point. This was done to reduce thermal lag and any other temperature measurement errors. Test results are listed in Table A-1.

Figure A-1 is a graph of these results. It shows that the indicated temperature was always slightly higher than the true stage temperature, especially at temperatures over +200°C. The accuracy and precision of the indicated temperature both deteriorate at higher temperatures.

Figure A-2 shows the calibration curve determined for the stage used in this study. It shows the value of the temperature correction which must be applied to the readout temperature at all values between about -57°C and +400°C. All corrections are negative, and must thus be subtracted from the indicated temperature.

**Table A-1**

**Standards used in stage calibration for study of fluid inclusions from the Deer Trail Mine, Washington, U.S.A.**

| Standard | Standard type; composition; and melting point | Indicated melting temperature °C | Average indicated melting temperature | Temperature correction. |
|---|---|---|---|---|
| A | Pure carbon dioxide, $CO_2$ | -55.8; -55.6; -55.7; -55.8 | -55.7 ± 0.2°C | -0.9 ± 0.2°C |
| | m.p. = -56.6°C | -55.7; -55.7; -55.7 | | |
| B | Pure water, $H_2O$ | 0.8; 0.3; 0.9; 0.5 | 0.7 ± 0.4°C | -0.7 ± 0.4°C |
| | m.p. = 0.01°C | 0.4; 1.0; 0.8 | | |
| C | Merck 9700, ???? | 100.2; 101.8; 103.2; 102.0 | 101.7 ± 1.5°C | -1.7 ± 1.5°C |
| | m.p. = 100.0°C | 102.9; 100.5; 101.8 | | |
| D | Ammonium nitrate, $NH_4NO_3$ | 171.9; 172.2; 171.4; 173.3 | 172.4 ± 1.0°C | -2.8 ± 1.0°C |
| | m.p. = 169.9°C | 172.8; 173.0; 172.5 | | |
| E | Sodium nitrate, $NaNO_3$ | 310.4; 312.5; 308.6; 311.4 | 310.6 ± 3.1°C | -3.8 ± 2.0°C |
| | m.p. = 306.8°C | 311.8; 310.1; 309.7 | | |
| F | Potassium dichromate, $K_2Cr_2O_7$ | 404.7; 402.9; 404.9; 406.2 | 403.7 ± 3.1°C | -5.7 ± 3.1°C |
| | m.p. = 398.0°C | 403.9; 402.7; 400.6 | | |

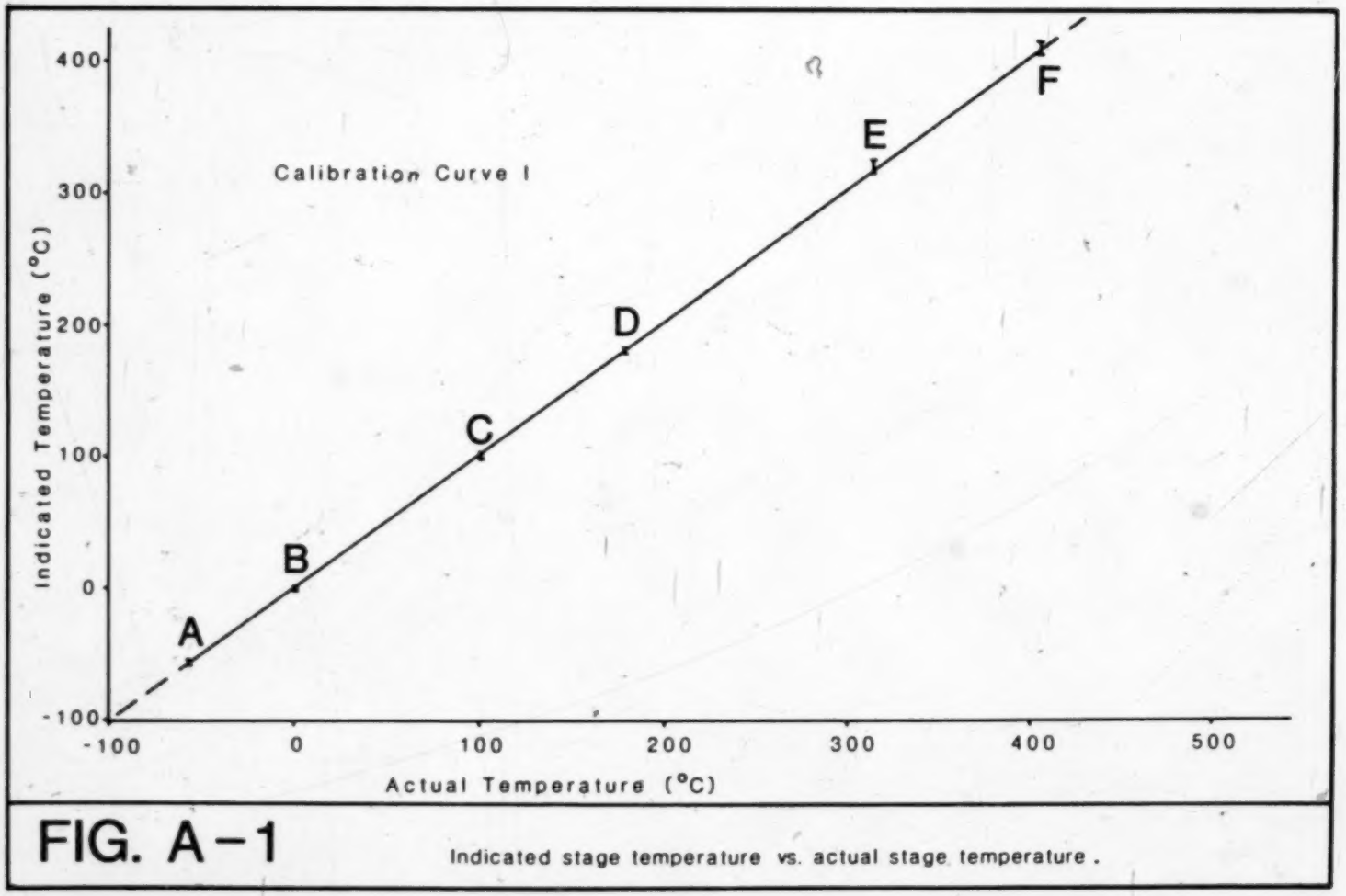


FIG. A-1 Indicated stage temperature vs. actual stage temperature.

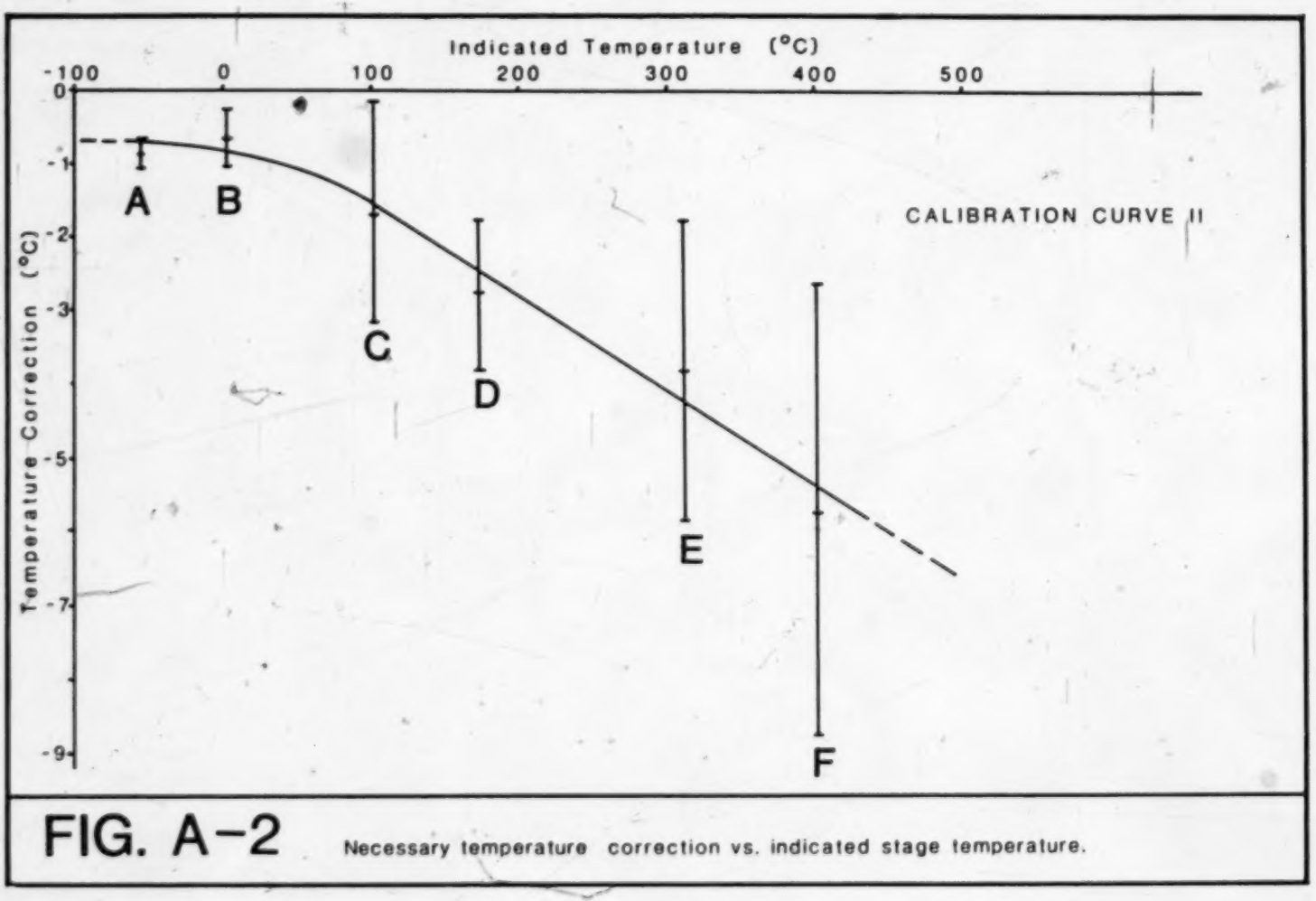


FIG. A-2 Necessary temperature correction vs. indicated stage temperature.

## E. SULFUR ISOTOPES

**Sample calculation of the boundary between two minerals on a $\log fS_2$ vs. $\log fO_2$ plot.**

pyrrhotite → pyrite

$$FeS + (0.5)S_2 \rightarrow FeS_2$$

At 250°C assume that the activity ($\alpha$) of Fe 0.55 (Barton and Skinner 1979).

$$K(eq) = \alpha FeS_2 \cdot \alpha FeS \cdot fS_2^{-.5}$$

$$K(eq) = \{1 / (\alpha FeS)(fS_2^{-.5})\}$$

$$\log K(eq) = -\log \alpha FeS - (1/2)\log fS_2$$

$$\log K(eq) = .222 - (1/2)\log fS_2$$

At 250°C the $\log K(eq)$ of this reaction is 7.01 (Table A-2).

$$7.01 = .222 - (1/2)\log fS_2$$

$$6.788 = -(1/2)\log fS_2$$

$$-13.576 = \log fS_2$$

Therefore, at 250°C the pyrrhotite/pyrite boundary is a straight line at $\log fS_2 = -13.576$.

An analogous procedure is used to calculate the $\log fO_2$ value in reactions involving oxygen.

**Calculation of system pH as controlled by $fCO_2$ in a system containing water, $CO_2$ and calcite in equilibrium.**

pH is assumed to be buffered by the following reactions;

$\alpha H_2CO_3(app) \rightarrow B \times fCO_2$ (app = apparent $\alpha$ of $H_2CO_3 = \alpha H_2CO_3 + \alpha HCO_3^-$

$H_2CO_3 \rightarrow H^+ + HCO_3^-$; equilibrium coefficient = Ka.

$HCO_3^- \rightarrow H^+ + CO_3^{2-}$; equilibrium coefficient = Kb.

$[CaCO_3](min) \rightarrow Ca^{2+} + CO_3^{2-}$; equilibrium coefficient = Kc

$H_2O \rightarrow H^+ + OH^-$; equilibrium coefficient = Kw.

$$2mCa^{2+} + mH^+ = mHCO_3^- + 2mCO_3^{2-} + mOH^-$$

**Table A-2**

**Equilibrium coefficients at listed temperatures and 80 bars for all thermodynamic reactions used in calculations throughout the thesis.**

| Reaction | 25°C | 100°C | 150°C | 200°C | 250°C | 300°C |
|---|---|---|---|---|---|---|
| * $H_2CO_3(aq) \rightarrow H^+ + HCO_3^-$ | ---- | -6.45 | -6.73 | -7.08 | -7.63 | -8.86 |
| * $HCO_3^- \rightarrow H^+ + CO_3^{2-}$ | ---- | -10.16 | -10.29 | -10.68 | -11.43 | -13.38 |
| * $[CaCO_3](min) \rightarrow Ca^{2+} + CO_3^{2-}$ | ---- | -9.39 | -10.25 | -11.37 | -12.72 | -14.10 |
| * $H_2O \rightarrow H^+ + OH^-$ | -14.0 | -12.26 | -11.64 | -11.27 | -11.13 | -11.39 |
| # $H_2S(aq) \rightarrow H^+ + HS^-$ | ---- | ---- | ---- | ---- | -7.55 | ---- |
| # $HS^- \rightarrow H^+ + S^{2-}$ | ---- | ---- | ---- | ---- | -11.30 | ---- |
| # $H_2S(aq) + (2)O_2 \rightarrow HSO_4^- + H^+$ | ---- | ---- | ---- | ---- | 61.37 | ---- |
| # $HSO_4^- \rightarrow H^+ + SO_4^{2-}$ | ---- | ---- | ---- | ---- | -5.05 | ---- |
| # $H_2S(aq) + (2)O_2 \rightarrow (2)H^+ + SO_4^{2-}$ | ---- | ---- | ---- | ---- | 56.32 | ---- |
| % $HS^- + (2)O_2 \rightarrow H^+ + SO_4^{2-}$ | ---- | ---- | ---- | ---- | 63.87 | ---- |
| % $S^{2-} + (2)O_2 \rightarrow SO_4^{2-}$ | ---- | ---- | ---- | ---- | 75.17 | ---- |
| & $FeS + (0.5)S_2 \rightarrow FeS_2$ | ---- | ---- | ---- | ---- | 7.01 | ---- |
| & $(3)FeS + (2)O_2 \rightarrow (1.5)S_2 + Fe_3O_4$ | ---- | ---- | ---- | ---- | 56.53 | ---- |
| & $(3)FeS_2 + (2)O_2 \rightarrow (3)S_2 + Fe_3O_4$ | ---- | ---- | ---- | ---- | 35.51 | ---- |
| & $(2)FeS_2 + (1.5)O_2 \rightarrow (2)S_2 + Fe_2O_3$ | ---- | ---- | ---- | ---- | 29.56 | ---- |
| & $(2)Fe_3O_4 + (0.5)O_2 \rightarrow (3)Fe_2O_3$ | ---- | ---- | ---- | ---- | 17.65 | ---- |

| | | | | | | |
|---|---|---|---|---|---|---|
| & $(2)Ag + (0.5)S_2 \rightarrow Ag_2S$ | ---- | ---- | ---- | ---- | 6.80 | ---- |
| & $(1.5)O_2 + CaCO_3 + (0.5)S_2 \rightarrow CaSO_4 + CO_2$ | ---- | ---- | ---- | ---- | 58.24 | ---- |
| & $(1.5)O_2 + BaCO_3 + (0.5)S_2 \rightarrow BaSO_4 + CO_2$ | ---- | ---- | ---- | ---- | 58.80 | ---- |
| & $C + O_2 \rightarrow CO_2$ | ---- | ---- | ---- | ---- | 39.44 | ---- |
| & $(5)CuFeS_2 + S_2 \rightarrow (4)FeS_2 + Cu_2FeS_4$ | ---- | ---- | ---- | ---- | 8.61 | ---- |
| & $(5)CuFeS_2 + (3)O_2 \rightarrow Cu_2FeS_4 + (2)Fe_2O_3 + (3)S_2$ | ---- | ---- | ---- | ---- | 67.72 | ---- |
| & $(15)CuFeS + (8)O_2 \rightarrow (3)Cu_2FeS_4 + (4)Fe_3O_4 + (9)S_2$ | ---- | ---- | ---- | ---- | 167.87 | ---- |

---

* = Values from Helgeson (1969). Pressure effect negligable.

\# = Values from Ohmoto, et al (1983). Based on data from Helgeson (1969) with new data for the dissociation of $H_2S$.

% = Values calculated from equations given in Ohmoto, et al (1983). Pressure effect on equilibrium coefficients from Ohmoto (1983) negligable.

& = Values calculated through the use of the computer program SUPCRT, a program which works from basic $\Delta G$ values of the reaction components to calculate the equilibrium coefficient of the reaction at the defined temperature and pressure.

Equilibrium coefficients are calculated by the following method;

equation : min a + gas → min b

$\Delta Gr^\circ = G(\text{min b}) - G(\text{min a}) - G(\text{gas})$

$0 = \Delta Gr = \Delta Gr^\circ + RT\ln K$

thus; $\Delta Gr^\circ = -RT\ln K$ and; $\Delta Gr^\circ / (RT \times 2.303) = \log K$

Where ; R = 8.3144, T = temperature in °K, $\Delta Gr^\circ$ = the change in Gibbs free energy for the reaction.

and G(min) or G(gas) = the Gibbs free energy in kilocalories for that component of the reaction at the specified T and P values.

From the above equations the following relationship may be obtained.

$$\alpha H^{+} = \frac{Ka^{2} \times Kb \times B^{2} \times fCO_{2}^{2} \times \alpha Ca^{2+}}{Kc \times 2 \times \alpha HCO_{3}^{-}} \quad \text{(equation \#1)} \qquad \text{(Robinson 1971)}$$

Which is equivalent to: $(3)\log\alpha H^{+} = (2)\log Ka + \log Kb + (2)\log B + (2)\log fCO_{2} + \log\alpha Ca^{2+} - \log Kc - \log 2 - \log\alpha HCO_{3}^{-}$ (equation #1)

$B = 55.5$ / Henry's law constant for $CO_2$ in a one molar ( $I=1$ ) solution at any given temperature (Holland 1965).

To calculate the $\log\alpha$ of the $Ca^{+}$ and $HCO_3^{-}$ ions in solution use the Debye - Huckle theory for individual ionic activity;

$$-\log\alpha(ion) = \frac{A \times z^{2}(ion) \times I^{.5}}{1 + a^{o}(ion) \times B \times I^{.5}} \quad \text{(equation \#2)}$$

Where;

$a^{o}(ion)$ = effective ionic radius.

$z(ion)$ = ionic charge.

$I$ = ionic strength of the solution

$A, B$ = constants at a given temperature (Helgeson 1967).

Substituting the values for the activity of the $Ca^{2+}$ and $HCO_3^{-}$ ions, calculated from equation #2, into equation #1 allows the calculation of the systems pH at various $fCO_2$ values at each temperature of interest.

i.e., $(3)\log\alpha H^{+} = (2)\log Ka + \log Kb + (2)\log B + (2)\log fCO_2 + \log\alpha Ca^{2+} - \log Kc - \log 2 - \log\alpha HCO_3^{-}$.

All of the above values are now known, except $(3)\log\alpha H^{+}$ and $(2)\log fCO_2$ so the equation now reduces to;

$$(3)pH = X - (2)\log fCO_2$$

Now insert the required $fCO_2$ values to find the pH value at each point of interest.

## D. OXYGEN AND HYDROGEN ISOTOPES

All samples to be used in the hydrogen isotope study were broken into pieces of 0.1 to 0.5 cm in diameter. Calcite and sphalerite were used 'as is', as were most of the quartz samples. Exceptionally 'dirty' quartz was leached in aqua regia for approximately 24 hours to remove all sulfides and/or calcite.

Inclusion fluids from six of the samples was released by crushing. Samples used in this method were first heated under vacuum to approximately 80°C for two hours to drive off all surface and fracture water. They were then crushed under vacuum and all liberated water was frozen off in a liquid nitrogen bath. This method was found to be unsatisfactory as the amount of water liberated, only about 1 to 3 $\mu$l, was generally too small to ensure an accurate analyses. Also, this method released water from all inclusions within the sample at once, including primaries, pseudo-secondaries and secondaries. The water produced is thus a combination of all fluids present in the sample and, unless all fluids have identical $\delta D$ compositions, the analytical results are meaningless, reflecting only the average $\delta D$ value of all fluids present.

To try to avoid these problems, a second method was used. Samples were again broken into small pieces and cleaned when necessary, but this time the fluid inclusion water was released by heating the sample under vacuum. Samples were first placed in nickel sample tubes and heated to approximately 125°C, again to drive off all surface and fracture water. Heating was continued for approximately two hours, or until no measurable pressure change was noted in the vessel after sealing for one half hour. Next the sample was heated to a temperature high enough to decrepitate the secondary inclusions but leave the primaries intact. This temperature varied for each depositional stage and sample type, i.e., calcite, quartz, sphalerite, but was generally around 275°C to 300°C for ore stage material, as determined through observations made during the fluid inclusion study. The released secondary inclusion water was frozen off in a $CO_2$-alcohol slush to prevent the capture of any $CO_2$ released.

Next the water from the primary inclusions, actually the fluid from all inclusions which decrepitated at temperatures above approximately 300°C, which included primaries, pseudo-secondaries and any rare high temperature secondaries which may have been present, was collected. To do this the sample tube was re-evacuated and then heated to approximately 650°C. Liberated water was collected for two hours, again by freezing with an alcohol - $CO_2$ slush.

In the case of the post-ore stage calcite and the very late calcite sample the initial heating was held to 100°C to prevent unwanted decrepitation of their low temperature primary fluid inclusions. Primary fluids were then collected at approximately 400°C.

The δD values for fluids captured by the crushing method generally fell between or near those of fluids released in low and high temperature decrepitation (Table 6-1). For example, the water captured during crushing of sample DTM-12 had a δD value of -151‰, while that captured at 300°C had a value of -152‰. The δD value of water captured at 650°C was -142‰. This indicates that in this case the secondary fluids were isotopically lighter than those present in primary inclusions within the sample. It also indicates that secondary fluid inclusions were in this case dominant over primary inclusions with the result that the water collected during crushing reflected the lower D value of the secondary fluids. The difference between the δD values of primary and secondary fluids is most pronounced in the early ore stage quartz and sphalerite samples, and is least obvious or absent in minerals deposited by fluids with low δD values.

As expected, the crushing method provides water samples whose δD value reflects the average composition of the fluids within inclusions in the sample. Heating, on the other hand, allows at least a crude separation of the fluids into their original groups and provides much more meaningful results.